DISS. ETH No. 18659

SILK FIBROIN AS A VEHICLE FOR DRUG DELIVERY IN TISSUE REGENERATION

A dissertation submitted to

ETH ZURICH

for the degree of

Doctor of Sciences

presented by

Esther Wenk

eidg. dipl. Apothekerin, ETH Zurich

born on September 29, 1978

citizen of Schmerikon, SG, Switzerland

accepted on the recommendation of

Prof. Dr. J.C. Leroux, examiner

Prof. Dr. H.P. Merkle, co-examiner

PD Dr. Dr. L. Meinel, co-examiner

2009

TABLE OF CONTENTS

BACKGROUND AND PURPOSE

Tissue damage or loss, as a consequence of ageing, pathology or injury, leads to a reduced quality of life for many and is associated with significant social and economic costs [1]. The need for efficacious therapies to regenerate damaged or lost tissue by guiding and controlling tissue differentiation and growth is therefore evidenced. A major role in this context is generally attributed to the use of growth factors as therapeutics. When systemically administered, growth factors often undergo fast biological clearance, which translates into short half-lives and calls for unfavorable dosage regimens of high frequency. Moreover, because growth factors may adopt multiple functions in different tissues, their systemic delivery would largely enhance the risk for adverse side effects. Instead, as an approach to mimic nature, growth factors should be locally released, possibly following the course of the different phases in physiological tissue repair [1]. Therefore, spatiotemporal delivery of growth factors plays a key role in therapeutic tissue regeneration. Only tightly controlled drug delivery is expected to allow safe and successful administration of growth factors in therapeutic tissue repair.

Various demands must be considered when it comes to design appropriate delivery systems: (i) the capacity of the system to deliver the growth factor to the correct site, at the appropriate time and in the proper dose; (ii) the presence of a substratum that stimulates cell recruitment and attachment, and, at least for some time, provides a structural support for the developing neotissue; (iii) the presence of pores with appropriate size and interconnectivity to ensure efficient nutrient supply and waste removal, support cell migration and promote angiogenesis; and finally (iv) the biocompatibility and biodegradability of the delivery system in order to preclude an immune or inflammatory response as well as exclude toxic waste products that could inhibit or end the repair process [2]. In this work, several of these points are being addressed.

Microparticulate carriers have considerable potential as platform for the delivery of therapeutics [3, 4]. Whether ingested or injected, they offer opportunities to protect a protein therapeutic from degradation or denaturation,

control its release profile, or be functionalized to achieve targeted release [3]. Unfortunately, many of the common technologies to prepare microparticles are detrimental to sensitive biologicals because they involve harsh preparation conditions, such as the presence of non-aqueous solvents, water/solvent interfaces, cross-linking reagents for hardening, or elevated temperatures [5, 6]. For that reason appropriate formulation protocols must be developed that maintain drug stability and potency.

For many applications in tissue regeneration, such as in bone repair, structural support is needed to accommodate cells and neotissue. For this purpose the growth factor could be loaded onto or into a 3D scaffold that provides mechanical stability. The incorporation of the growth factor could be achieved by simple adsorption or embedment. However, such approaches allow only limited control over loading and release kinetics. The embedment of growth factor loaded microparticles into scaffolds is a further option to improve control over the release kinetics not only through the scaffold itself but also through the degradation and release kinetics of the microparticles.

The design of scaffolds that mimic the extracellular matrix (ECM), e.g., by introducing mechanical and/or biochemical cues, has been suggested to optimize cell recruitment and differentiation in tissue repair [7]. The ECM represents a hydrated protein- and proteoglycan-based gel network consisting of collagens, non-collageneous glycoproteins such as elastin, laminin or fibronectin, and hydrophilic proteoglycans with large glycosaminoglycan side chains [8]. Beyond its function to provide a physiological matrix for cellular accommodation, the ECM of mammalian cells also acts as a local storage to sequester growth factors, delivers them on demand, protects their potency, and, in some cases, enhances their binding to cell surface receptors [8]. For instance, fibroblast growth factor 2 (FGF-2), a heparin-binding growth factor, specifically interacts with a major component of the ECM, the sulfated glycosaminoglycan heparan sulfate [9-11]. Mimicking the role of the physiologic ECM through modified biomaterials with appropriate functional groups may, therefore, lead to advanced opportunities for both scaffold design and drug delivery.

Against this background, the present PhD thesis aims to establish drug delivery systems based on silk fibroin (SF) with the capacity to control loading and release of growth factors. Silk fibroin is a natural, fibrous protein produced by spiders or insects such as *Nephila clavipes* and the domestic silkworm *Bombyx mori* [12]. A major advantage of SF as compared to other biomaterials is its convenient processability in aqueous systems, which allows mild fabrication conditions that are favorable for the incorporation of sensitive biologicals such as growth factors. This and other of its unique properties such as superior mechanical strength as well as well-established biocompatibility and long-term biodegradability [12-14] led to its exploration as a biomaterial for various biomedical applications [15-18].

The introductory chapter to this PhD thesis first summarizes properties of SF that affect the release of therapeutics from SF delivery systems. Furthermore, various fabrication methods of SF drug delivery systems and applications are reviewed. To further contribute to SF as a biomaterial for drug delivery, the first experimental chapter introduces a new approach to fabricate SF spheres that allows the incorporation of highly sensitive biologicals such as growth factors for tissue regeneration. Since microparticles themselves cannot provide structural support, the combination of growth factor loaded PLGA microparticles with SF scaffolds was subject of another experimental chapter, affording adjustable and controlled growth factor release kinetics. The final chapter covers the implementation of natural concepts for growth factor storage and delivery, using chemically modified SF that mimics the ECM and binds FGF-2.

References

1.	Gerstenfeld LC, Cullinane DM, Barnes GL, Graves DT, Einhorn TA. Fracture healing as a post-natal developmental process: molecular, spatial, and temporal aspects of its regulation. J Cell Biochem 2003;88(5):873-884.

2.	Lieberman JR, Daluiski A, Einhorn TA. The role of growth factors in the repair of bone. Biology and clinical applications. J Bone Joint Surg Am 2002;84-A(6):1032-1044.

3.	Freiberg S, Zhu XX. Polymer microspheres for controlled drug release. Int J Pharm 2004;282(1-2):1-18.

4.	Sinha VR, Trehan A. Biodegradable microspheres for protein delivery. J Control Release 2003;90(3):261-280.

5.	Wang L-Y, Gu Y-H, Su Z-G, Ma G-H. Preparation and improvement of release behavior of chitosan microspheres containing insulin. Int J Pharm 2006;311:187-195.

6.	Bilati U, Allemann E, Doelker E. Strategic approaches for overcoming peptide and protein instability within biodegradable nano- and microparticles. Eur J Pharm Biopharm 2005;59(3):375-388.

7.	Ma PX. Biomimetic materials for tissue engineering. Adv Drug Deliv Rev 2008;60(2):184-198.

8.	Lutolf MP, Hubbell JA. Synthetic biomaterials as instructive extracellular microenvironments for morphogenesis in tissue engineering. Nat Biotechnol 2005;23(1):47-55.

9.	Nugent MA, Iozzo RV. Fibroblast growth factor-2. Int J Biochem Cell Biol 2000;32(2):115-120.

10.	Ornitz DM. FGFs, heparan sulfate and FGFRs: complex interactions essential for development. Bioessays 2000;22(2):108-112.

11.	Harmer NJ. Insights into the role of heparan sulphate in fibroblast growth factor signalling. Biochem Soc Trans 2006;34(Pt 3):442-445.

12.	Altman GH, Diaz F, Jakuba C, Calabro T, Horan RL, Chen J, et al. Silk-based biomaterials. Biomaterials 2003;24(3):401-416.

13. Horan RL, Antle K, Collette AL, Wang Y, Huang J, Moreau JE, et al. In vitro degradation of silk fibroin. Biomaterials 2005;26(17):3385-3393.

14. Meinel L, Hofmann S, Karageorgiou V, Kirker-Head C, McCool J, Gronowicz G, et al. The inflammatory responses to silk films in vitro and in vivo. Biomaterials 2005;26(2):147-155.

15. Meinel L, Betz O, Fajardo R, Hofmann S, Nazarian A, Cory E, et al. Silk based biomaterials to heal critical sized femur defects. Bone 2006;39(4):922-931.

16. Hofmann S, Knecht S, Langer R, Kaplan DL, Vunjak-Novakovic G, Merkle HP, et al. Cartilage-like tissue engineering using silk scaffolds and mesenchymal stem cells. Tissue Eng 2006;12(10):2729-2738.

17. Kirker-Head C, Karageorgiou V, Hofmann S, Fajardo R, Betz O, Merkle HP, et al. BMP-silk composite matrices heal critically sized femoral defects. Bone 2007;41(2):247-255.

18. Altman GH, Horan RL, Lu HH, Moreau J, Martin I, Richmond JC, et al. Silk matrix for tissue engineered anterior cruciate ligaments. Biomaterials 2002;23(20):4131-4141.

SUMMARY

In physiological tissue repair biological signaling is a crucial factor controlling cellular recruitment, proliferation and differentiation. However, under critical conditions the local availability of endogenous signaling factors may be insufficient to sustain repair. Therefore, localized delivery of exogenous growth factors may be mandatory, e.g., for the repair of large (critical) bone defects. Incorporation of growth factors into polymer scaffolds has been shown to provide options for both mechanical stabilization of the defect and controlled delivery of therapeutics. The present PhD thesis investigates into silk fibroin (SF) as a biomaterial for the controlled delivery of growth factors in tissue engineering. This naturally occurring protein polymer has several unique properties making it a favorable vehicle for the incorporation and delivery of such therapeutics.

As an introduction to this PhD thesis, **Chapter I** reviews molecular and physical properties of SF that affect the release of therapeutics from SF delivery systems and their biomedical application. Various methods used for the fabrication of SF delivery systems are described, including mild, all-aqueous processes that have expanded their range of applicability even to sensitive drug candidates such as protein therapeutics and nucleic acids. For illustration, we discuss a variety of examples for the incorporation of drugs into SF systems, their interaction with the SF matrix and their release. Further, various applications of SF delivery systems ranging from tissue engineering to ocular drug delivery are presented.

Microparticulate carriers have considerable potential as platform for the delivery of therapeutics. **Chapter II** describes the fabrication of drug loaded SF spheres under very mild processing conditions. The spheres were fabricated using the laminar jet break-up of an aqueous SF solution, which was induced by a nozzle vibrating at controlled frequency and amplitude. As determined by SEM, the obtained SF particles were spherical in shape with diameters in the

range of 101 μm to 440 μm, depending on the diameter of the nozzle and the treatment to induce water insolubility of SF. Treatments with either methanol or exposure to water vapor resulted in an increase in β-sheet content as analyzed by FTIR. High encapsulation efficiencies, close to 100%, were obtained when salicylic acid and propranolol hydrochloride-loaded SF spheres were left untreated or exposed to water vapor. Methanol treatment resulted in drug leaching and lowered the overall encapsulation efficiency. When 9% SF solutions were used for SF sphere preparation, release rates were more sustained than from spheres made from 3% SF solutions, and propranolol hydrochloride release was more sustained than salicylic acid release. However, no difference in the release profiles was observed between methanol and water vapor treated SF spheres. Because of its very mild conditions, which are potentially advantageous for the encapsulation of sensitive drugs, we also tested this technology for the encapsulation of insulin-like growth factor I (IGF-I). Again encapsulation efficiencies were close to 100%, even after treatment with methanol. IGF-I was continuously released over 7 weeks in bioactive form, as analyzed by the proliferation of MG-63 cells. The results favor further investigations into SF spheres as a platform for the controlled delivery of sensitive biologicals.

Whereas previous studies demonstrated that spheres represent a feasible system to deliver growth factors in a controlled and sustained manner, an osteoconductive environment is necessary to enhance cell recruitment and attachment and provide a structural support for cells and new tissue formed in the scaffold during the initial stages post-implantation. Therefore, the development of prototype scaffolds for either direct implantation or *in vitro* tissue engineering purposes that feature spatiotemporal control of growth factor release is highly desirable. **Chapter III** describes the preparation of SF scaffolds with interconnective pores by a porogen leaching protocol, carrying embedded microparticles that were loaded with IGF-I. Treatments with methanol or water vapor induced water insolubility of SF based on an increase in β-sheet content as analyzed by FTIR. Pore interconnectivity was demonstrated by SEM. Porosities were in the range of 70% to 90%, depending on the treatment applied, and were better preserved when methanol or water vapor treatments were performed prior to porogen leaching. IGF-I was

encapsulated into two different types of poly(lactide-co-glycolide) microparticles (PLGA MP) using uncapped PLGA (50:50) with molecular weights of either 14 or 35 kDa to control IGF-I release kinetics from the SF scaffold. Embedded PLGA MP were located in the walls or intersections of the SF scaffold. Embedment of the PLGA MP into the scaffolds led to more sustained release rates as compared to the free PLGA MP, whereas the hydrolytic degradation of the two PLGA MP types was not affected. The PLGA types used had distinct effects on IGF-I release kinetics. Particularly the supernatants of the lower molecular weight PLGA formulations turned out to release bioactive IGF-I. Our studies justify future investigations of the developed constructs for tissue engineering applications.

The development of biomaterials that mimic the physiological binding of growth factors to the extracellular matrix (ECM) is an appealing strategy for advanced growth factor delivery systems. *In vivo*, fibroblast growth factor 2 (FGF-2) binds to the sulfated glycosaminoglycan heparan sulfate, which is a major component of the ECM. Therefore, in **Chapter IV** we tested whether SF decorated with a sulfonated moiety could mimic the natural ECM environment and lead to sustained delivery of this heparin-binding growth factor. Using a diazonium coupling reaction, modified SF derivatives containing approximately 20, 40, 55 and 70 sulfonic acid groups per SF molecule were obtained. Films of the SF derivative decorated with 70 sulfonic acid groups per SF molecule resulted in a 2-fold increase in FGF-2 binding as compared to native SF. More than 99% of bound FGF-2 could be retained on all SF derivatives. However, protection of FGF-2 potency was only achieved with at least 40 sulfonic acid groups per SF molecule, as observed by reduced metabolic activity and enhanced levels of phosphorylated extracellular signal-regulated kinases (pERK1/2) in cultured human mesenchymal stem cells (hMSCs). This study introduces a first step towards the development of an ECM-mimicking biomaterial for sustained, non-covalent binding, controlled delivery and preserved potency of a biomolecule.

In conclusion, SF represents an attractive biomaterial for the fabrication of growth factor delivery systems. The performed experiments add further options to incorporate sensitive drugs, consider their interaction with SF matrices and inform on the sustained release from such matrices. They encourage further investigations into SF as a vehicle for the controlled release of growth factors for tissue regeneration, both *in vitro* and *in vivo*.

ZUSAMMENFASSUNG

Biologische Signalgebung spielt für die physiologische Regeneration von Geweben eine entscheidende Rolle. Sie beeinflusst die Rekrutierung geeigneter Zellen ebenso wie deren Proliferation und Differenzierung. Unter kritischen Voraussetzungen reicht jedoch die lokale Verfügbarkeit endogener signalgebender Faktoren oft nicht zur Regeneration aus. In solchen Fällen ist die lokale Zufuhr von exogenen Wachstumsfaktoren erforderlich. Dies trifft vor allem auch für die Regeneration kritischer Knochendefekte zu. Es konnte gezeigt werden, dass mit Wachstumsfaktoren beladene Polymergerüste diese Defekte nicht nur mechanisch stabilisieren, sondern auch eine kontrollierte Freigabe von Wachstumsfaktoren ermöglichen. Thema dieser Dissertation ist der Einsatz von Seidenfibroin (SF) als Biomaterial für die Herstellung einiger Systeme zur kontrollierten Freigabe von Wachstumsfaktoren.

Gegenstand von **Kapitel I** ist eine Einführung in die Thematik der molekularen und physikalischen Eigenschaften von SF, welche die Freisetzung von Wirkstoffen und die biomedizinische Anwendung der Systeme betreffen. Beschrieben werden zunächst verschiedene Techniken, die für die Herstellung von SF-Freisetzungssystemen entwickelt wurden. Darunter befinden sich auch vergleichsweise milde Prozesse auf der Basis von wässrigen SF-Lösungen, die eine Beladung mit empfindlichen Wirkstoffkandidaten wie therapeutischen Proteinen und Nukleinsäuren ermöglichen. Zur besseren Anschauung wird die Beladung von SF-Systemen mit solchen Therapeutika, deren Interaktion mit der SF-Matrix und ihr Freisetzungsverhalten anhand von Beispielen diskutiert. Zusätzlich werden verschiedene Anwendungsgebiete für SF-Freigabesysteme vorgestellt, die von der Geweberegeneration bis hin zu Freisetzungssystemen für die Anwendung am Auge reichen.

Mikropartikuläre Träger verfügen über ein breites Potential als Plattform für die Freisetzung von Therapeutika. **Kapitel II** beschreibt die Herstellung von sphärischen SF-Partikeln unter milden Herstellungsbedingungen. Deren Fertigung erfolgte mit Hilfe der *laminar jet break-up*-Technologie, bei der eine

wässrige SF-Lösung unter Druck durch eine mit kontrollierter Frequenz und Amplitude pulsierende Düse gepresst wird. Mittels SEM konnte die Morphologie dieser sphärischen Partikel näher bestimmt werden. Je nach Durchmesser der Düse und Art der Behandlung zur Verminderung ihrer Löslichkeit in Wasser besassen die Partikel Durchmesser im Bereich von 101 bis 440 µm. FTIR-Messungen zeigten, dass sowohl deren Behandlung mit Methanol als auch mit Wasserdampf zu einer Zunahme des Gehalts an β-Faltblattstruktur führten, was die Löslichkeit der SF-Partikel in Wasser herabsetzte. Hohe Verkapselungseffizienzen für Salicylsäure oder Propranololhydrochlorid nahe 100% konnten erreicht werden, wenn die SF-Partikel unbehandelt blieben bzw. nur mit Wasserdampf behandelt wurden. Methanolbehandlung führte zu einem Verlust an Wirkstoff und somit zu verminderter Verkapselungseffizienz. Wurde die Konzentration der SF-Lösung für die Herstellung der SF-Partikel von 3% auf 9% erhöht, erfolgte eine weitere Verzögerung der Freisetzung. Die Freisetzungsraten mit Salicylsäure waren geringer als die mit Propranololhydrochlorid. Es bestand jedoch kein Unterschied zwischen den Freisetzungsraten aus Partikeln, die mit Methanol oder mit Wasserdampf behandelt wurden. Aufgrund besonders milder Herstellungsbedingungen, die Vorteile für die Verkapselung von empfindlichen Wirkstoffen erwarten liessen, wurde die Methode auch für die Verkapselung von Insulin-ähnlichem Wachstumsfaktor I (IGF-I) getestet. Wiederum lag die Verkapselungseffizienz nahe 100%, in diesem Fall auch nach Behandlung mit Methanol. Mit Hilfe der Proliferation von MG-63-Zellen wurde festgestellt, dass IGF-I in bioaktiver Form während 7 Wochen kontinuierlich freigesetzt wurde. Diese Resultate regen zu weiteren Forschungsarbeiten über SF-Partikel als Plattform für die kontrollierte Freisetzung von empfindlichen Wirkstoffen an.

Bereits frühere Studien konnten zeigen, dass Mikropartikel geeignete Systeme für die kontrollierte und verzögerte Freigabe von Wachstumsfaktoren darstellen. Die Regeneration von Knochengewebe erfordert jedoch zusätzlich eine osteokonduktive Umgebung, einmal zur gesteigerten Rekrutierung und Adhäsion von Zellen, zum anderen aber auch zur strukturellen Unterstützung von Zellen und neuem Gewebe unmittelbar nach Implantation. Dies erklärt den Wunsch nach geeigneten Polymergerüsten, die nicht nur direkt implantiert oder

für die Zellkultur von Geweben geeignet sind, sondern gleichzeitig auch die Freigabe von Wachstumsfaktoren räumlich und zeitlich kontrollieren. **Kapitel III** beschreibt dazu Herstellung und Testung von porösen SF-Gerüsten, in die mit IGF-I beladene Mikropartikel eingebettet wurden. Eine Behandlung mit Methanol oder Wasserdampf führte zu wasserunlöslichen SF-Gerüsten. Mittels FTIR wurde festgestellt, dass dies zu einem erhöhten Gehalt an β-Faltblattstrukturen führte. SEM Aufnahmen zeigten eine gute Interkonnektivität der Poren. Die Porositäten der SF-Gerüste lagen je nach Behandlung im Bereich von 70% - 90%. Wurde die Behandlung mit Methanol oder Wasserdampf vor der Extraktion des verwendeten porogenen Zuschlags durchgeführt, liess sich die Porenstruktur sehr gut erhalten. Poly(milch-co-glykolsäure) (PLGA) mit Molekulargewichten von 14 und 35 kDA wurden eingesetzt, um mit IGF-I beladene PLGA-Mikropartikel (PLGA MP) herzustellen und deren Freisetzungskinetik zu kontrollieren. Nach Einbettung befanden sich die PLGA MP entweder in den Wänden oder den Kreuzungspunkten der SF-Gerüste. Im Vergleich zu freien PLGA MP führte deren Einbettung zu einer zusätzlichen Kontrolle der Freisetzung. Der Kinetik des hydrolytischen Abbaus der PLGA MP blieb nach Einbettung unverändert. Die unterschiedlichen Molekular-gewichte der PLGA MP ergaben unterschiedliche Freisetzungskinetiken von IGF-I. Ausserdem konnte gezeigt werden, dass Überstände aus Freigabe-untersuchungen von PLGA-Formulierungen mit geringerem Molekulargewicht bioaktives IGF-I enthielten. Unsere Studien rechtfertigen weitere Forschungs-arbeiten mit den hier entwickelten Konstrukten im Hinblick auf Anwendungen im Bereich *tissue engineering*.

Die Entwicklung von Biomaterialien, die die physiologische Bindung von Wachstumsfaktoren an die extrazelluläre Matrix nachahmen, ist eine attraktive Strategie, zur weiteren Entwicklung von Freigabesystemen für Wachstums-faktoren beizutragen. Fibroblasten-Wachstumsfaktor 2 (FGF-2) bindet *in vivo* an das aus sulfatisierten Glykosaminoglykanen bestehende Heparansulfat, das einen Hauptbestandteil der ECM bildet. Aus diesen Gründen wurde in **Kapitel IV** untersucht, ob mit Sulfonsäuregruppen dekorierte SF-Derivate die Funktion der natürlichen ECM zu imitieren vermögen und in der Lage sind, eine lang anhaltende Freigabe dieses Heparin-bindenden Wachstumsfaktors zu

ermöglichen. Die mit 20, 40, 55 und 70 Sulfonsäuregruppen pro SF-Molekül modifizierten SF-Derivate wurden mittels Diazonium-Kupplungsreaktion synthetisiert. Filme eines SF-Derivats, welches mit 70 Sulfonsäuregruppen pro SF-Molekül ausgestattet war, führten im Vergleich zu nativem SF zu einer zweifachen Zunahme der Bindung von FGF-2. Alle SF-Derivate konnten mehr als 99% des gebundenen FGF-2 zurückhalten. Der Schutz der Bioaktivität von FGF-2 war jedoch nur durch SF-Filme mit mindestens 40 Sulfonsäuregruppen pro SF-Molekül gewährleistet. Dies wurde an Hand einer reduzierten metabolischen Aktivität und einer erhöhten Phosphorylierung von extrazellulären Signal-regulierten Kinasen (pERK1/2) in Zellkulturen von humanen mesenchymalen Stammzellen (hMSCs) festgestellt. Die vorliegende Studie beinhaltet einen ersten Schritt in Richtung der Entwicklung eines ECM-imitierenden Biomaterials, welches die nachhaltige, nicht-kovalente Bindung eines Biomoleküls ermöglicht, seine Freisetzung kontrolliert und seine biologische Wirksamkeit schützt.

Zusammenfassend konnte diese Dissertation zeigen, dass SF ein attraktives Biomaterial für die Herstellung von mit Wirkstoff beladenen Freisetzungs-systemen darstellt. Die durchgeführten Experimente tragen zum Stand des Wissens über die Beladung von SF mit empfindlichen Wirkstoffen bei, berücksichtigen deren Wechselwirkungen mit SF und berichten über Möglich-keiten zur kontrollierten Freisetzung aus diesem Material. Die Resultate regen zu weiteren Forschungsarbeiten über SF als Vehikel für die kontrollierte Freisetzung von Therapeutika an, besonders im Hinblick auf den Einsatz von Wachstumsfaktoren für die Regeneration von Geweben *in vitro* und *in vivo*.

CHAPTER I

SILK FIBROIN AS A VEHICLE FOR DRUG DELIVERY APPLICATIONS

Esther Wenk, Hans P. Merkle, Lorenz Meinel

Institute of Pharmaceutical Sciences, ETH Zurich, Wolfgang-Pauli-Strasse 10, CH-8093 Zurich, Switzerland

Abstract

Silk fibroin (SF), a naturally occurring protein polymer, has several unique properties making it a favorable matrix for the incorporation and delivery of a range of therapeutic agents. SF is biocompatible, slowly biodegradable, and endowed with excellent mechanical properties and processability. Novel manufacturing techniques including mild all-aqueous processes have expanded its range of application even to sensitive protein and nucleic acid therapeutics. SF matrices were demonstrated to successfully deliver protein drugs and preserve their potency. Adjustments in SF crystallinity, concentration and structure, the design of the delivery systems as well as the molecular weight and structure of the embedded agents represent important variables when it comes to precisely tailor the release kinetics of SF matrices. Other strategies to fine-tune the release from SF matrices comprise the embedment of drug loaded micro- or nanoparticles or the coating of micro- or nanoparticles with SF films. In conjunction with their potential for controlled drug delivery, SF matrices may also serve as scaffolds in regenerative medicine. For instance, growth factor loaded SF scaffolds were suggested for the tissue engineering of bone and cartilage, as well as for vascular and nerve regeneration devices and wound healing products. Moreover, SF matrices were proposed for oral, transmucosal and ocular drug delivery. This article reviews SF properties and fabrication processes that affect the release from SF drug delivery systems. For illustration, we discuss a variety of examples for the incorporation of drugs into SF systems and their release.

Contents of Chapter I

1. Introduction

The unique properties of silk fibroin (SF) such as slow biodegradation, superior mechanical properties, favorable processability in combination with biocompatibility, have fueled wide interest in this material for a variety of applications, ranging from textiles to biomedical use [1]. In fact, SF is currently emerging as an important protein biomaterial of broad biomedical applicability. This review is particularly directed towards the application of native and modified SF for controlled drug delivery in a wider sense.

Investigations in delivery systems that release a therapeutic compound in a controlled manner have continued to expand in number due to advantages over conventional dosage forms. For many drug applications controlled drug delivery has even become a prerequisite to achieve therapeutic efficacy and/or avoid adverse side effects [2-4]. Beyond more conventional drug formulations, delivery concepts are also largely expanding into the field of regenerative medicine. For instance, the development of microporous scaffolds that are capable to concurrently accommodate cells and release a drug in a controlled fashion will be critical to exploit the therapeutic potential of growth factors in tissue regeneration, and concerns both *in vitro* cell culture and implantation *in vivo*. Controlled drug delivery systems are not only to protect and stabilize the incorporated drug but also help to maintain significant local levels for sustained therapeutic response at low frequency of administration.

Biomaterials for controlled drug delivery systems have to meet several requirements. They need to be biocompatible, biodegradable, non-toxic, cheap and straightforward to process. The ability to fabricate a variety of drug delivery constructs with different morphologies such as films, gels, foams, microparticles and scaffolds contributes to a broad application spectrum of the biomaterial. Mild processing technologies are preferred, and the amount of organic solvents must be minimized or even circumvented when it comes to incorporate sensitive biologics and in order to reduce detrimental and/or toxic effects of residual solvents. Moreover, the release profiles of a delivery system should be adjustable in order to achieve spatiotemporal control of clinically relevant therapeutic concentrations. Especially if a construct is designed to perform a

dual function, e.g., serve as a controlled drug delivery platform and as a scaffold for tissue regeneration, not only its release properties should be considered, but also its load-bearing capacity and elasticity, the porosity of the material and its interconnectivity as well as its propensity for cellular interactions. To set up a suitable package combining all necessary specifications for both, the drug delivery and the implant function, and for a given scenario, poses a substantial challenge with great potential for regenerative tissue repair.

A variety of polymers have been investigated for drug delivery purposes. Synthetic macromolecules including polyesters, polyorthoesters, polyan-hydrides, polyphosphazenes, and polyphosphoesters have found broad application [5]. Natural polymers including alginates, chitosan, cellulose, collagen, gelatin and elastin remain attractive due to their biocompatibility and biodegradability, their similarity to biological macromolecules and the potential for chemical or physical modification [6, 7]. However, there remains a need for biomaterials that can be highly controlled in terms of composition and sequence, structure and architecture, mechanical properties and function. To address these requirements, the exploration of SF as a biomaterial for controlled drug delivery has widely expanded over the last few years. This article will review recent developments in this area of research.

2. Silk properties

Drug loading, release kinetics and physico-chemical stability of a drug delivery system are features, which can be tailored by changing the properties of its matrix. Here we review SF properties that we expect to affect the controlled release of a drug from a SF based delivery system and its application.

2.1. Molecular properties of silk

SF is a natural polymer produced by a variety of insects and spiders. It is, therefore, subject to a wide diversity in sequence, structure and properties. The best characterized silks are the cocoon silk from the domesticated silkworm *Bombyx mori* and the dragline silk from the spider *Nephila clavipes* [8].

Silk from *B. mori* is made of two structural proteins, the fibroin heavy chain (~ 325 kDa) and light chain (~ 25 kDa). Glue-like proteins named sericins (20 kDa to 310 kDa) hold the chains together. Sericins have been associated with immune response, but due to their higher hydrophilicity as compared to fibroin they can be easily removed by boiling silk in alkaline solutions [1, 9]. The heavy chain of SF contains alternating hydrophobic and hydrophilic blocks similar to those seen in amphiphilic block co-polymers. The hydrophobic blocks consist of highly conserved sequence repeats of GAGAGS and less conserved repeats of GAGAGX (where X is either V or Y) that make up the crystalline regions of SF by folding into intermolecular β-sheets. The hydrophilic part of the core is non-repetitive and very short compared to the size of the hydrophobic repeats [9, 10].

Due to its amino acid sequence, SF provides opportunities for chemical modification. Amines, alcohols, phenols, carboxyl groups, and thiols have been explored as potentially reactive side groups for the chemical modification of SF. For instance, carboxylic acid side groups from aspartic and glutamic acids, representing 2-3% of the total amino acid content of SF, have been derivatized with primary amines of peptides such as the RGD sequence, with the aim to improve cell adhesion [11]. To expand the range of functionalization, tyrosine residues, representing 10% of the total amino acid content of SF, were modified with a variety of functional groups [12-14]. Such modifications led to changes in SF hydrophilicity [14, 15] and charge and are, therefore, expected to alter the interaction between drug molecules and SF. It is envisioned that by introducing distinct functional groups into SF and by varying the degree of functionalization per SF molecule, a variety of drugs in different amounts can be loaded and released with distinct kinetics, providing a wide range of adjustable drug release systems. In addition to drug delivery contributions, functionalization may also promote cell adhesion and spreading or address cellular signaling pathways through specific cell-matrix interactions.

2.2. Physical properties of SF

2.2.1. Molecular weight

The molecular weight of a polymer strongly influences its mechanical properties and biodegradability, and, therefore, its qualification for drug delivery. For instance, because of the variety of available molecular weights affecting its biodegradation and, therefore, its drug release kinetics, customized polyesters such as poly(lactide-co-glycolide) (PLGA) of various lactide:glycolide ratios have been widely used for drug delivery applications [16-18]. Natural silks exhibit large molecular weights. Lower molecular weights of SF can be obtained by processing silk. For instance, prolonged boiling of silk cocoons in Na_2CO_3 solutions, a common method to remove sericin from fibroin, was shown to cause extensive hydrolytic degradation of the SF protein [19]. However, this method is not well documented and controlled, and might produce a wide molecular weight distribution. SF with diverse molecular weights may be also obtained by adding NaOH to aqueous SF solutions at different processing temperatures [20] or by enzymatic degradation. A better controlled approach to produce SF analogues with distinct molecular weights is genetic engineering [21]. It has to be considered that SF analogues with much lower molecular weights may have compromised mechanical properties. Thus, the application of such analogues to load-bearing body sites must be further explored. In summary, variations in the processing of SF or its genetic engineering can produce SF with different molecular weights, which may influence bulk viscosity, further processing into drug delivery systems, bulk crystallinity, degradation rates and, thereby, the release kinetics of embedded drugs [22, 23].

2.2.2. Crystallinity and water insolubility

The hydrophobic blocks of SF make up the crystalline regions of SF by their capacity to form intermolecular β-sheets. Different treatments dehydrate and destabilize the random coil and/or the unstable silk I state of SF, leading to silk II (predominant) conformation, which is more stable and characterized by an increase in β-sheet content. The most common method to enrich SF in β-

sheet structure and thus induce water insolubility is a treatment with methanol [24-27]. Additionally, high temperatures [28], a pH close to the isoelectric point of SF (around 4), the use of salts [29-32] and shear-force [33, 34] were shown to increase its β-sheet content. However, when sensitive molecules such as growth factors need to be incorporated into SF, milder conditions to evoke β-sheets are preferred. Exposure to water vapor has been demonstrated to be such a mild alternative to induce water insolubility [35, 36]. Moreover, slow freezing rates, being a consequence of higher freezing temperatures (above -20°C), resulted in an increase in β-sheet based crystallinity [37, 38].

Crystallinity is the basis for the superior mechanical strength of SF. Nevertheless, an excessive increase in crystallinity reduces its flexibility and leads to more brittle materials. Annealing in water or water vapor treatments were shown to induce less β-sheet structure and retain better elasticity as compared to methanol treatments [24, 39]. Conformational analysis of SF films and nanofibers with 13C-MAS NMR demonstrated the percentage of silk II after water vapor treatment (30% - 47%) to be lower as compared to a treatment with methanol (74%) [24, 36]. Recently, a time dependent increase in β-sheet structure was observed when treating SF microparticles with saturated NaCl solution, obtaining β-sheet contents of about 34%, 51% and 67% when treating for 1 h, 4 h and 15 h, respectively. The β-sheet content of SF microparticles treated with methanol for 30 min was analyzed to be 58%, comparable to longer treatments with NaCl [32]. Additionally, inclusion of elastin-like domains in SF could reduce crystallinity [21, 40]. Alterations in both crystallinity and hydrophobicity offer options to affect the interaction between drug molecules and SF. Moreover, a change in crystallinity influences the degradation rate of SF (see below), which could be an attractive approach towards drug delivery systems with distinct release kinetics.

2.2.3. Solubility

Crystalline SF is insoluble in most solvents that are widely used to dissolve polymers typical for drug delivery applications, as well as in water. Commonly applied to dissolve SF are highly concentrated salt solutions of lithium bromide,

lithium thiocyanate, calcium thiocyanate or calcium chloride. [9]. Such electrolyte solutions are able to disrupt the hydrogen bonds that stabilize β-sheets [41]. After solubilization, dialysis against water or buffers is performed to remove the electrolytes. The resulting aqueous SF solutions can then be freeze-dried, followed by dissolution of the dry SF in hexafluoroisopropanol (HFIP). Such solutions may be further processed into the desired drug delivery device [42-44]. However, HFIP is an expensive and toxic solvent. Moreover, in contact with sensitive biologicals, e.g. growth factors, HFIP may exert detrimental effects on protein folding and biological potency. The alternative use of aqueous SF solutions offers more gentle processing conditions to fabricate drug delivery systems for such biologicals. Interestingly, the processing of aqueous instead of HFIP solutions of SF offers several advantages: (i) the option to load SF based constructs with drugs, porogens or microparticles that are insoluble in aqueous solutions. In fact, we recently introduced an aqueous process to fabricate microporous SF scaffolds by prior loading with paraffin spheres as elutable porogen, as well as with PLGA microparticles to release a growth factor [18]. Further advantages of processing aqueous instead of HFIP solutions of SF are: (ii) the ease of sterilization by filtration and (iii) the absence of residual solvents in the fabricated matrix.

A common problem with the processing of aqueous SF solutions still exists, namely the premature reprecipitation into its water insoluble, β-sheet enriched silk II state. Especially highly concentrated SF solutions tend to aggregate in a matter of hours to days due to inter- and intramolecular interactions of the protein. Various approaches that prevent the formation of β-sheet structure were studied in order to maintain higher SF concentrations in a soluble state. For instance, phosphorylation of genetically engineered silk has been shown to increase the overall aqueous solubility of the protein through a combination of steric hindrance and charge [45]. Recently, the modification of the tyrosine residues in SF by a diazonium coupling reaction with 4-sulfanilic acid led to a sulfonated SF derivative that demonstrated to inhibit spontaneous protein aggregation or gelation for more than one year, whereas unmodified SF was found to gel within one month [14]. Nevertheless, the sulfonated SF derivative could still transform into a β-sheet enriched structure when treated

with methanol. Periodic interruption of a silk-like polymer (SLP) featuring (GAGAS)$_n$ blocks with the elastin-like sequence (GVGVP)$_n$ to produce genetically engineered silk-elastin-like polymers (SELPs) was also found to increase the solubility while decreasing the β-sheet based crystallinity [40]. The possibility to control the solubility of SF not only allows for longer storage times for SF solutions but also for an increase in SF concentration without aggregation. As a consequence thereof, it is possible to fabricate SF matrices with different characteristics than matrices prepared from solutions with lower SF concentration, e.g., matrices with denser structures which may influence release kinetics.

2.2.4. Stability

The stability of a polymer is an important feature for the storage of a drug delivery device. Aggregation and gelation of SF solutions through enrichment in β-sheet content during storage has been discussed above. Untreated SF matrices are low in β-sheet content, remain hygroscopic and thus highly sensitive to humidity. Incubation at high humidity has been shown to change the conformational state of SF, leading to increased β-sheet contents [36, 46]. Nevertheless, no systematic investigations exist on the storage stability of SF matrices.

SF displays an exceptional thermal stability, being virtually unaffected by temperatures up to 140 °C. The glass transition temperature T_g of proteins is considered to be a major determinant of protein self-assembly. Silk taken from the posterior part of the middle division of the silk gland of the silkworm *B. mori* and dry SF films demonstrated a T_g of approximately 175 °C, above which there is free molecular movement to transform into the stable β-sheet conformation, showing stability up to around 250 °C [47, 48]. The T_g of frozen SF solution was reported to be in the range of about -34 to -20 °C [38]. The higher the pre-freezing temperature above the glass transition, the longer the time needed for ice crystals to form and grow in size. This affects the pore size within SF matrices, leading to bigger pores [49], as well as an increase in crystallinity [37, 38].

2.2.5. Swelling properties

The release of drugs from matrices such as hydrogels depends partially on the degree of swelling, which in turn depends on the ionization of the network, its degree of crosslinking and its hydrophilic/hydrophobic balance [50]. Changes in polymer compositions can influence the degree of swelling. For instance, an increase in the length of elastin repeating units in the backbone of SELP hydrogels, while keeping the length of silk repeating units constant, can result in an increased degree of swelling due to a decrease in cross-linking density [51]. This can potentially increase the cumulative amount and rate of drug release. The swelling ratio of SF scaffolds has also been shown to decrease with an increase in SF concentration. Blending of SF with other materials such as chitosan [52], hyaluronic acid [53] and chitosan [54] led to increased swelling when compared with plain SF.

2.2.6. Mechanical properties

Many polymers including PLGA and collagen lack sufficient mechanical strength for load-bearing purposes [55, 56]. Enhanced mechanical strength, however, is an important issue when a device is not only used for the delivery of a drug but also as a scaffold with load-bearing function, as frequently needed in bone repair. For instance, the physical properties of collagen are rather limited unless crosslinked. However, crosslinking reactions may have adverse effects on adjacent native tissue [56] such as cellular toxicity and inflammatory responses [57-59]. In contrast, owing to its robust β-sheet conformation, crystalline SF exhibits outstanding mechanical properties and does not need to be crosslinked. Among natural and synthetic fibers SF is unique in terms of mechanical strength and resilience [60]. The compressive strength and modulus of SF matrices was reported to increase with increasing SF concentration, decreasing pore size and more uniform pore distribution [60]. In general, the mechanical characteristics of SF scaffolds were superior as compared to other matrices including scaffolds prepared from collagen [61], and chitosan [49, 61].

2.2.7. Degradation and biodegradation

The biodegradation rate of a drug delivery system for tissue regeneration should be adjustable to kinetically match the evolving environment during healing and regeneration [62]. The degradation of many commonly used polymers in drug delivery is fast [63], typically in the range of weeks or months as with many poly(lactide-co-glycolide) (PLGA) copolymers. This is a disadvantage when the integrity of a load-bearing system has to be preserved. Moreover, by hydrolytic degradation some polymers such as the widely used PLGA generate acidic moieties, resulting in a local decrease in pH [64], which may cause an inflammatory response both in the implant and the adjacent tissue [65] and initiate acid catalyzed protein degradation [66].

The hydrolytic degradation of SF has been shown to be slow. In fact, we demonstrated in a recent study that the hydrolytic degradation of water vapor treated SF scaffolds *in vitro* is minor, with only about 4% mass loss within 7 weeks [18]. Being a protein, biodegradation of SF predominantly occurs through proteolytic enzymes, with non-toxic degradation products and unproblematic metabolization *in vivo*. The implantation site, the mechanical environment and the size of the drug delivery device are likely to affect the degradation rate *in vivo*. The biodegradation of SF has been described to directly relate to its β-sheet content. For instance, the annealing of SF films with water is known to induce conformational transition. When incubated in the presence of a protease, the mass-loss of such water-annealed SF films, typically having a lower β-sheet content due to the slow annealing process, was more pronounced than that of methanol-treated films showing predominantly silk II conformation [39]. Furthermore, SF scaffolds have been prepared by adding NaCl particles to either SF aqueous solutions (all-aqueous-derived) or to SF dissolved in HFIP (HFIP-derived) to induce conformational transition [67]. After fabrication the NaCl particles were leached out in water. The biodegradation of such prepared 3D porous scaffolds was studied in rats. Most all-aqueous-derived scaffolds were completely degraded after 6 months, whereas HFIP-derived scaffolds still existed showing varying degrees of biodegradation. Total β-sheet content was not significantly different between all-aqueous- and HFIP-derived scaffolds, but

the size, distribution and nature of the crystals may vary, contributing to the different biodegradation rates, along with different structural, morphological and surface characteristics. Scaffolds prepared from solutions of higher SF concentration degraded more slowly than those made from solutions of lower concentrations. The experiments demonstrate that short-term drug delivery systems can be best matched by systems prepared by an all-aqueous process or water-annealing due to its faster degradation time while long-term delivery devices can be better met by slower degrading HFIP-derived systems or methanol-treated devices. On the other hand, previous reports on SELPs have shown that their *in vivo* degradation can be controlled by varying the composition and sequence of the polymers [68]. Using a protein-engineering approach, biodegradation rates in response to tissue-specific enzymes may be tailored by incorporating protease specific cleavage sites into SF.

2.3. Biocompatibility

The foreign body response following implantation of SF *in vivo* has been described to be comparable to or even less than the most popular materials in use today as biomaterials [1, 69, 70]. Throughout a one-year implantation study in rats, all-aqueous- and HFIP-derived scaffolds were well tolerated by the host animals, and the host immune response to the implanted scaffolds was low and local [67], consistent with another study with SF films [69].

3. Fabrication and sterilization of silk-based drug delivery devices

3.1. Fabrication

The possibility to shape a polymer into various morphologies makes it an attractive material for controlled drug delivery applications. For SF a wide range of drug delivering platforms have been reported, including hydrogels, films, coatings, microparticles, nanoparticles, conduits, scaffolds and tablets. Diverse drug molecules were incorporated therein ranging from low molecular model compounds such as propranolol hydrochloride and salicylic acid, large

molecular model compounds like horseradish peroxidase and lysozyme, up to biologicals such as various growth factors.

Drug delivery devices made of SF may be fabricated by a variety of techniques. Their choice depends on mode of application, processability, desired release kinetics and stability of the drug. Fabrication may involve exposure of SF to heat, shear forces, pH extremes, organic solvents, freezing and drying. All of them might cause alterations in SF such as changes in β-sheet content (see above). Such changes and the influence of the fabrication technology on porosity and surface area of the device may affect its drug release kinetics. When incorporating sensitive biologicals such as growth factors, organic solvents and high temperature must be avoided to maintain their biologic potency [71]. Here we will discuss various methods used for the fabrication of SF drug delivery systems.

3.1.1. Film casting

Because they are straightforward to prepare SF films are attractive systems to study proof-of-principles [14, 72, 73]. They may be fabricated by casting solutions of SF in water or in HFIP on plates or into molds. The SF films are dried and then treated with either methanol or exposed to water vapor in order to induce water insolubility. SF films may be suitable in order to test the influence of the fabrication process on the stability of the loaded drug or the interaction of the drug with SF. However, it has to be considered that 2D films may show different characteristics than 3D systems. For instance, SF films may exhibit different release kinetics than 3D matrices. Folding and winding of 2D films open access to 3D structures.

3.1.2. Gelation

Due to the fact that gelation of SF induces an increase in β-sheet content, SF hydrogels do not need to be post-treated with any solvent to induce water insolubility [31]. With SF, having a pI of about 4.2, hydrogels were prepared by lowering the pH of a SF solution in the presence of the drug with citric acid to

pH 4 to induce gelation [74, 75]. This pH may be acceptable for certain drugs, but could have detrimental effects on others. Blending of SF with poly(ethylene)oxide (PEO) [31] or poloxamer [76] induced gelation through an increase in β-sheet content at around pH 7 due to the dehydration of SF, and may, therefore, be beneficial for the incorporation of drugs, which are sensitive to low pH values. Other methods that were used to prepare SF hydrogels, including increases in temperature and SF content, led to enhanced interactions among SF chains [31, 74]. Addition of Ca^{2+} decreased the repulsion among SF molecules and resulted in a stronger potential for the formation of β-sheets [31]. Recently, rapid formation of SF hydrogels using ultrasonication was reported [77], allowing the incorporation of drugs right after ultrasonication and just before gelation, thus avoiding detrimental effects. Through different fabrication conditions, the pore size of SF hydrogels may be controlled, which influences the permeation of a drug through the matrix. For instance, increases in SF concentration and gelation temperature, and a decrease in Ca^{2+} concentrations were shown to result in smaller pores in freeze-dried hydrogels [31].

SELPs (see section 2.2.3.) are liquid at room temperature. Mixing of the drug with the solution can be performed on site and under mild conditions, and the mix then directly injected into the application site. SELPs irreversibly self-assemble under physiological conditions depending on the number of silk-like blocks in the repeat unit [78, 79]. Such *in situ* gel-forming polymers offer the advantage that gelation occurs without the need of harsh preparation conditions. Therefore, changes to the polymer or to any drug incorporated in the polymer solution can be minimized.

3.1.3. Freeze-drying

A common method that is frequently applied for the preparation of SF matrices is the freeze-drying of aqueous SF solutions after shaping the desired drug delivery system using an appropriate mold. Freeze-drying is a mild fabrication process and leads to porous structures which largely affect drug release kinetics. Previous studies reported on the influence of different freezing temperatures prior to lyophilization on the pore size in SF matrices [49, 80].

Lowering the temperature resulted in smaller, highly interconnected pores and high porosity, apparently due to the shortening of time needed for the growth of ice crystals, whereas higher freezing temperatures led to larger pores and lower porosity. Moreover, higher SF concentration resulted in smaller pores and less interconnectivity [49, 80]. Slow freezing rates, being a consequence of higher freezing temperature (above -20°C), resulted in an increase in β-sheet content [37, 38] and may be expected to circumvent the use of other methods to induce water insolubility.

Better control of pore formation in SF matrices was achieved through incorporation of particulates such as paraffin spheres or salt crystals of distinct size as porogens that can be eluted from the device after fabrication [81-83], e.g., using hexane for paraffin spheres or water for NaCl crystals, respectively. In addition to their use as porogen, the commonly used NaCl crystals have been shown to induce a conformational transition from random coil to β-sheet [49, 60], making methanol treatments (see 2.2.2.) unnecessary. However, high salt concentrations may have a negative impact on the integrity and potency of biologicals such as growth factors. Additionally, the long periods of soaking in water necessary to leach out NaCl crystals completely, may lead to a loss of loaded drug.

3.1.4. Electrospinning

In electrospinning, a strong electrical field is applied between a grounded target and a polymer solution that is pumped from a storage chamber through a small capillary orifice. When the voltage reaches a critical value, the charge overcomes the surface tension of the deformed drop of the polymer solution formed at the capillary orifice, and a jet is produced. Evaporation of the solvent occurs, and the dry fibers accumulate on the surface of the grounded target forming a nonwoven mesh [84-86]. The process has become popular in tissue engineering as the structures generated are formed by nanoscale fibers that mimic the structure of the extracellular matrix (ECM). The physiological ECM acts as a local storage for growth factors, releases them on demand, prevents their enzymatic degradation, and, in some cases, enhances binding to cell

surface receptors [87]. Using electrospinning, various drug delivery devices could be produced through the control of fiber diameter and porosity of fiber mats by adjustment of solution properties and fabrication parameters such as applied voltage, viscosity, composition and feeding rate of the polymer solution [88, 89]. The large specific surface area and the short diffusion path typical for the produced nanofibers are expected to result in fast degradation and release as compared to matrices prepared with other fabrication methods. Various studies have demonstrated the feasibility of preparing SF matrices through electro-spinning by using either aqueous SF solutions [89-92] or solutions of SF dissolved in HFIP [93, 94]. Aqueous SF solutions are commonly mixed with PEO in order to increase the viscosity of the solution and to obtain a suitable surface tension to generate stable, continuous spinning [84, 95]. Our laboratory has recently developed a new approach that circumvents the use of PEO by preparing concentrated SF solutions with high viscosity (C. Li et al., unpublished data). Such concentrated SF solutions were obtained without gel formation by controlling the pH of the solution. In contrast to SF/PEO fibers, pure SF fibers do not need an additional step for the removal of PEO before application, which prevents a possible loss of incorporated drug. The presence of PEO was shown to inhibit initial adhesion of human mesenchymal stem cells (hMSCs) to electrospun SF/PEO mats [96]. On the other hand, SF/PEO mats containing growth factor were successfully used as a bioactive dressing for wound healing using human dermal fibroblasts (HDF) without prior PEO removal [97]. A conformational transition leading to a higher β-sheet content and water insolubility of electrospun SF fibers can be induced by either methanol treatment, exposure to water vapor, or by increased voltage and SF concentration [98]. Water insolubility without any post-treatment can be reached by the addition of genipin, an excellent natural cross-linker of very low toxicity, to SF solutions, resulting in the production of small-diameter fibers [99]. The structural rearrangement was assumed to be the consequence of both the addition of genipin and the processing conditions.

The opportunities of drug loaded electrospun fibers are particularly interesting. For drug delivery purposes, aqueous SF solutions may be directly loaded with drugs, either by dissolution or colloidal dispersion, and then

electrospun [89, 97]. This appears to be particularly beneficial for the incorporation of growth factors. We have experimental evidence that electrospun SF fibers protect the growth factors from denaturation as shown by biological cell activity [89, 97]. This may be explained by the nearly instantaneous immobilization of the growth factors in the electrospun fibers. We generally expect the presence of SF to form a proteinacious environment and protect the notoriously delicate nature of growth factors during formulation and on the shelf.

3.1.5. Processing microparticles: laminar jet break-up, electrospinning, spray-drying, self-assembling

The fabrication of spheres or microparticles loaded with drug is another option to formulate drug delivery devices with SF. Recently we prepared SF spheres by a laminar jet break-up induced by a nozzle vibrating at controlled frequency and amplitude [46], an approach that was previously used mainly for the preparation of alginate beads, e.g., for cell immobilization [100-102]. The advantage of this process is its simplicity and scaleability. The fabrication of SF spheres was carried out under mild conditions, using aqueous SF solutions and working at room temperature or below, an advantage for the encapsulation of sensitive biologicals. Within a given range, size and morphology of the spheres may be tuned by varying the diameter of the nozzle, the concentration of the SF solution and the final treatment to induce water insolubility. The use of organic solvents could be fully circumvented by using aqueous SF solutions and inducing water insolubility by exposing the spheres to water vapor. Typically, close to 100% encapsulation efficiencies could be achieved with both low and high molecular weight compounds [46].

Electrospinning may be another approach for the fabrication of micro- or nanoparticles. A reduction in the electrospinning voltage and/or SF concentration or viscosity resulted in a string-of-pearls structure or even beads instead of fibers [98, 103, 104]. Thus the fabrication of drug loaded SF nano- or microparticles by adjusting the parameters during electrospinning is assumed to

be possible. The produced particles may be collected in pre-cooled methanol or frozen in liquid nitrogen.

Another method for the fabrication of SF spheres is spray-drying of an aqueous SF solution [105]. Too rapid drying of the SF microparticles impedes the transition into β-sheet conformation. Therefore, spray-dried SF microparticles need to be further treated, e.g., with water vapor to achieve water insolubility. Nevertheless, it may be envisaged that the high inlet air temperature common for spray-drying could be detrimental to encapsulated biologicals.

Self-assembling of SF in aqueous solution induced at specific ethanol concentrations and freezing temperature is another option to obtain SF microparticles [106]. As ethanol is a poor solvent for SF, its presence prompts molecular interactions between the SF chains. The preparation of a water-in-oil emulsion is another approach to form microspheres. This method was accomplished with SF derived from cocoons of *B. mori* and genetically engineered spider-silk protein using paraffin and toluene, respectively, as oil phase [107, 108]. Because of its amphiphilic nature, the protein adsorbs to oil/water interfaces and assembles to form a film at the surface of the water droplet, encapsulating its content. Through adjustment of the shear rate during emulsification, the size of the microcapsules may be conveniently controlled. Moreover, assembly of engineered spider silk protein was provoked by the salting-out effect. The formation of microparticles was induced by high concentrations of potassium phosphate [109].

Another method to fabricate SF microparticles was developed using lipid vesicles as templates [32]. The lipid was subsequently removed by methanol or sodium chloride treatments, which resulted in SF microparticles that were enriched in β-sheet structure.

3.1.6. Layer-by-layer deposition

The stepwise deposition of nanoscale coatings onto surfaces - also coined as layer-by-layer deposition - has gained much interest in surface engineering [110, 111]. Unlike classical layer-by-layer deposition, which is based on the

alternate deposition of oppositely charged polyelectrolytes onto surfaces, the primary driving force for the surface assembly of SF is by hydrophobic interactions, while electrostatic interactions play a secondary role [112]. The feasibility to coat hydrophobic and hydrophilic materials, and the possibility to control the composition and the thickness of the films by the number of deposited SF layers, SF concentration, salt concentration in the dipping solution, and rinsing method makes the layer-by-layer deposition of SF attractive for controlled drug release applications. Drug molecules may be incorporated either in or between layers. A virtually unlimited range of shapes and materials could be coated which opens diverse opportunities for tunable systems to control drug release. The β-sheet content of the coatings could be controlled by methanol treatments, but also by drying with nitrogen gas [112], which may be a favorable approach when incorporating sensitive biologicals.

A special type of layer-by-layer deposition of SF is the direct ink writing of aqueous SF solutions [113]. The deposition of the ink in a layer-by-layer fashion was through a fine nozzle to produce a 3D array of silk fibers of 5 μm in diameter. The extruded fibers could be enriched in β-sheet structure when deposited in a methanol-rich reservoir, and retained a pore structure necessary for solute exchange. Direct ink writing with SF solutions charged with drug loadings at different concentrations may be a tool to fabricate drug delivery systems featuring complex drug deposition gradients for spatiotemporal control of drug release. Obviously, as ink writing avoids harsh fabrication conditions such as high temperatures, processing of sensitive biologicals could be an interesting option.

3.1.7. Direct compression

For a wide range of drugs, tablets are the preferred dosage form for oral drug delivery [114]. The advantage of direct compression of tablets is the simplicity of the process, the avoidance of heat and contact of the drug molecules with solvents and, therefore, the loss of activity and leaching of the drug. By direct compression SF tablets have been prepared using SF powder without any excipients [115], excluding any interference with the incorporated

drug. Nevertheless, at this time this is the only reference to the direct compression of SF.

3.1.8. Film coating

The spray coating technology is extensively used in order to generate film-coated tablets. The coating is generally applied for reasons such as taste masking, to prolong release, avoid irritation upon ingestion, prevent inactivation of the drug, and improve drug stability and patient compliance. However, so far spray coating of solid dosage forms has not yet been reported for SF.

3.2. Sterilization

Sterility is a critical issue for many synthetic polymers to be used for implantation or cell culture purposes. Because of their often low glass transition temperature, the formulation of implantable delivery systems or 3D cell culture scaffolds thereof may rely on aseptic processing whereas sterilization by autoclaving is rare or might be unfeasible. This is in large contrast to crystalline SF, which can be sterilized by autoclaving [83, 116, 117] without major deformation, loss of porosity or damage in mechanical strength. A recent study suggested that when autoclaving aqueous SF solutions SF even retained important features of its original solution-state structure and its capability for structural transition to a β-sheet state in forming a gel. The study showed that the time necessary for gelation induced by sonication of the SF solution did not significantly change after autoclaving. [77]. However, sterilization by autoclaving or heat may have detrimental effects on incorporated labile drugs and certainly on proteins. In this case, drugs have to be aseptically incorporated after the sterilization process, or other sterilization methods have to be chosen. As alternative, γ-irradiation was explored for the sterilization of SF matrices. However, γ-irradiation may compromise SF structure causing a decrease of its average molecular size and crystallinity, loss of tensile strength and reduced thermal stability due to physicochemical degradation [118, 119]. Another alternative for the sterilization of SF matrices is the use of 70% ethanol [89, 120]. Again, changes in crystallinity [121] as well as leaching of drug and loss

of activity has to be considered. All in all, the influence of different sterilization methods on SF properties still has yet to be studied systematically.

4. Silk-based drug delivery strategies and systems

4.1. Drug incorporation

The most common and straightforward way to channel drugs into the fabrication of SF delivery systems is by dissolving or mixing them directly in the SF solution before processing. Such protocols were suggested for the preparation of drug loaded SF hydrogels [74, 75], films [72, 73], scaffolds [82, 89] and microparticles [32, 46, 108]. The challenge of this method is to ensure that there is no negative impact of the fabrication process on the integrity and biological potency of the drug. Alternatively, the drug may be incorporated post-fabrication, such as by adsorption [42, 44] or covalent coupling [120, 122, 123] of the drug to the pre-fabricated SF system. The incorporation of drug loaded nano- or microparticles either during the fabrication process or into a pre-fabricated device are further options [18, 124] (Fig. 1). A modular system, onto which the drug may be bound or conjugated just prior to implantation, would be advantageous. This would allow the SF matrix to be prepared in advance and stored stably under appropriate conditions for extended periods of times. The drug would be introduced just prior to use such that its stability and biological potency would be best maintained. Moreover, the drug would not be exposed to harsh fabrication conditions or leach out during fabrication. Nevertheless, the capacity of a drug to bind to or form a conjugate with a SF matrix depends on its physicochemical and chemical properties and could be rather limited. For instance, owing to the mainly negatively charged side chains of the hydrophilic spacers of its heavy chain [125, 126], SF has a pI of about 4.2. Therefore, it is more likely to interact with positively than with negatively charged drugs at a pH above 4.2 [46, 127]. On the other hand, hydrophobic interactions were shown to be the main cause of interactions between SF and drugs with hydrophobic moieties [46], due to the hydrophobic blocks in the heavy chain of SF. In order to improve the capacity of a drug to bind to a SF matrix and to enhance drug loading, several approaches have been suggested. For instance,
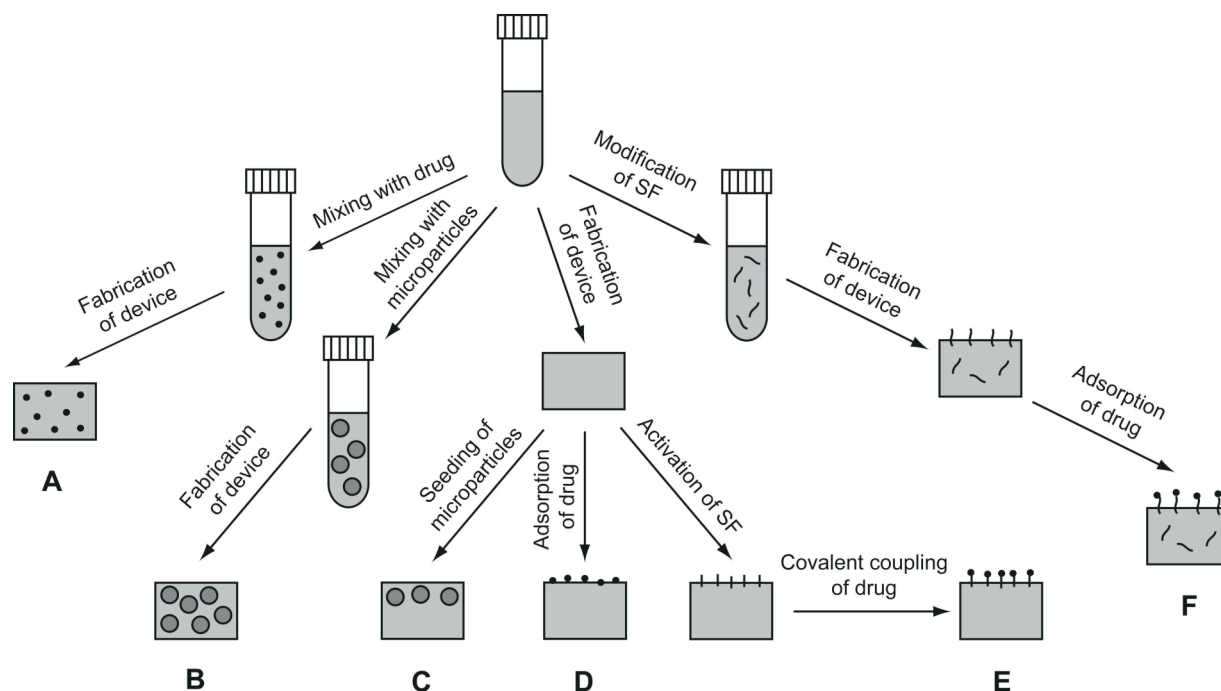
Fig. 1. *SF drug delivery systems prepared using different drug molecule incorporation strategies. Physical incorporation of the drug molecule (A), or embedment of drug loaded microparticles (B) by mixing with the SF solution prior to fabrication of the SF device. Seeding of drug loaded microparticles (C), adsorption (D), or covalent coupling of the drug (E) post fabrication of the SF device. Adsorption of the drug to the SF device after modification of SF in solution (F).*

drug binding to SF matrices may be improved by SF modifications. We decorated SF with varying numbers of sulfonic acid moieties and were able to adjust the amount of non-covalently bound FGF-2 to SF films [15]. We demonstrated that films of the SF derivative decorated with approximately 70 sulfonic acid groups per SF molecule resulted in a two-fold increase in FGF-2 binding as compared to native SF. Both sustained delivery and preservation of FGF-2 potency could be demonstrated with such SF derivatives. Another study describes the improvement of drug loading of SF microparticles. Freeze-thaw cycles were used to enhance drug loading approximately two-fold when preparing SF microparticles by using lipid vesicles as templates, probably due to a better mix between SF and the drug [32]. In order to enhance the drug loading

of SF matrices highly loaded microparticles can be embedded. We recently embedded insulin-like growth factor I (IGF-I) loaded PLGA microparticles [18], and rhBMP-2 and IGF-I loaded SF microparticles [124] into SF scaffolds. In addition to the adjustable loading of the scaffolds, the drug was protected during the fabrication process of the scaffolds. The incorporation of pre-fabricated drug-loaded nanoparticles into electrospun SF mats during electrospinning may be also envisioned. Again, this approach has the potential to protect the drug against harsh processing parameters, and control its release kinetics not only by retention in the SF nanofiber itself, but also by the composition of the nanoparticles. The incorporation of unloaded hydroxyapatite nanoparticles into SF nanofibers upon electrospinning has been previously reported and shown promise as an osteoinductive biomaterial [89].

The covalent coupling of drugs to the SF matrix can sustain its release compared to simple adsorption. However, harsh coupling conditions may result in a loss of activity and drug. Moreover, additional washing steps have to be included in the process in order to remove side products and additives.

Drug loading can be determined either directly by dissolution of the drug delivery device, or indirectly by measuring the drug that was not incorporated. Dissolution is preferably performed prior to inducing water insolubility. For instance, untreated SF spheres were dissolved in water to determine the content of encapsulated salicylic acid, propranolol hydrochloride and IGF-I [46]. On the other hand, the content of methanol treated and thus water insoluble SF spheres with increased β-sheet structure was determined indirectly by measuring the drug content of the untreated SF spheres and the amount of the drug that leached out during methanol treatment [46]. Methanol treated scaffolds were dissolved in 9M LiBr at 37°C to determine ^{125}I-BMP-2 loading [44]. Moreover, the solubilization of methanol and NaCl treated SF microparticles was performed using HFIP in order to determine HRP loading [32]. However, the adverse potential of LiBr and HFIP has to be considered, which might compromise the potency of protein therapeutics and result in incomplete determination of drug content. The actual bioactivity of a released enzyme or growth factor may be tested with an enzymatic reaction or with a cellular assay.

4.3. Control of drug release

Suitable drug release kinetics is often a prerequisite to trigger physiological signaling or cope with given pathological conditions. In this section we will discuss the release of a variety of drugs from SF drug delivery devices and how their release kinetics may be controlled.

4.3.1. Release of model drugs from SF matrices

The release kinetics of SF matrices were frequently studied using model drugs. Generally, release was controlled by both the characteristics of the incorporated drug and those of the polymer matrix. In terms of the incorporated drugs, release kinetics were shown to depend on the molecular weight. As demonstrated for dextrans, an increase in molecular weight resulted in reduced release rates [72]. Furthermore, drug release depended on its interaction with SF. For instance, we recently demonstrated that the release of propranolol hydrochloride from SF spheres was more sustained as compared to salicylic acid [46]. This was explained by the electrostatic interaction between the positively charged propranonol ($pK_a = 9.5$) and the negatively charged SF ($pI = 4.2$) at the pH of the release study (pH 7.4). In contrast, repulsive forces were concluded to govern the interaction between salicylic acid ($pK_a = 3.0$) and SF, leading to enhanced release. Additionally, dissimilar hydrophobicities were further assumed to explain the differences in interaction and release of the two drug models in this study.

As to the SF matrix, higher SF concentrations resulted in lower burst and release rates. This was not only demonstrated with propranolol hydrochloride and salicylic acid encapsulated in SF spheres [46], but also with theophylline in SF tablets [75, 115] and buprenorphine in hydrogels [74], possibly due to the more closely packed structure, decreased swelling and mean pore size, and/or the longer diffusional pathways. Further factors to influence the release kinetics were surface morphology, lipid content, distribution of the drug in the SF matrix, and crystallinity induced by methanol or NaCl treatment, as exemplified by the release of HRP from SF microparticles [32]. The microparticles were prepared using phospholipid vesicles as templates. Further treatments with

methanol or NaCl were to remove the phospholipids as far as possible and induce SF assembly through β-sheet formation. NaCl treatment resulted in SF microparticles with a phospholipid content of about 17%. In contrast, methanol treatment resulted in a rough surface full of defects, providing channels to enhance removal of the lipid contents allowing only 1% residual phospholipids. Depending on the concentration of residual phospholipids either multilamellar (high phospholipid content) or unilamellar (low phospholipid content) structures were formed. High phospholipid contents caused the HRP release to increase [32].

SF hydrogels containing glycerol were suggested as oral dosage form for elderly patients. Increases in glycerol content were shown to lower the release rates of benfotiamine from such formulations [75]. The release of trypan blue as well as FITC-inulin, embedded in semi-interpenetrating hydrogel networks of SF and polyacrylamide, was found to drop with increasing acrylamide fractions. This resulted from decreasing swelling ratios of the gels.

Further materials that were used to blend SF include hydroxyapatite [128], collagen [129], chitosan [52, 54, 130], PEG [131], keratin [132], hyaluronic acid [53], and poloxamer [76], but remain yet to be tested for drug delivery applications. All of them are assumed not only to change the mechanical properties but also the release kinetics due to changes in porosity, swelling, solubility and drug-matrix interactions, thus providing a wide range of opportunities to customize the delivery properties of SF.

Release of drug molecules from genetically engineered SELP hydrogels has been reviewed elsewhere [21]. The release kinetics from such hydrogels was found to be a function of hydrogel hydration, crosslinkage, pore size, degradability, size, hydrophobicity, charge and concentration. Another opportunity to control drug release from SF hydrogels could be the incorporation of drug loaded nano- or microparticles.

4.3.2. Drug release controlled by SF coatings

Microparticles and liposomes have been coated with SF in order to improve cellular recognition and prolong release. For instance, PLGA and alginate microparticles were coated by the layer-by-layer assembly technology [133]. The resulting SF coatings not only slowed down the decomposition of the alginate microparticles as compared to the corresponding uncoated microparticles, but also dramatically sustained the release of HRP from PLGA microparticles and of Rh-BSA from alginate microparticles. The release could be further controlled through a treatment with methanol to induce water insolubility of the coatings. Since the degradation of SF is both surface- as well as enzyme-mediated, the extent of degradation and release of embedded drugs may be controlled through the number of layers used. Release control was by hindrance to permeate across a barrier of several SF layers, and was demonstrated for Rhodamine B, Evans Blue and Azoalbumin incorporated in the SF coatings [127]. Remarkably, the initial burst was suppressed. This makes such SF coated microparticles superior to other systems such as plain PLGA microparticles which commonly show a significant burst effect causing drug levels to peak, making local or systemic toxicity more likely [134].

Through diffusional hindrance the barrier imposed by SF coatings can also result in reduced swelling. For instance, the release of emodin from 1,2-dimyristol-*sn*-glycero-3-phosphocholine (DMPC) liposomes was described to be the consequence of the swelling of the liposomal lamellae followed by quick diffusion of the drug. When the liposomes were coated with SF layers, the swelling of the liposomal lamellae was restricted, and emodin release was diffusion controlled and slow [135]. Furthermore, SF coated liposomes showed higher efficacy in harming breast cancer cells due to an increased uptake/retention of the emodin loaded system. The sustained availability of emodin led to the downregulation of an increased number of signaling pathways resulting in superior inhibition of cell growth as compared to uncoated liposomes [136].

Overall, the results from SF coated microparticles and liposomes suggest the development of further modifications (Fig. 2). For instance, drugs may not

only be embedded in the bulk of the particles (Fig. 2A), but also incorporated into (Fig. 2B) or sandwiched between the SF coatings (Fig. 2C). Layer-by-layer assembled SF coatings could be also useful for sequential release, e.g., by embedment of one drug into the microparticles or liposomes and a second or third one into the SF coating (Fig. 2D, E). Owing to a potential functionalization of SF, targeted drug delivery of microparticles and liposomes by coupling ligands to the SF coating could also be envisioned (Fig. 2F).
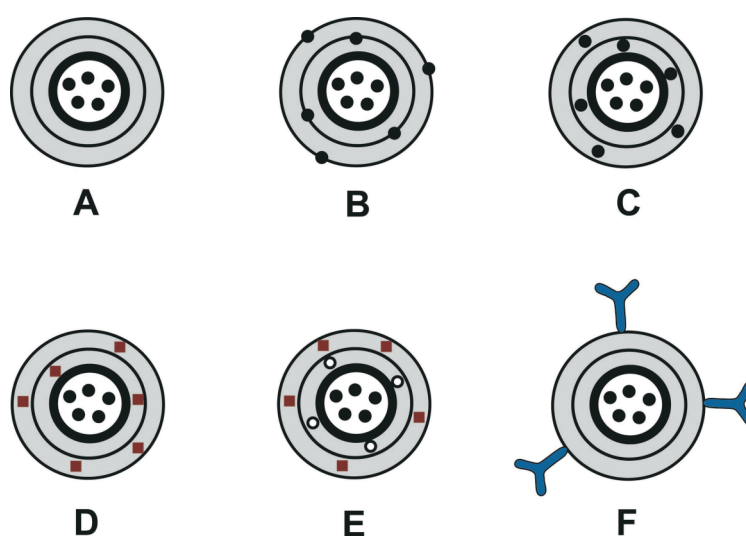
Fig. 2. *SF coated microparticles or liposomes with the drug encapsulated in the microparticle or liposome (A), and additionally incorporated between (B) or within SF layers (C). Sequential release could be obtained by encapsulation of one drug in the microparticle or liposome and a second (D) or third one (E) in the multilayers of the SF coating. Targeted drug delivery could be envisioned by attaching ligands to the SF coating (F).*

Stent implantation is often associated with an excessive proliferation of vascular smooth muscle cells (SMCs), extracellular matrix synthesis, thrombosis, and chronic inflammatory reaction. To prevent thrombosis and restenosis, a promising approach is to coat the stent with a polymeric layer loaded with therapeutic agents. The capacity of heparin, paclitaxel and clopidogrel loaded, multilayered SF coatings to regulate the adhesion, viability

and growth of human aortic endothelial cells (HAECs) and human coronary artery SMCs was demonstrated *in vitro*. The results were supported by an *in vivo* study using a porcine model, which demonstrated the integrity of the SF coatings on metallic stents, the maintenance of the endothelial cell phenotype and the reduction of platelet adhesion on the drug-loaded SF coatings [137]. Nevertheless, clear-cut clinical benefits await to be demonstrated.

Polymer coatings are common tools to enable sustained drug release from solid oral dosage forms. Owing to toxicity and environmental problems, coating with organic polymer solutions should be replaced by aqueous polymer solutions [138]. Because of its solubility in water, coating with aqueous SF solutions is feasible. For instance, aqueous SF solutions were used to coat theophylline tablets by a dip-coating technique [139]. Release depended on the thickness and the brittleness of the coating. When dried at 45°C to cause β-sheet formation of SF, the coating became brittle and developed cracks, rendering low sustainment of theophylline release. For reduced brittleness, aqueous SF solutions were blended with PEO as plastisizer. Crosslinkage of a SF coating with 1-ethyl-3(3-dimethyl aminopropyl) carbodiimide (EDC) induced an increase in β-sheet content, but also led to more elastic coatings. Both methods led to nearly zero order theophylline release [139].

The combination of different drug carriers, such as microparticles, scaffolds and coatings in one system, has been envisioned to enhance the level of drug release control. For instance, adenosine has recently been encapsulated into SF microparticles, which were further integrated into a SF scaffold. This scaffold was soaked in a SF/adenosine solution and coated with adenosine-loaded SF layers. The system successfully retarded kindling epileptogenesis in a dose-dependent manner [140]. Nevertheless, the advantage of the combined system over the individual forms of the drug delivery device has to be further determined. Additionally, the advantage of the control of release kinetics has to be weighed against the enhanced complexity of the fabrication process of a combined system.

**4.3.3 Growth factor delivery for tissue regeneration using SF matrices**

The combination of SF matrices with growth factors has shown significant potential for tissue regeneration. Especially the incorporation of the osteoinductive growth factor BMP-2 into SF matrices has gained much interest [42, 44, 120]. For instance, BMP-2 incorporated into electrospun SF/PEO fibers was shown to cause increased *in vitro* calcification rates as compared to BMP-2 free controls [89]. The release of the growth factor from the scaffold was assumed to be facilitated by the dissolution of the PEO component rendering the SF matrix more permeable. This led to the conclusion that blending of SF with different fractions of PEO may result in different release and mineralization kinetics. As yet this hypothesis awaits experimental confirmation.

In the same work enhanced mineralization was not only observed with electrospun scaffolds when loaded with BMP-2, but also when loaded with hydroxyapatite nanoparticles. This was either because of an improved adsorption of adhesion ligands to the hydroxyapatite surface providing signals for cellular differentiation, or due to partial dissolution of hydroxyapatite [89]. In addition to the loading of electrospun SF fibers with a first growth factor, the loading of the hydroxyapatite nanoparticles with a second growth factor may be envisioned to result in delivery systems with release kinetics that mimic physiological patterns.

In another *in vitro* study, pre-fabricated SF scaffolds were loaded with BMP-2, simply by exposing the scaffolds to an aqueous BMP-2 solution [44]. Loading with BMP-2 was to improve delivery control whereas prior efforts simply used soluble growth factor as medium supplement. The cumulative release rate of bound BMP-2 within one week was 75%, and was attributed to diffusion through the scaffold's porous structure, and the turbulent flow around the scaffold, as achieved by spinner flask culture conditions. Because of the minor hydrolytic degradation of SF, release rate control by degradation of the scaffold was unlikely. BMP-2 release was observed to practically end after one week which implied that 25% of the initial BMP-2 was firmly adsorbed to the SF scaffold. When such BMP-2 loaded SF scaffolds were seeded with hMSCs they led to localized mineralization at the center of the scaffolds. The authors

assumed that mineralization occurred where BMP-2 was retained and that the growth factor at the surface of the protein was released into the medium. It was hypothesized that adsorbed BMP-2 was better protected against inactivation than soluble BMP-2, and was more efficiently presented to BMP-2 receptors on the cells to induce differentiation of hMSCs. [44].

In contrast to the traditional approach to let the growth factor be released from the matrix, a more recent approach, denoted as substrate-mediated delivery, aims at a firm attachment of the growth factor to the matrix (Fig. 3). This approach mimics the physiological role of the ECM, acting as storage for growth factors such as FGF-2, BMP-2 and VEGF [141-143]. When recognized by cell surface receptors they induce a biological effect while still bound to the ECM [144-146]. As pointed out previously [147], this type of interaction may not trigger the same signaling pathway as a soluble factor, because the internalization of a factor may stimulate other signaling pathways than those activated at the surface. Moreover, signaling by certain growth factors firmly attached to a biomaterial may induce a stronger response than signaling by a soluble factor, while other factors show better results when being released [148].
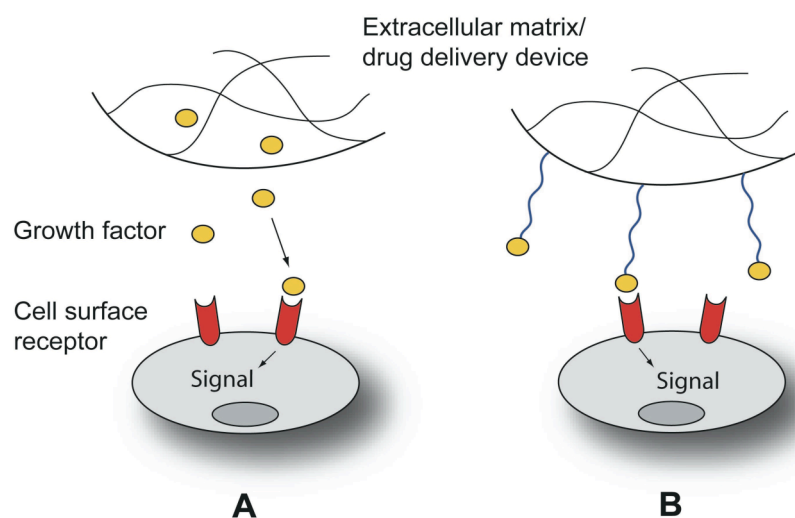
Fig. 3. *Release of a growth factor from the extracellular matrix (ECM) or a drug delivery device (A). Substrate-mediated delivery of a growth factor, where the drug binds to cell surface receptors while still bound to the ECM or the drug delivery device (B).*

In this context, BMP-2 was covalently coupled to SF films using carbodiimide chemistry [120]. The differentiation of hMSCs induced by BMP-2 coupled to the surface of the SF films was more efficient than when induced by a comparable amount of soluble BMP-2 added to the medium. Two reasons were considered by the authors to explain their observation: the higher local concentration or the slower degradation of coupled BMP-2.

Substrate-mediated delivery might not only be achieved by covalent coupling of a growth factor to a SF matrix but also by simple adsorption or embedment, caused by a strong interaction between the growth factors and SF. For instance, analogous to nature where the sulfated glycosaminoglycan heparan sulfate is the physiological storage site of FGF-2 in the ECM, we tested the hypothesis of whether SF could be decorated with moieties containing sulfonic acid groups in order to endow it with high capacity for non-covalent storage and advanced delivery of this heparin-binding growth factor for tissue engineering purposes [15]. More than 99% of bound FGF-2 could be retained on the SF derivatives within 6 days. Nevertheless, FGF-2 was able to efficiently induce a biological response, as observed by reduced metabolic activity and enhanced levels of phosphorylated extracellular signal-regulated kinases (pERK1/2) in cultured hMSCs. It remains to be investigated whether the biological response was exclusively induced by bound FGF-2. The strong interaction between FGF-2 and SF may originate from an enhanced ionic interaction between the negatively charged sulfonic acid groups of the SF derivative and the basic amino acid residues of FGF-2 [149]. An additional contribution is also likely to occur from the interaction between the mainly negatively charged side chains of the hydrophilic spacers of the heavy chain of SF [125, 126] and the basic amino acid residues of FGF-2. Moreover, an interaction between the hydrophobic (GAGAS)$_n$ blocks of the heavy chain of SF and the hydrophobic core of FGF-2 [150] may be considered. The interaction of other growth factors with SF matrices has also been demonstrated to originate from electrostatic and hydrophobic interactions and to influence release. For instance, release of nerve growth factor (NGF) from SF matrices was prolonged, but remained incomplete, i.e. 0.3 – 13% within 22 days, depending on the preparation method [73]. At pH 7.4, NGF with a pI of 9.3 carries a positive net charge, and can therefore interact

with the negatively charged SF (pI = 4.2). In contrast, it was recently shown that IGF-I, having a lower pI of 8.4 and a lower molecular weight (7.4 kDa for IGF-I versus 26 kDa for NGF), was released more completely (i.e. around 30% of the initial loading after four weeks) [46, 82]. Nevertheless, the main impact of the interaction between IGF-I and SF was assumed to be hydrophobic [46]. The burst release of IGF-I was significantly reduced and the release prolonged when SF scaffolds were treated with methanol as compared to untreated scaffolds. This was the result of an enrichment in β-sheets, which should hinder the diffusion of IGF-I within the SF structure [82]. IGF-I release was linearly correlated to the initial load, which may help to achieve predictable drug release profiles. SF was even able to preserve IGF-I potency during methanol treatment which contributed to the observed chondrogenic differentiation [82]. Overall, the capacity of SF to accommodate and protect sensitive growth factors seems to be remarkable.

As an alternative to the direct loading of a scaffold with a growth factor we also tested scaffolds containing embedded biodegradable PLGA microparticles loaded with IGF-I. We hypothesized that the biodegradation of the microparticles could further help to better control the release of the growth factor from the scaffold. In fact, the embedment of microparticles into the scaffolds resulted in a control of IGF-I release by both degradation of different types of PLGA microparticles and diffusional resistance through the SF matrix. PLGA degradation was not influenced by the SF matrix [18]. Therefore, by embedding microparticles with different degradation rates into SF matrices, complex release characteristics may be feasible (Fig. 4). For instance, different types of microparticles with distinct release kinetics that are loaded with different growth factors could be combined in one matrix. The spatially separated deposition of two different types of microparticles containing different growth factors would then allow dual growth factor delivery, which may be a prerequisite for the repair of osteochondral defects (Fig. 4C). In fact, the sequential delivery of BMP-2 and IGF-I from a two-layered gelatin system has previously been shown to have a better effect on bone formation as compared to a simultaneous release [151]. Recently, BMP-2 and IGF-I were loaded into SF scaffolds and alginate gel scaffolds as concentration gradient as the result of

gradient incorporation of BMP-2 and IGF-I loaded SF microparticles [124]. Besides the two growth factors, also the two different carrier matrices of the SF microparticles, featuring distinct growth factor loading and release properties, affected hMSC differentiation. The study confirmed that hMSCs exhibited osteogenic and chondrogenic differentiation along the concentration gradients of BMP-2 in the SF scaffolds, as demonstrated by increasing transcript levels of osteogenic and chondrogenic markers with increasing BMP-2 concentrations. IGF-I was shown to enhance the effect of BMP-2. However, when using alginate gel scaffolds instead of SF scaffolds, the level of osteochondrogenic differentiation did not follow the gradient trend of BMP-2 or IGF-I. In contrast to the β-sheet structure of SF that acts as a physical barrier to restrict diffusion of the growth factors and therefore retains gradients, the fast diffusion from the alginate gels leads to a loss of the growth factor gradient.

4.3.4. Gene delivery

In contrast to the delivery of either naked DNA or DNA complexed to non-viral or viral vectors, their incorporation into polymeric matrices may provide prolonged delivery, protect from enzymatic degradation and minimize toxicity. In this context, SELP hydrogels were described as attractive gene delivery systems. *In vitro* release of DNA was shown to be a function of SELP concentration and cure time of the hydrogels influencing swelling properties. Additionally, release from SELPs can be tailored by changing the macromolecular architecture using genetic engineering [152, 153]. The introduction of longer elastin-like units containing more lysine residues resulted in a reduced interaction of the SELP backbone with negatively charged plasmid DNA which led to an increase in release rates [153]. Furthermore, the release rate of plasmid DNA was inversely related to its molecular weight and influenced by its conformation and the geometry of the SELP hydrogel [154]. A decrease in SELP concentration and an increase in elastin content was shown to result in an increase in adenoviral release over a longer time span, due to the larger pore size of the matrix, and a decrease in rate and formation of β-sheets [155, 156].
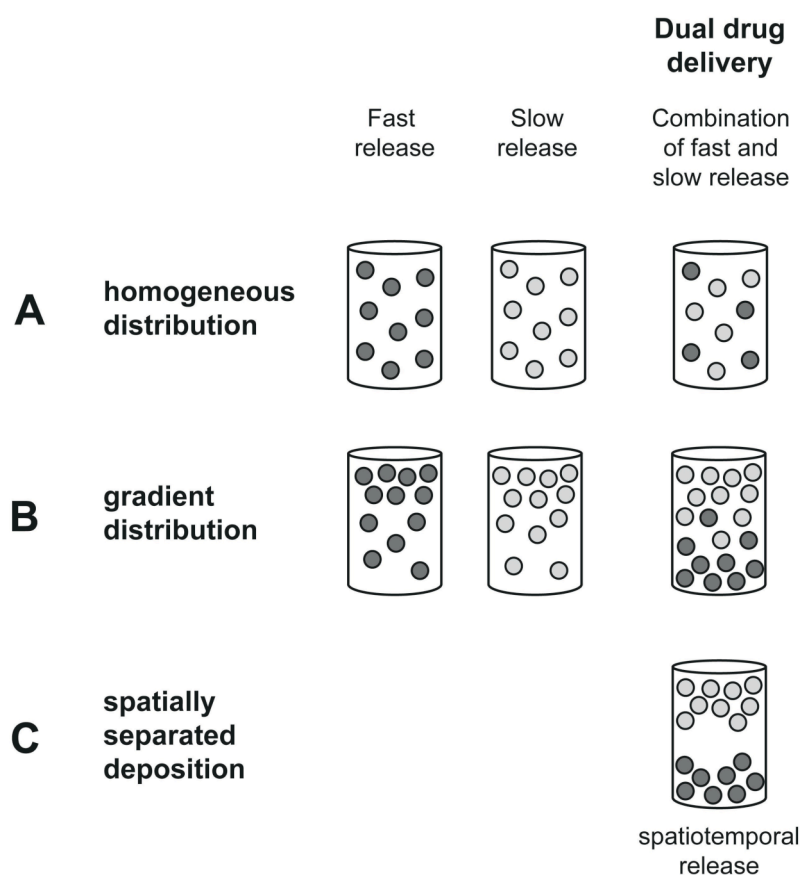
Fig. 4. *Embedment of fast and slow degrading drug molecule loaded microparticles in SF matrices: homogeneous distribution of one or the combination of two types of drug loaded microparticles (A), gradient distribution of one or the combination of two types of drug loaded microparticles (B), and spatially separated deposition of two types of drug loaded microparticles, leading to a spatiotemporal release (C). Barrels schematically indicate SF drug delivery device, ○ slow degrading microparticle loaded with drug molecule 1, ◉ fast degrading microparticle loaded with drug molecule 2*

4.3.5. Bioconjucates

Most protein drugs demonstrate poor *in vivo* stability and short half-lives. For improvement, SF bioconjugates have been prepared by covalent conjugation of a drug or enzyme to SF using the cross-linking reagent glutaraldehyde. Due to the strongly polar side groups in the SF molecule, SF does not have to be activated prior to crosslinking. For instance, insulin coupled to SF [157] and SF nanoparticles [122] demonstrated improved *in vitro* stability and half-life in

human serum. Additionally, the pharmacological activity in diabetic rats was lengthened, thus reducing the frequency of administration. L-asparaginase used in the treatment of acute lymphoblastic leukemia was covalently bioconjugated to SF [158]. The enzyme was characterized by its higher activity, heat and storage stability, resistance to trypsin digestion and affinity to the substrate L-asparagine as compared to that of uncoupled enzyme. Nevertheless, the denaturation potential of glutaraldehyde has to be considered and possible side products of the reaction have to be removed.

5. Applications of silk-based drug delivery systems

So far, the main focus of SF drug delivery systems has been on tissue regeneration applications. Due to its superior mechanical strength and its long-term biodegradability, SF drug delivery devices have been mainly used for bone and cartilage tissue engineering [42, 44, 89, 120, 124], and more recently also for vascular [137] and nerve regeneration [73]. The ability to create concentration gradients of growth factors in SF matrices by either using a suitable fabrication process leading to spatial deposition of the growth factor or the gradient incorporation of microparticles [124] could provide a platform for guidance of neurite outgrowth [159, 160]. Electrospun SF mats loaded with epidermal growth factor (EGF) have been recently demonstrated to enhance wound re-epithelialization [97]. Scaffolds made of SF/chitosan blends and seeded with human adipose-derived stem cells were previously shown to enhance wound healing in mice [130]. SF films turned out to be suitable as wound dressings as they are transparent, allowing easy inspection, they drain exudates from wounds and possibly retain water, proteins and electrolytes [161]. Obviously, incorporation of growth factors would be a logical step for further improvements in wound healing. The transparency of SF films has also been exploited for a possible use in cornea tissue engineering. Surface patterned transparent SF films were demonstrated to provide a suitable environment to control cell alignment and ECM synthesis [162]. The surface patterning may be combined with the binding of bioactive molecules to the SF surface to further control the material-cell interactions.

Other studies focused on applications in cancer therapy, using SF coated drug delivery systems, such as liposomes [135, 136]. Moreover, further SF devices were analyzed for their potential in the treatment of epilepsy [140].

The use of SF for oral drug delivery has found less attention but is assumed to lead to some interesting applications. For instance, protease digestion of SF tablets was shown to be slow, so that the tablets kept their shape during mechanical stimulation in the gastro-intestinal tract [115], giving SF tablets potential as long lasting oral drug delivery systems. Microparticles fabricated from genetically engineered spider silk were shown to remain intact in the stomach and release compounds into the small intestine [163]. Mucoadhesive SF films as potential vehicle for transmucosal delivery were fabricated by blending SF with hydroxy propyl methyl cellulose (HPMC) and poly(ethylene glycol) (PEG) [164]. Herein SF was used as film forming biomaterial due to its superior mechanical characteristics, HPMC as mucoadhesive polymer and PEG as plasticizer.

Overall, intensified explorations of the potential role of SF in drug interactions and release kinetics may certainly lead to future extensions in the application profile of SF based drug delivery systems.

6. Conclusions

Better understanding of how SF properties, fabrication processes and post-treatment protocols influence the features of SF based devices has led to rising interest in SF as a biomaterial for drug delivery. Owing to its biocompatibility SF is experiencing increased popularity for controlled release applications, and its aqueous processability allows the fabrication of highly tunable morphologies under mild conditions. The simplicity of adjusting release profiles by tools such as varying its concentration, applying multiple coatings or changing the β-sheet content, makes SF especially attractive. Moreover, simple surface modifications may affect drug binding and release, and even allow targeted drug delivery. The option to combine different SF drug delivery systems in one construct leads to a

sheer unlimited range of drug delivery devices providing distinct release kinetics.

Despite the excellent properties of SF that make it an attractive biomaterial for controlled delivery, a number of challenges remain. As a natural product the properties of silk may vary between both species and individuals of the same species. Moreover, inconsistencies in the degumming process may render the quality control of SF delivery systems and predictions for their release kinetics difficult. Genetically engineered SF proteins may overcome such deficiencies.

References

1. Altman GH, Diaz F, Jakuba C, Calabro T, Horan RL, Chen J, et al. Silk-based biomaterials. Biomaterials 2003;24(3):401-416.

2. Wamsley HL, Iwaniec UT, Wronski TJ. Selected extraskeletal effects of systemic treatment with basic fibroblast growth factor in ovariectomized rats. Toxicol Pathol 2005;33(5):577-583.

3. Parveen S, Sahoo SK. Polymeric nanoparticles for cancer therapy. J Drug Target 2008;16(2):108-123.

4. Nelson JL, Roeder BL, Carmen JC, Roloff F, Pitt WG. Ultrasonically activated chemotherapeutic drug delivery in a rat model. Cancer Res 2002;62(24):7280-7283.

5. Nair LS, Laurencin CT. Polymers as biomaterials for tissue engineering and controlled drug delivery. Adv Biochem Eng Biotechnol 2006;102:47-90.

6. Malafaya PB, Silva GA, Reis RL. Natural-origin polymers as carriers and scaffolds for biomolecules and cell delivery in tissue engineering applications. Adv Drug Del Rev 2007;59(4-5):207-233.

7. Mano JF, Silva GA, Azevedo HS, Malafaya PB, Sousa RA, Silva SS, et al. Natural origin biodegradable systems in tissue engineering and regenerative medicine: present status and some moving trends. J R Soc Interface 2007;4(17):999-1030.

8. Kaplan DL, Adams WW, Farmer B, Viney C. Silk: Biology, Structure, Properties, and Genetics. In: Kaplan DL, Adams WW, Farmer B, Viney C, editors. Silk polymers: materials science and biotechnology: ACS Symp Ser, 1994. p. 2-16.

9. Kaplan DL, Mello CM, Arcidiacono S, Fossey S, Senecal K, Muller W. Silk. In: McGrath K, Kaplan DL, editors. Protein-based materials. Boston: Birkhauser, 1997. p. 103-131.

10. Bini E, Knight DP, Kaplan DL. Mapping domain structures in silks from insects and spiders related to protein assembly. J Mol Biol 2004;335(1):27-40.

11. Sofia S, McCarthy MB, Gronowicz G, Kaplan DL. Functionalized silk-based biomaterials for bone formation. J Biomed Mater Res 2001;54(1):139-148.

12. Zhou CZ, Confalonieri F, Jacquet M, Perasso R, Li ZG, Janin J. Silk fibroin: structural implications of a remarkable amino acid sequence. Proteins 2001;44(2):119-122.

13. Gotoh Y, Tsukada M, Minoura N, Imai Y. Synthesis of poly(ethylene glycol)-silk fibroin conjugates and surface interaction between L-929 cells and the conjugates. Biomaterials 1997;18(3):267-271.

14. Murphy AR, St John P, Kaplan DL. Modification of silk fibroin using diazonium coupling chemistry and the effects on hMSC proliferation and differentiation. Biomaterials 2008;29(19):2829-2838.

15. Wenk E, Murphy AR, Kaplan DL, Meinel L, Merkle HP, Uebersax L. The use of sulfonated silk fibroin derivatives to control binding, delivery and potency of FGF-2 in tissue regeneration. Biomaterials 2010:31(6):1403-13.

16. Park TG. Degradation of poly(D,L-lactic acid) microspheres: effect of molecular weight. J Control Release 1994;30:161-173.

17. Zilberman M, Grinberg O. HRP-loaded bioresorbable microspheres: effect of copolymer composition and molecular weight on microstructure and release profile. J Biomater Appl 2008;22(5):391-407.

18. Wenk E, Meinel AJ, Wildy S, Merkle HP, Meinel L. Microporous silk fibroin scaffolds embedding PLGA microparticles for controlled growth factor delivery in tissue engineering. Biomaterials 2009;30(13):2571-81.

19. Trefiletti V, Conio G, Pioli F, Cavazza B, Perico A, Patrone E. The spinning of silk, 1: Molecular weight, subunit structure, and molecular shape of Bombyx mori fibroin. Makromol Chem 1980;181:1159-1179.

20. Cai K, Yao K, Lin S, Yang Z, Li X, Xie H, et al. Poly(D,L-lactic acid) surfaces modified by silk fibroin: effects on the culture of osteoblast in vitro. Biomaterials 2002;23(4):1153-1160.

21. Megeed Z, Cappello J, Ghandehari H. Genetically engineered silk-elastinlike protein polymers for controlled drug delivery. Adv Drug Del Rev 2002;54(8):1075-1091.

22. Zuo B, Dai L, Wu Z. Analysis of structure and properties of biodegradable regenerated silk fibroin fibers. J Mater Sci 2006;41:3357-3361.

23. Freiberg S, Zhu XX. Polymer microspheres for controlled drug release. Int J Pharm 2004;282(1-2):1-18.

24. Asakura T, Kuzuhara A, Tabeta R, Saito H. Conformation characterization of Bombyx mori silk fibroin in the solid state by high-frequency 13C cross polarization-magic angle spinning NMR, X-ray diffraction, and infrared spectroscopy. Macromolecules 1985;18:1841-1845.

25. Monti P, Freddi G, Bertoluzza A, Kasai N, Tsukada M. Raman spectroscopic studies of silk fibroin from Bombyx mori. J Raman Spectrosc 1998;29:297-304.

26. Marsh RE, Corey RB, Pauling L. An investigation of the structure of silk fibroin. Biochim Biophys Acta 1955;16(1):1-34.

27. Ishida M, Asakura T, Yokoi M, Saito H. Solvent- and mechanical-treatment-induced conformational transition of silk fibroins studied by high-resolution solid-state 13C NMR spectroscopy. Macromolecules 1990;23:88-94.

28. Motta A, Fambri L, Migliaresi C. Regenerated silk fibroin films: thermal and dynamic mechanical analysis. Macromol Chem Phys 2002;203:1658-1665.

29. Dicko C, Kenney JM, Knight D, Vollrath F. Transition to a beta-sheet-rich structure in spidroin in vitro: the effects of pH and cations. Biochemistry (Mosc) 2004;43(44):14080-14087.

30. Zong XH, Zhou P, Shao ZZ, Chen SM, Chen X, Hu BW, et al. Effect of pH and copper(II) on the conformation transitions of silk fibroin based on EPR, NMR, and Raman spectroscopy. Biochemistry (Mosc) 2004;43(38):11932-11941.

31. Kim UJ, Park J, Li C, Jin HJ, Valluzzi R, Kaplan DL. Structure and properties of silk hydrogels. Biomacromolecules 2004;5(3):786-792.

32. Wang X, Wenk E, Matsumoto A, Meinel L, Li C, Kaplan DL. Silk microspheres for encapsulation and controlled release. J Control Release 2007;117(3):360-370.

33. Jin HJ, Kaplan DL. Mechanism of silk processing in insects and spiders. Nature 2003;424(6952):1057-1061.

34. Xie F, Zhang H, Shao H, Hu X. Effect of shearing on formation of silk fibers from regenerated Bombyx mori silk fibroin aqueous solution. Int J Biol Macromol 2006;38(3-5):284-288.

35. Wenk E, Wandrey AJ, Merkle HP, Meinel L. Silk fibroin spheres as a platform for controlled drug delivery. J Control Release 2008;132(1):26-34.

36. Min BM, Jeong L, Lee KY, Park WH. Regenerated silk fibroin nanofibers: water vapor-induced structural changes and their effects on the behavior of normal human cells. Macromol Biosci 2006;6(4):285-292.

37. Nam J, Park YH. Morphology of regenerated silk fibroin: effects of freezing temperature, alcohol addition, and molecular weight. J Appl Polym Sci 2001;81:3008-3021.

38. Li M, Lu S, Wu Z, Yan H, Mo J, Wang L. Study on porous silk fibroin marterials. I. Fine structure of freeze dried silk fibroin. J Appl Polym Sci 2001;79:2185-2191.

39. Jin HJ, Park J, Karageorgiou V, Kim UJ, Valluzzi R, Cebe P, et al. Water-stable silk films with reduced beta-sheet content. Adv Funct Mater 2005;15:1241-1247.

40. Cappello J, Crissman J, Dorman M, Mikolajczak M, Textor G, Marquet M, et al. Genetic engineering of structural protein polymers. Biotechnol Prog 1990;6(3):198-202.

41. Phillips DM, Drummy LF, Conrady DG, Fox DM, Naik RR, Stone MO, et al. Dissolution and regeneration of Bombyx mori silk fibroin using ionic liquids. J Am Chem Soc 2004;126(44):14350-14351.

42. Kirker-Head C, Karageorgiou V, Hofmann S, Fajardo R, Betz O, Merkle HP, et al. BMP-silk composite matrices heal critically sized femoral defects. Bone 2007;41(2):247-255.

43. Meinel L, Hofmann S, Betz O, Fajardo R, Merkle HP, Langer R, et al. Osteogenesis by human mesenchymal stem cells cultured on silk biomaterials: comparison of adenovirus mediated gene transfer and protein delivery of BMP-2. Biomaterials 2006;27(28):4993-5002.

44. Karageorgiou V, Tomkins M, Fajardo R, Meinel L, Snyder B, Wade K, et al. Porous silk fibroin 3-D scaffolds for delivery of bone morphogenetic protein-2 in vitro and in vivo. J Biomed Mater Res A 2006;78(2):324-334.

45. Winkler S, Wilson D, Kaplan DL. Controlling beta-sheet assembly in genetically engineered silk by enzymatic phosphorylation/ dephosphorylation. Biochemistry (Mosc) 2000;39(41):12739-12746.

46. Wenk E, Wandrey AJ, Merkle HP, Meinel L. Silk fibroin spheres as a platform for controlled drug delivery. J Control Release 2008;132(1):26-34.

47. Nakamura S, Magoshi J, Magoshi Y. Thermal properties of silk proteins in silkworm. In: Kaplan D, Adams WW, Farmer B, Viney C, editors. Silk polymers: Materials science and biotechnology: ACS Symp Ser, 1994. p. 211-221.

48. Drummy LF, Phillips DM, Stone MO, Farmer BL, Naik RR. Thermally induced alpha-helix to beta-sheet transition in regenerated silk fibers and films. Biomacromolecules 2005;6(6):3328-3333.

49. Nazarov R, Jin HJ, Kaplan DL. Porous 3-D scaffolds from regenerated silk fibroin. Biomacromolecules 2004;5(3):718-726.

50. Peppas NA, Khare AR. Preparation, structure and diffusional behavior of hydrogels in controlled release. Adv Drug Deliv Rev 1993;11:1-35.

51. Haider M, Leung V, Ferrari F, Crissman J, Powell J, Cappello J, et al. Molecular engineering of silk-elastinlike polymers for matrix-mediated gene delivery: biosynthesis and characterization. Mol Pharm 2005;2(2):139-150.

52. Rujiravanit R, Kruaykitanon S, Jamieson AM, Tokura S. Preparation of crosslinked chitosan/silk fibroin blend films for drug delivery system. Macromol Biosci 2003;3:604-611.

53. Garcia-Fuentes M, Giger E, Meinel L, Merkle HP. The effect of hyaluronic acid on silk fibroin conformation. Biomaterials 2008;29(6):633-642.

54. Gobin AS, Froude VE, Mathur AB. Structural and mechanical characteristics of silk fibroin and chitosan blend scaffolds for tissue regeneration. J Biomed Mater Res A 2005;74(3):465-473.

55. Holland TA, Mikos AG. Biodegradable polymeric scaffolds. Improvements in bone tissue engineering through controlled drug delivery. Adv Biochem Eng Biotechnol 2006;102:161-185.

56. Lee SH, Shin H. Matrices and scaffolds for delivery of bioactive molecules in bone and cartilage tissue engineering. Adv Drug Deliv Rev 2007;59(4-5):339-359.

57. Schmidt CE, Baier JM. Acellular vascular tissues: natural biomaterials for tissue repair and tissue engineering. Biomaterials 2000;21(22):2215-2231.

58. Chang Y, Tsai CC, Liang HC, Sung HW. In vivo evaluation of cellular and acellular bovine pericardia fixed with a naturally occurring crosslinking agent (genipin). Biomaterials 2002;23(12):2447-2457.

59. Bhrany AD, Lien CJ, Beckstead BL, Futran ND, Muni NH, Giachelli CM, et al. Crosslinking of an oesophagus acellular matrix tissue scaffold. J Tissue Eng Regen Med 2008;2(6):365-372.

60. Kim UJ, Park J, Kim HJ, Wada M, Kaplan DL. Three-dimensional aqueous-derived biomaterial scaffolds from silk fibroin. Biomaterials 2005;26(15):2775-2785.

61. Kim SE, Cho YW, Kang EJ, Kwon IC, Bae Lee E, Kim JH, et al. Three-dimensional porous collagen/chitosan complex sponge for tissue engineering. Fibers Polym 2001;2:64-70.

62. Luo Y, Engelmayr G, Auguste DT, da Silva Ferreira L, Karp JM, Saigal R, et al. Three-dimensional scaffolds. In: Lanza R, Langer R, Vacanti J, editors. Principles of tissue engineering. 3 ed: Academic Press, 2007. p. 359-373.

63. Pachence JM, Bohrer MP, J. K. Biodegradable polymers. In: Lanza R, Langer R, Vacanti J, editors. Principles of tissue engineering. 3 ed: Academic Press, 2007. p. 323-339.

64. Fu K, Pack DW, Klibanov AM, Langer R. Visual evidence of acidic environment within degrading poly(lactic-co-glycolic acid) (PLGA) microspheres. Pharm Res 2000;17(1):100-106.

65. Zolnik BS, Burgess DJ. Evaluation of in vivo-in vitro release of dexamethasone from PLGA microspheres. J Control Release 2008;127(2):137-145.

66. Houchin ML, Topp EM. Chemical degradation of peptides and proteins in PLGA: a review of reactions and mechanisms. J Pharm Sci 2008;97(7):2395-2404.

67. Wang Y, Rudym DD, Walsh A, Abrahamsen L, Kim HJ, Kim HS, et al. In vivo degradation of three-dimensional silk fibroin scaffolds. Biomaterials 2008;29(24-25):3415-3428.

68. Cappello J. Genetically engineered protein polymers. In: Domb AJ, Kost J, Wiseman DM, editors. Handbook of biodegradable polymers. Amsterdam: Harwood Academic Publishers, 1997. p. 387-416.

69. Meinel L, Hofmann S, Karageorgiou V, Kirker-Head C, McCool J, Gronowicz G, et al. The inflammatory responses to silk films in vitro and in vivo. Biomaterials 2005;26(2):147-155.

70. Uebersax L, Apfel T, Nuss KMR, Vogt R, Kim HY, Meinel L, et al. Biocompatibility and osteoconduction of macroporous silk fibroin implants in cortical defects in sheep. Silk fibroin scaffolding for growth factor delivery in tissue repair, Diss ETH No 17551, 2008. p. 131.

71. Pace CN, Trevino S, Prabhakaran E, Scholtz JM. Protein structure, stability and solubility in water and other solvents. Philos Trans R Soc Lond B Biol Sci 2004;359(1448):1225-1234; discussion 1234-1225.

72. Hofmann S, Foo CT, Rossetti F, Textor M, Vunjak-Novakovic G, Kaplan DL, et al. Silk fibroin as an organic polymer for controlled drug delivery. J Control Release 2006;111(1-2):219-227.

73. Uebersax L, Mattotti M, Papaloizos M, Merkle HP, Gander B, Meinel L. Silk fibroin matrices for the controlled release of nerve growth factor (NGF). Biomaterials 2007;28(30):4449-4460.

74. Fang JY, Chen JP, Leu YL, Wang HY. Characterization and evaluation of silk protein hydrogels for drug delivery. Chem Pharm Bull (Tokyo) 2006;54(2):156-162.

75. Hanawa T, Watanabe A, Tsuchiya T, Ikoma R, Hidaka M, Sugihara M. New oral dosage form for elderly patients. II. Release behavior of benfotiamine from silk fibroin gel. Chem Pharm Bull (Tokyo) 1995;43(5):872-876.

76. Kang GD, Nahm JH, Park JS, Moon JY, Cho CS, Yeo JH. Effects of poloxamer on the gelation of silk fibroin. Macromol Rapid Commun 2000;21:788-791.

77. Wang X, Kluge JA, Leisk GG, Kaplan DL. Sonication-induced gelation of silk fibroin for cell encapsulation. Biomaterials 2008;29(8):1054-1064.

78. Dinerman AA, Cappello J, Ghandehari H, Hoag SW. Solute diffusion in genetically engineered silk-elastinlike protein polymer hydrogels. J Control Release 2002;82(2-3):277-287.

79. Cappello J, Crissman JW, Crissman M, Ferrari FA, Textor G, Wallis O, et al. In-situ self-assembling protein polymer gel systems for administration, delivery, and release of drugs. J Control Release 1998;53(1-3):105-117.

80. Mandal BB, Kundu SC. Non-bioengineered silk fibroin protein 3D scaffolds for potential biotechnological and tissue engineering applications. Macromol Biosci 2008;8(9):807-818.

81. Uebersax L, Hagenmuller H, Hofmann S, Gruenblatt E, Muller R, Vunjaknovakovic G, et al. Effect of scaffold design on bone morphology in vitro. Tissue Eng 2006;12(12):3417-3429.

82. Uebersax L, Merkle HP, Meinel L. Insulin-like growth factor I releasing silk fibroin scaffolds induce chondrogenic differentiation of human mesenchymal stem cells. J Control Release 2008;127(1):12-21.

83. Hofmann S, Hagenmuller H, Koch AM, Muller R, Vunjak-Novakovic G, Kaplan DL, et al. Control of in vitro tissue-engineered bone-like structures using human mesenchymal stem cells and porous silk scaffolds. Biomaterials 2007;28(6):1152-1162.

84. Jin HJ, Fridrikh SV, Rutledge GC, Kaplan DL. Electrospinning Bombyx mori silk with poly(ethylene oxide). Biomacromolecules 2002;3(6):1233-1239.

85. Kriegel C, Arrechi A, Kit K, McClements DJ, Weiss J. Fabrication, functionalization, and application of electrospun biopolymer nanofibers. Crit Rev Food Sci Nutr 2008;48(8):775-797.

86. Sill TJ, von Recum HA. Electrospinning: applications in drug delivery and tissue engineering. Biomaterials 2008;29(13):1989-2006.

87. Lutolf MP, Hubbell JA. Synthetic biomaterials as instructive extracellular microenvironments for morphogenesis in tissue engineering. Nat Biotechnol 2005;23(1):47-55.

88. Zong X, Kim K, Fang D, Ran S, Hsiao B, Chu B. Structure and process relationship of electrospun bioabsorbable nanofiber membranes. Polymer 2002;43:4403-4412.

89. Li C, Vepari C, Jin HJ, Kim HJ, Kaplan DL. Electrospun silk-BMP-2 scaffolds for bone tissue engineering. Biomaterials 2006;27(16):3115-3124.

90. Meinel AJ, Kubow KE, Klotzsch E, Garcia-Fuentes M, Smith ML, Vogel V, et al. Optimization strategies for electrospun silk fibroin tissue engineering scaffolds. Biomaterials 2009;30(17):3058-67.

91. Soffer L, Wang X, Zhang X, Kluge J, Dorfmann L, Kaplan DL, et al. Silk-based electrospun tubular scaffolds for tissue-engineered vascular grafts. J Biomater Sci Polym Ed 2008;19(5):653-664.

92. Zhu J, Shao H, Hu X. Morphology and structure of electrospun mats from regenerated silk fibroin aqueous solutions with adjusting pH. Int J Biol Macromol 2007;41(4):469-474.

93. Jeong L, Yeo IS, Kim HN, Yoon YI, Jang da H, Jung SY, et al. Plasma-treated silk fibroin nanofibers for skin regeneration. Int J Biol Macromol 2009;44(3):222-228.

94. Park KE, Jung SY, Lee SJ, Min BM, Park WH. Biomimetic nanofibrous scaffolds: preparation and characterization of chitin/silk fibroin blend nanofibers. Int J Biol Macromol 2006;38(3-5):165-173.

95. Zhang X, Baughman CB, Kaplan DL. In vitro evaluation of electrospun silk fibroin scaffolds for vascular cell growth. Biomaterials 2008;29(14):2217-2227.

96. Jin HJ, Chen J, Karageorgiou V, Altman GH, Kaplan DL. Human bone marrow stromal cell responses on electrospun silk fibroin mats. Biomaterials 2004;25(6):1039-1047.

97. Schneider A, Wang XY, Kaplan DL, Garlick JA, Egles C. Biofunctionalized electrospun silk mats as a topical bioactive dressing for accelerated wound healing. Acta Biomater 2008;5(7)2570-2578.

98. Wang H, Zhang Y, Shao H, Hu X. Electrospun ultra-fine silk fibroin fibers from aqueous solutions. J Mater Sci 2005;40:5359-5363.

99. Silva SS, Maniglio D, Motta A, Mano JF, Reis RL, Migliaresi C. Genipin-modified silk-fibroin nanometric nets. Macromol Biosci 2008;8(8):766-774.

100. Brandenberger H, Nüssli D, Piech V, Widmer F. Monodisperse particle production: a new method to prevent drop coalescence using electrostatic forces. J Electrostat 1999;45:227-238.

101. Seifert D, Phillips J. Production of small, monodispersed alginate beads for cell immobilization. Biotechnol Prog 1997;13:562-568.

102. Serp D, Cantana E, Heinzen C, Von Stockar U, Marison IW. Characterization of an encapsulation device for the production of monodisperse alginate beads for cell immobilization. Biotechnol Bioeng 2000;70(1):41-53.

103. Sukigara S, Gandhi M, Ayutsede J, Micklus M, Ko F. Regeneration of Bombyx mori silk by electrospinning-part 1: processing parameters and geometric properties. Polymer 2003;44:5721-5727.

104. Meechaisue C, Wutticharoenmongkol P, Waraput R, Huangjing T, Ketbumrung N, Pavasant P, et al. Preparation of electrospun silk fibroin fiber mats as bone scaffolds: a preliminary study. Biomed Mater 2007;2(3):181-188.

105. Hino T, Tanimoto M, Shimabayashi S. Change in secondary structure of silk fibroin during preparation of its microspheres by spray-drying and

exposure to humid atmosphere. J Colloid Interface Sci 2003;266(1):68-73.

106. Cao Z, Chen X, Yao J, Huang L, Shao Z. The preparation of regenerated silk fibroin microspheres. Soft Matter 2007;3:910-915.

107. Srisuwan Y, Srihanam P, Baimark Y. Preparation of silk fibroin microspheres and its application to protein adsorption. J Macromol Sci A 2009;46:521-525.

108. Hermanson KD, Huemmerich D, Scheibel T, Bausch AR. Engineered microcapsules fabricated from reconstituted spider silk. Adv Mater 2007;19:1810-1815.

109. Slotta UK, Rammensee S, Gorb S, Scheibel T. An engineered spider silk protein forms microspheres. Angew Chem Int Ed Engl 2008;47(24):4592-4594.

110. Tang Z, Wang Y, Podsiadlo P, Kotov N. Biomedical Applications of Layer-by-Layer Assembly: From Biomimetics to Tissue Engineering. Adv Mater 2006;18:3203-3224.

111. Decher G. Fuzzy nanoassemblies: towards layered polymeric multicomposites. Science 1997;277:1232-1237.

112. Wang X, Kim HJ, Xu P, Matsumoto A, Kaplan DL. Biomaterial coatings by stepwise deposition of silk fibroin. Langmuir 2005;21(24):11335-11341.

113. Ghosh S, Parker ST, Wang X, Kaplan DL, Lewis JA. Direct-write assembly of microperiodic silk fibroin scaffolds for tissue engineering applications. Adv Funct Mater 2008;18:1883-1889.

114. Gohel MC, Jogani PD. A review of co-processed directly compressible excipients. J Pharm Pharm Sci 2005;8(1):76-93.

115. Katayama H, Issiki M, Yoshitomi H. Application of fibroin in controlled release tablets containing theophylline. Biol Pharm Bull 2000;23(10):1229-1234.

116. Meinel L, Hofmann S, Karageorgiou V, Zichner L, Langer R, Kaplan D, et al. Engineering cartilage-like tissue using human mesenchymal stem cells and silk protein scaffolds. Biotechnol Bioeng 2004;88(3):379-391.

117. Hofmann S, Knecht S, Langer R, Kaplan DL, Vunjak-Novakovic G, Merkle HP, et al. Cartilage-like tissue engineering using silk scaffolds and mesenchymal stem cells. Tissue Eng 2006;12(10):2729-2738.

118. Tsukada M, Freddi G, Minoura N. Changes in the fine structure of silk fibroin fibers following gamma irradiation. J Appl Polym Sci 1994;51:823-829.

119. Kojthung A, Meesilpa P, Sudatis B, Treeratanapiboon L, Udomsangpetch R, Oonkhanond B. Effects of gamma radiation on biodegradation of bombyx mori silk fibroin. Int Biodeterior Biodegradation 2008;62:487-490.

120. Karageorgiou V, Meinel L, Hofmann S, Malhotra A, Volloch V, Kaplan D. Bone morphogenetic protein-2 decorated silk fibroin films induce osteogenic differentiation of human bone marrow stromal cells. J Biomed Mater Res A 2004;71(3):528-537.

121. Chen X, Shao Z, Knight DP, Vollrath F. Conformation transition kinetics of Bombyx mori silk protein. Proteins 2007;68(1):223-231.

122. Yan HB, Zhang YQ, Ma YL, Zhou LX. Biosynthesis of insulin-silk fibroin nanoparticles conjugates and in vitro evaluation of a drug delivery system. J Nanopart Res 2009;11:1937-46.

123. Vepari CP, Kaplan DL. Covalently immobilized enzyme gradients within three-dimensional porous scaffolds. Biotechnol Bioeng 2006;93(6):1130-1137.

124. Wang X, Wenk E, Zhang X, Meinel L, Vunjak-Novakovic G, Kaplan DL. Growth factor gradients via microsphere delivery in biopolymer scaffolds for osteochondral tissue engineering. J Control Release 2009;134(2):81-90.

125. Zhou CZ, Confalonieri F, Medina N, Zivanovic Y, Esnault C, Yang T, et al. Fine organization of Bombyx mori fibroin heavy chain gene. Nucleic Acids Res 2000;28(12):2413-2419.

126. Foo CW, Bini E, Hensman J, Knight DP, Lewis RV, Kaplan DL. Role of pH and charge on silk protein assembly in insects and spiders. Appl Phys A 2006;82:223-233.

127. Wang X, Hu X, Daley A, Rabotyagova O, Cebe P, Kaplan DL. Nanolayer biomaterial coatings of silk fibroin for controlled release. J Control Release 2007;121(3):190-199.

128. Du C, Jin J, Li Y, Kong X, Wei K, Yao J. Novel silk fibroin/hydroxyapatite composite films: structure and properties. Mater Sci Eng C 2009;29:62-68.

129. Yeo IS, Oh JE, Jeong L, Lee TS, Lee SJ, Park WH, et al. Collagen-based biomimetic nanofibrous scaffolds: preparation and characterization of collagen/silk fibroin bicomponent nanofibrous structures. Biomacromolecules 2008;9(4):1106-1116.

130. Altman AM, Yan Y, Matthias N, Bai X, Rios C, Mathur AB, et al. IFATS Series: Human adipose-derived stem cells seeded on a silk fibroin-chitosan scaffold enhance wound repair in a murine soft tissue injury model. Stem Cells 2008;27(1):250-258.

131. Acharya C, Dutta A, Kundu SC. Surface Treatment of Pure and PEG-4000 Blended Fibroin Films and their Characterizations as Matrices for in vitro Fibroblast Culture. J Biomater Appl 2008 Sep 18;23(6):497-517.

132. Vasconcelos A, Freddi G, Cavaco-Paulo A. Biodegradable materials based on silk fibroin and keratin. Biomacromolecules 2008;9(4):1299-1305.

133. Wang X, Wenk E, Hu X, Castro GR, Meinel L, Wang X, et al. Silk coatings on PLGA and alginate microspheres for protein delivery. Biomaterials 2007;28(28):4161-4169.

134. Huang X, Brazel CS. On the importance and mechanisms of burst release in matrix-controlled drug delivery systems. J Control Release 2001;73(2-3):121-136.

135. Gobin AS, Rhea R, Newman RA, Mathur AB. Silk-fibroin-coated liposomes for long-term and targeted drug delivery. Int J Nanomedicine 2006;1(1):81-87.

136. Cheema SK, Gobin AS, Rhea R, Lopez-Berestein G, Newman RA, Mathur AB. Silk fibroin mediated delivery of liposomal emodin to breast cancer cells. Int J Pharm 2007;341(1-2):221-229.

137. Wang X, Zhang X, Castellot J, Herman I, Iafrati M, Kaplan DL. Controlled release from multilayer silk biomaterial coatings to modulate vascular cell responses. Biomaterials 2008;29(7):894-903.

138. Tarvainen M, Peltonen S, Mikkonen H, Elovaara M, Tuunainen M, Paronen P, et al. Aqueous starch acetate dispersion as a novel coating material for controlled release products. J Control Release 2004;96(1):179-191.

139. Bayraktar O, Malay O, Ozgarip Y, Batigun A. Silk fibroin as a novel coating material for controlled release of theophylline. Eur J Pharm Biopharm 2005;60(3):373-381.

140. Wilz A, Pritchard EM, Li T, Lan JQ, Kaplan DL, Boison D. Silk polymer-based adenosine release: therapeutic potential for epilepsy. Biomaterials 2008;29(26):3609-3616.

141. Macri L, Silverstein D, Clark RA. Growth factor binding to the pericellular matrix and its importance in tissue engineering. Adv Drug Deliv Rev 2007;59(13):1366-1381.

142. Badylak SF. The extracellular matrix as a biologic scaffold material. Biomaterials 2007;28(25):3587-3593.

143. Dawson JI, Oreffo RO. Bridging the regeneration gap: stem cells, biomaterials and clinical translation in bone tissue engineering. Arch Biochem Biophys 2008;473(2):124-131.

144. Smith JC, Singh JP, Lillquist JS, Goon DS, Stiles CD. Growth factors adherent to cell substrate are mitogenically active in situ. Nature 1982;296(5853):154-156.

145. Tanghetti E, Ria R, Dell'Era P, Urbinati C, Rusnati M, Ennas MG, et al. Biological activity of substrate-bound basic fibroblast growth factor (FGF2): recruitment of FGF receptor-1 in endothelial cell adhesion contacts. Oncogene 2002;21(24):3889-3897.

146. Vincent TL, McLean CJ, Full LE, Peston D, Saklatvala J. FGF-2 is bound to perlecan in the pericellular matrix of articular cartilage, where it acts as a chondrocyte mechanotransducer. Osteoarthritis Cartilage 2007;15(7):752-763.

147. Haugh JM, Schooler K, Wells A, Wiley HS, Lauffenburger DA. Effect of epidermal growth factor receptor internalization on regulation of the phospholipase C-gamma1 signaling pathway. J Biol Chem 1999;274(13):8958-8965.

148. Dinbergs ID, Brown L, Edelman ER. Cellular response to transforming growth factor-beta1 and basic fibroblast growth factor depends on release kinetics and extracellular matrix interactions. J Biol Chem 1996;271(47):29822-29829.

149. Coltrini D, Rusnati M, Zoppetti G, Oreste P, Isacchi A, Caccia P, et al. Biochemical bases of the interaction of human basic fibroblast growth factor with glycosaminoglycans. New insights from trypsin digestion studies. Eur J Biochem 1993;214(1):51-58.

150. Nugent MA, Iozzo RV. Fibroblast growth factor-2. Int J Biochem Cell Biol 2000;32(2):115-120.

151. Raiche AT, Puleo DA. In vitro effects of combined and sequential delivery of two bone growth factors. Biomaterials 2004;25(4):677-685.

152. Megeed Z, Cappello J, Ghandehari H. Controlled release of plasmid DNA from a genetically engineered silk-elastinlike hydrogel. Pharm Res 2002;19(7):954-959.

153. Hwang D, Moolchandani V, Dandu R, Haider M, Cappello J, Ghandehari H. Influence of polymer structure and biodegradation on DNA release from silk-elastinlike protein polymer hydrogels. Int J Pharm 2008;368(1-2):215-219.

154. Megeed Z, Haider M, Li D, O'Malley BW, Jr., Cappello J, Ghandehari H. In vitro and in vivo evaluation of recombinant silk-elastinlike hydrogels for cancer gene therapy. J Control Release 2004;94(2-3):433-445.

155. Dandu R, Ghandehari H, Cappello J. Characterization of structurally related adenovirus-laden silk-elastinlike hydrogels. J Bioact Compat Polym 2008;23:5-19.

156. Cresce AW, Dandu R, Burger A, Cappello J, Ghandehari H. Characterization and real-time imaging of gene expression of adenovirus embedded silk-elastinlike protein polymer hydrogels. Mol Pharm 2008;5(5):891-897.

157. Zhang YQ, Ma Y, Xia YY, Shen WD, Mao JP, Zha XM, et al. Synthesis of silk fibroin-insulin bioconjugates and their characterization and activities in vivo. J Biomed Mater Res B Appl Biomater 2006;79(2):275-283.

158. Zhang YQ, Zhou WL, Shen WD, Chen YH, Zha XM, Shirai K, et al. Synthesis, characterization and immunogenicity of silk fibroin-L-asparaginase bioconjugates. J Biotechnol 2005;120(3):315-326.

159. Cao X, Shoichet MS. Defining the concentration gradient of nerve growth factor for guided neurite outgrowth. Neuroscience 2001;103(3):831-840.

160. Kapur TA, Shoichet MS. Immobilized concentration gradients of nerve growth factor guide neurite outgrowth. J Biomed Mater Res A 2004;68(2):235-243.

161. Sugihara A, Sugiura K, Morita H, Ninagawa T, Tubouchi K, Tobe R, et al. Promotive effects of a silk film on epidermal recovery from full-thickness skin wounds. Proc Soc Exp Biol Med 2000;225(1):58-64.

162. Lawrence BD, Marchant JK, Pindrus MA, Omenetto FG, Kaplan DL. Silk film biomaterials for cornea tissue engineering. Biomaterials 2009;30(7):1299-1308.

163. Liebmann B, Hümmerich D, Scheibel T, Fehr M. Formulation of poorly water-soluble substances using self-assembling spider silk protein. Colloids Surf A Physicochem Eng Asp 2008;331:126-132.

164. Kundu J, Patra C, Kundu SC. Design, fabrication and characterization of silk fibroin-HPMC-PEG blended films as vehicle for transmucosal delivery. Mater Sci Eng C 2008;28:1376-1380.

CHAPTER II

SILK FIBROIN SPHERES AS A PLATFORM FOR CONTROLLED DRUG DELIVERY

Esther Wenk, Anne J. Wandrey, Hans P. Merkle, Lorenz Meinel

Institute of Pharmaceutical Sciences, ETH Zurich, Wolfgang-Pauli-Strasse 10,

CH-8093 Zurich, Switzerland

Abstract

The goal of this proof-of-concept study was the fabrication of drug loaded silk fibroin (SF) spheres under very mild processing conditions. The spheres were fabricated using the laminar jet break-up of an aqueous SF solution, which was induced by a nozzle vibrating at controlled frequency and amplitude. SF particles were spherical in shape as determined by SEM with diameters in the range of 101 μm to 440 μm, depending on the diameter of the nozzle and the treatment to induce water insolubility of SF. Both treatments, either methanol or exposure to water vapor, resulted in an increase in β-sheet content as analyzed by FTIR. High encapsulation efficiencies, close to 100%, were obtained when salicylic acid and propranolol hydrochloride-loaded SF spheres were left untreated or exposed to water vapor. Methanol treatment resulted in drug leaching and lowered the overall encapsulation efficiency. When 9% SF solutions were used for SF sphere preparation, release rates were more sustained than from spheres made with 3% SF solutions, and propranolol hydrochloride release was more sustained than salicylic acid release. However, no difference in the release profiles was observed between methanol and water vapor treated SF spheres. Because of its very mild conditions, which are potentially advantageous for the encapsulation of sensitive drugs, we also tested this method for the encapsulation of insulin-like growth factor I (IGF-I). Again encapsulation efficiencies were close to 100%, even after treatment with methanol. IGF-I was continuously released over 7 weeks in bioactive form, as analyzed by the proliferation of MG-63 cells. These results favor further investigation of SF spheres as a platform for the controlled release of sensitive biologicals.

1. Introduction

Microparticulate carriers have considerable potential as a platform for the delivery of therapeutic molecules [1, 2]. As delivery systems, they may be ingested or injected, protect the therapeutic from degradation or denaturation, control its release profile, and be functionalized to achieve targeted release [1]. Typical carriers for therapeutics are synthetic macromolecules, including polyesters, polyanhydrides, polyorthoesters, polyphosphazenes and pseudopolyamino acids, of which the polyesters are the best studied [2]. Nevertheless, the use of natural polymers remains attractive primarily because they resemble biological macromolecules, are often biocompatible or even biodegradable, are relatively inexpensive, and permit a variety of chemical modifications or functionalizations [3-5]. The current focus is on polysaccharides, including cellulose, chitosan, hyaluronic acid, alginate, dextran and starch, as well as on proteins such as collagen, gelatin, elastin, albumin and silk fibroin [3-5].

Silk fibroin is a natural, fibrous protein produced by spiders or insects such as *Nephila clavipes* and the domestic silkworm *Bombyx mori* [6]. Due to its unique properties such as processability, mechanical strength, biocompatibility and long-term degradability [6-8] it is currently being investigated for several biomedical applications [9-12]. An important advantage of SF as compared to other materials is its aqueous solubility and processability under very mild conditions, which makes it an attractive material for the formulation of delivery systems for sensitive biologics such as therapeutic proteins and peptides. For instance, we have investigated SF films for the embedment of model proteins such as horseradish peroxidase and lysozyme. The crystallinity of SF and the molecular weights of the proteins were the main parameters governing their release from the films [13]. Recently, we reported on the successful embedment of bioactive nerve growth factor and its release from tubular SF nerve conduits [14]. Moreover, electrospun SF scaffolds were found to preserve embedded BMP-2 in its bioactive form as demonstrated by osteogenic differentiation of human bone marrow-derived mesenchymal stem cells (hMSC) [15]. Similarly, when incorporated in macroporous, interconnective SF scaffolds, IGF-I

successfully induced the chondrogenic differentiation of such hMSC [16]. Other studies have reported on the protective properties of SF matrices for several proteins including alkaline phosphatase [17] and staphylococcal protein A [18].

Beyond films, scaffolds and nerve conduits, we suggest the use of SF for the preparation of SF spheres as a delivery system for sensitive biologicals that provides protection from degradation or denaturation, and affords sustained release. Unfortunately, many of the common methods used to prepare microspheres could be detrimental to sensitive biologicals because they require harsh preparation conditions such as the presence of non-aqueous solvents, water/solvent interfaces, cross-linking reagents for hardening, or elevated temperatures [19, 20]. For instance, SF microspheres have been produced by spray-drying, which required an inlet air temperature of 120°C [21]. Obviously, high temperatures are potentially detrimental to sensitive drugs and elicit denaturing conditions for protein therapeutics. For that reason it is essential to select formulation processes that maintain drug stability and bioactivity. For instance, SF microspheres have been fabricated under mild conditions using lipid vesicles as templates to stably load them with horseradish peroxidase [22].

This study purposed to manufacture SF spheres without the need of additional excipients and under very mild conditions from aqueous SF solutions at room temperature or below. The potential use of such spheres is widespread and may range from the controlled delivery of labile drugs and protein therapeutics, to their use as a biocompatible platform for the delivery of growth factors for tissue repair. Spheres were formed from aqueous solutions by means of a laminar jet break-up technology [23]. The preparation method was first tested for its ability to adjust the size of the spheres by using two different nozzle diameters. To induce β-sheet formation and thus water insolubility, the resulting SF spheres were treated with methanol. An alternative but even milder method to render the spheres water-insoluble was by exposure to water vapor. Both methods have been previously established with SF scaffolds [9, 16, 24], spray-dried SF microspheres [21] and electrospun SF nanofibers [25]. We also performed a first pilot study on the controlled release properties of the SF spheres containing salicylic acid and propranolol hydrochloride as model drugs. The effects of different SF concentrations, the treatments with methanol and

water vapor, and the effect of the model drugs on the drugs' release profiles were assessed. As a crucial step towards the development of SF spheres for the delivery of sensitive biologicals, we also studied the fabrication and the release of IGF-I loaded SF spheres as a platform for controlled growth factor delivery.

2. Materials and Methods

2.1. Materials

Cocoons of *Bombyx mori* were kindly supplied by Trudel Silk Inc. (Zurich, Switzerland). Propranolol hydrochloride was from Sigma-Aldrich (Buchs, Switzerland), salicylic acid and phosphoric acid were from Haenseler (Herisau, Switzerland). Acetonitrile was from Merck (Darmstadt, Germany) and methanol from Scharlau (Tägerig, Switzerland). Recombinant human IGF-I was kindly provided by Chiron Corporation (Emeryville, CA). For a bioassay on its mitogenic activity, we used bovine serum albumin (BSA) and 3-[4,5-dimethylthiazol-2-yl]-2,5-diphenyltetrazolium bromide (MTT) from Sigma (Buchs, Switzerland), and human osteosarcoma MG-63 cells from ATCC (Manassas, VA). Eagle's MEM, fetal bovine serum (FBS), penicillin G and streptomycin, and non essential amino acids were from Invitrogen (Paisley, UK). All other substances used were of analytical or pharmaceutical grade and obtained from Fluka (Buchs, Switzerland).

2.2. Preparation of SF spheres

Aqueous SF solution was prepared from cocoons of the silkworm *Bombyx mori* as previously described [26]. Briefly, cocoons were boiled two times for 1 h in an aqueous solution of 0.02 M Na_2CO_3 and thoroughly rinsed with water to remove the sericin. The extracted SF was dissolved in a 9 M aqueous LiBr solution to obtain a 10% (w/v) solution. This solution was dialyzed against water for 2.5 days using Slide-a-Lyzer dialysis cassettes (Pierce, Woburn, MA; MWCO 3500 g/mol), followed by dialysis against a 13% (w/v) PEG (MW 6000 g/mol) solution at room temperature in order to obtain a concentrated SF solution. SF solutions with concentrations of 3% and 9% were prepared by

diluting the concentrated solution with water and by sterile filtration through a 0.22 μm filter.

SF spheres were prepared by using an Inotech IEM-40 encapsulator (Basel, Switzerland). Nozzles with diameters of either 200 μm or 80 μm were mounted. In both cases an oscillation frequency of 1300 Hz was sufficient to achieve jet break-up of the solution into droplets. A high voltage of 1700 V was applied. The produced droplets were continuously collected and shock-frozen in a liquid nitrogen bath (Fig. 1). The frozen SF spheres were freeze-dried at –25 °C for 12 h (Lyovac GT2, FINN-AQUA, Hurth, Germany). Freeze-dried spheres were either (i) left untreated, (ii) treated with a 90% aqueous methanol solution at room temperature for 30 min [24], or (iii) exposed to water vapor of 96% relative humidity by equilibration in the presence of a saturated aqueous Na_2SO_4 solution at room temperature for 24 h as previously described [21]. Hereafter, these treatments will be denoted as methanol and water vapor treatment, respectively.
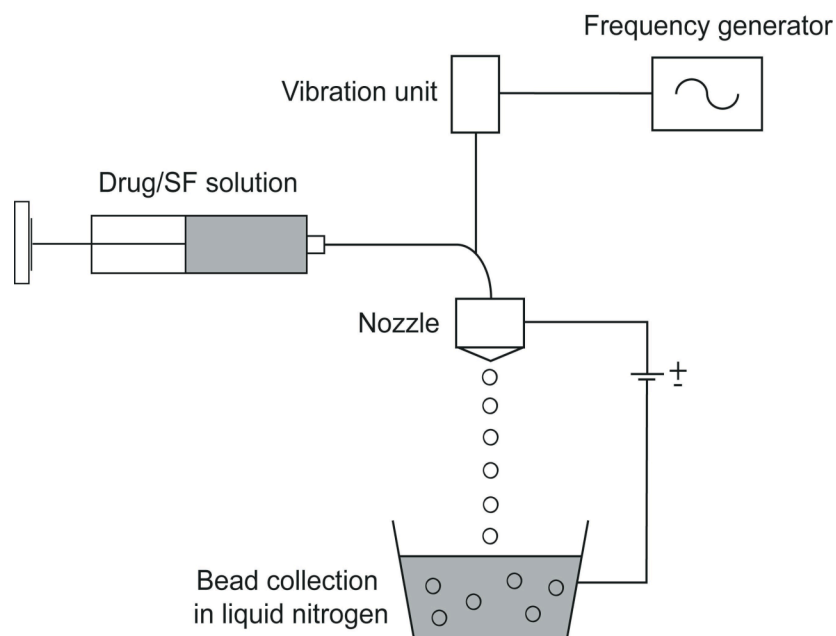
Fig. 1. *Illustration showing the experimental setup used for the preparation of SF spheres.*

To establish a proof-of-principle, most of the SF spheres in this study were made with the 200 μm nozzle. SF spheres produced with the 80 μm nozzle were only used to test whether the particle size of the SF spheres could be varied by using different nozzle diameters. To encapsulate the model drugs salicylic acid and propranolol hydrochloride, 5 mg of the compound was dissolved in 10 ml of either a 3% or 9% aqueous SF solution. To produce IGF-I loaded SF spheres, 420 μg of the growth factor was added to 10 ml of a 3% aqueous SF solution. Loaded SF spheres were then prepared as described above, using the 200 μm nozzle.

2.3. Characterization of SF spheres

2.3.1. Particle size analysis

The particle size of SF spheres was analyzed on the basis of microscopic images made with an Axiovert 35 microscope (Zeiss, Feldbach, Switzerland). The captured images were analyzed using ImageJ software. For each particle preparation we determined the average of the equivalent circular diameter of a total of 100 spheres.

2.3.2. Scanning electron microscopy (SEM)

Whole SF spheres and cross-sections thereof were platinum-coated and examined morphologically by scanning electron microscopy (SEM, Leo Gemini 1530, Zeiss, Oberkochen, Germany). Cross-sections were prepared by cutting dried SF spheres with a razor blade. SF spheres were examined before and after release experiments.

2.3.3. Fourier-transform infrared spectroscopy (FTIR)

Empty and loaded SF spheres were ground, the samples mixed with KBr and compressed to KBr disks. FTIR spectroscopy was performed with a 2000 FT-IR Spectrometer V3,01 (Perkin Elmer, Boston, MA).

2.4. Drug content and encapsulation efficiency

The actual contents of the model drugs salicylic acid and propranolol hydrochloride in the untreated SF spheres were determined by dissolving 10 mg of untreated spheres in 1 ml PBS of pH 7.4 (n = 5). The actual content of IGF-I in untreated SF spheres was analyzed (n = 4) by dissolving 5 mg of untreated spheres in 1 ml release medium (50 mM sodium acetate, 100 mM sodium chloride, 0.02% polysorbate 20, 0.02% sodium azide, pH 5.4); this medium was previously found to preserve IGF-I structure and activity [27]. Actual drug contents of SF spheres after methanol treatment were indirectly analyzed by the amount of drug that leaked into the supernatant and then subtracting this amount from that of untreated SF spheres. In contrast to methanol treatment, no drug leakage was expected to occur upon exposure to water vapor. Therefore, the actual drug content of water vapor treated SF spheres was assumed to be identical with that of untreated SF spheres. Salicylic acid and propranolol hydrochloride were assayed by HPLC as described below. IGF-I was analyzed either by HPLC or ELISA as described below. Because of the high dilution of methanol (< 0.02%) it was safe to exclude a potential interference with the ELISA protocol. Theoretical drug content was calculated assuming that the entire amount of drug added to the SF solution was encapsulated and no drug loss occurred at any stage of SF sphere preparation. Drug contents were expressed as the percentage of wt drug per wt SF spheres. Encapsulation efficiencies were calculated as the percentage of actual versus theoretical drug content.

2.5. In vitro drug release

Release of the model drugs salicylic acid and propranolol hydrochloride from 10 mg SF spheres was studied in 1 ml PBS of pH 7.4 at 37°C (n = 5). At each time point the whole release medium was collected and replaced by fresh buffer. The supernatants were analyzed by HPLC as described below. Data was expressed as percentage of the actual drug contents.

IGF-I release from 10 mg SF spheres was studied (n = 4) in 1 ml release medium (50 mM sodium acetate, 100 mM sodium chloride, 0.02% polysorbate

20, 0.02% sodium azide; pH 5.4, 37°C, 7 weeks); this release medium was previously found to preserve IGF-I structure and activity [27]. The release medium was fully exchanged with fresh medium after 0.5, 1, 1.5, 2.5, 5, 8, 10, 16, 21, 28, 34, 44, and 49 days. Medium samples were analyzed using an enzyme-linked immunosorbent assay (ELISA, DuoSet Human) according to the manufacturer's protocol (R&D Systems, Minneapolis, MN).

2.6. High pressure liquid chromatography (HPLC)

Released salicylic acid and propranolol hydrochloride were assayed by HPLC using a Merck system (Dübendorf, Switzerland) consisting of a sample cooler, an autoinjector (L-7200), a computer interface (D-7000), a pump (L-7100) and a UV detector (L-7455). Separation was performed on a LiChrospher® 100 RP-18 (5 μm) column (125 x 4 mm) at a flow rate of 1 ml/min. The mobile phase used for the analysis of salicylic acid consisted of 70% phosphate buffer (0.01 M KH_2PO_4 adjusted to pH 2.3 with H_3PO_4), 25% acetonitrile and 5% methanol (v/v/v). Detection was at 237 nm and quantified by peak area measurement. Propranolol hydrochloride was analyzed by using a mobile phase consisting of 0.2% sodium dodecyl sulfate, 7.2% phosphoric acid, 36% acetonitrile and 36% methanol (w/v/v/v) (USP XXII). Propranolol hydrochloride was detected at 220 nm and quantified by peak area measurement.

IGF-I content of SF spheres was assayed by using a Zorbax®300SB CN column (150 mm x 4.6 mm) at a flow rate of 1 ml/min. Two eluents were used: (A) consisting of 5% acetonitrile and 0.2% trifluoroacetic acid (TFA) in water, and (B) 80% acetonitrile and 0.2% TFA in water. The solvent was initially composed of 74% (v/v) eluent A. The solvent was changed over 30 min to 100% eluent B. Then, initial conditions were set to wash the column. IGF-I was detected at 214 nm and quantified by measuring peak area.

2.7. Bioassay for mitogenic activity of IGF-I

A bioassay was applied to demonstrate mitogenic activity of the supernatants as obtained from the IGF-I release tests. IGF-I is a well-known stimulator of the *in vitro* proliferation of MG-63 cells [28, 29]. MG-63 cells were grown in growth medium (MEM containing 8.9% FBS, 1.79 mM L-glutamine, 89 U/ml penicillin G and 89 µg/ml streptomycin). Medium was exchanged every 2 – 3 days. Cells were trypsinized and diluted to $2x10^5$ cells/ml in assay medium (MEM containing 0.456% BSA, 1.84 mM L-glutamine, 92 U/ml penicillin G and 92 µg/ml streptomycin). Using a 96-well plate, 100 µl of this cell suspension was added to each well, incubated at 37°C and 5% CO_2 for 24 hours, and the medium discarded. Supernatants of the *in vitro* IGF-I release study, which were collected in the time periods of 0.5 – 1 days, 1.5 - 2.5 days, 10 - 16 days and 28 - 34 days (each n = 4) were diluted 1:1000 in assay medium, 100 µl of the dilution added to the assay plate and incubated at 37°C and 5% CO_2 for 48 hours. Cells were stained with a 2% MTT solution in PBS for 4 hours. The formed formazan was solubilized with 3% sodium dodecyl sulfate (SDS) and 0.04 M HCl in 2-propanol. Absorbance was read at 570 nm. The absorbance of the solution taken from the control cells in assay medium without IGF-I (negative control) was defined as 100%. Additional samples were taken from solutions containing control cells which were incubated with 0.01, 0.1 and 1 ng IGF-I/ ml (positive controls). The dilution factor of 1:1000 was found to assure the range of an approximately semi-logarithmic relationship between absorbance and IGF-I concentration.

2.8. Statistics

Results are expressed as means ± standard deviations. Statistical analysis was performed using the Student t-test as well as one-way analysis of variance (ANOVA) followed by the Tukey HSD test for post-hoc comparison. Differences were considered significant when $p < 0.05$.

3. Results

3.1. Characterization of SF spheres

3.1.1. Macroscopic properties

SF particles had a spherical morphology. Untreated SF spheres prepared from a 9% SF solution were freely flowing compared to those prepared from a 3% SF solution, which had a tendency to lower flowability. Untreated SF spheres appeared white whereas methanol and water vapor treated spheres were slightly yellow. Prior to inducing water insolubility, the SF spheres were soft and dissolved in water immediately and completely. However, upon treatment with methanol or exposure to water vapor they appeared to be insoluble in water. Solubility tests showed no significant difference between methanol and water vapor treated SF spheres. Less than 5% of both methanol and water vapor treated SF spheres dissolved within 3 weeks (data not shown).

3.1.2. Particle size analysis

Untreated SF spheres prepared using a nozzle with a diameter of 200 μm had an average diameter of 402 μm ± 54 μm (3% SF solution) and 440 μm ± 59 μm (9% SF solution) (Fig. 2). The different treatments significantly influenced the size of the spheres resulting in decreased diameters ($p < 0.05$). Methanol treated SF spheres had an average diameter of 229 μm ± 42 μm (3% SF solution) and 301 μm ± 68 μm (9% SF solution), whereas SF spheres exposed to water vapor had an average diameter of 189 μm ± 30 μm (3% SF solution) and 235 μm ± 54 μm (9% SF solution). An increase in the concentration of the SF solution from 3% to 9% resulted in spheres with significantly increased diameters ($p < 0.05$; Fig. 2).

The same trends were also observed with the 80 μm nozzle, resulting in significantly smaller particles as compared to those prepared with a 200 μm nozzle ($p < 0.05$; Fig. 2). Untreated SF spheres had an average diameter of 262 μm ± 66 μm (3% SF solution) and 296 μm ± 80 μm (9% SF solution). Methanol treated SF spheres were significantly smaller ($p < 0.05$) and had an average diameter of 139 μm ± 58 μm (3% SF solution) and 163 μm ± 30 μm (9% SF

solution). SF spheres exposed to water vapor were also significantly smaller than untreated SF spheres and showed an average diameter of 101 μm ± 23 μm (3% SF solution) and 138 μm ± 37 μm (9% SF solution). When using the 80 μm nozzle, an increase in the concentration of the SF solution from 3% to 9% resulted in spheres with significantly increased diameters ($p < 0.05$), except for the methanol treated SF spheres, where the difference was non-significant ($p > 0.05$).
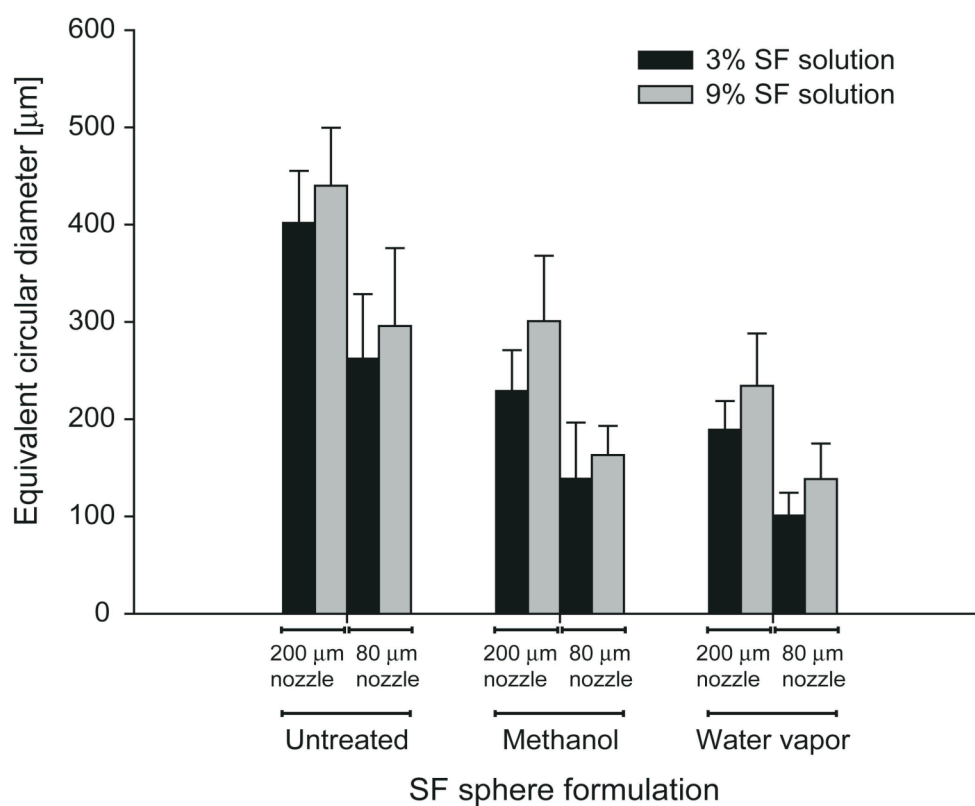
Fig. 2. *Equivalent circular diameters of untreated, methanol and water vapor treated SF spheres, prepared from either a 3% or 9% SF solution using a nozzle with a diameter of either 200 μm or 80 μm (means ± SD). See text for statistical tests.*

3.1.3. Scanning electron microscopy (SEM)

Surface analysis of the SF spheres by scanning electron microscopy revealed that the surface of untreated spheres was covered with a dense and quite complete skin layer of SF (Fig. 3).
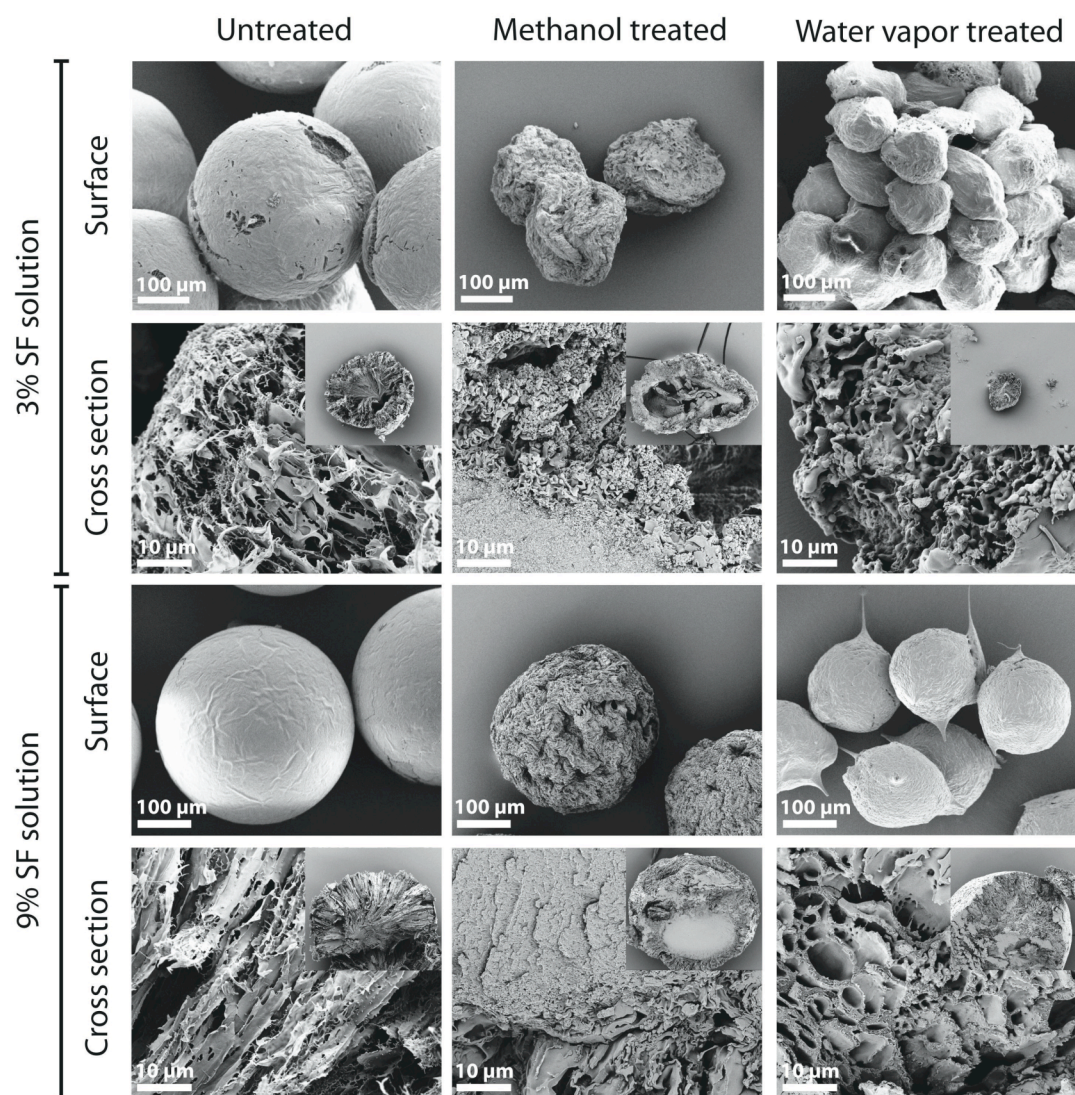
Fig. 3. *SEM images of untreated, methanol and water vapor treated SF spheres prepared from either a 3% or a 9% SF solution using a nozzle with a diameter of 200 µm. Scale bar first and third row = 100 µm, scale bar second and fourth row = 10 µm.*

Upon cross-sectioning, untreated SF spheres exhibited a sheet-like morphology with thin fibers protruding from the edges of the sheets. The inner part of the untreated SF spheres was denser than the outer part. SF spheres prepared from a 9% SF solution had a more compact structure than those prepared from a 3% SF solution. Treatment of the SF spheres with methanol or water vapor rendered the structure more compact. Differences in densities between the inner and outer parts of the spheres were still observed after the treatments and were especially pronounced in the methanol treated SF spheres. Indeed, methanol treated SF spheres prepared from a 9% SF solution showed two layers, an inner compact layer and an outer more porous, leaf-like layer. The inner section of the methanol treated SF spheres prepared from a 3% SF solution was hollow with some dense structures (Fig. 3).

We also performed SEM studies with SF spheres that were subject to previous drug release experiments. No detectable differences in morphology between SF spheres before and after release experiments were observed (data not shown).

3.1.4. Fourier-transform infrared spectroscopy (FTIR)

FTIR spectra of untreated and methanol and water vapor treated SF spheres without drug and prepared from either 3% or 9% SF solutions were recorded (Fig. 4). Characteristic absorption bands of untreated SF spheres were observed around 1658 cm^{-1} (amide I) and at 1540 cm^{-1} (amide II). These bands shifted to 1629 cm^{-1} (amide I) and 1517 cm^{-1} (amide II) upon treatment with methanol. The band shifts were also observed in the water vapor treated samples but seemed to be less pronounced. Samples of drug-loaded SF spheres resulted in similar spectra and band shifts (data not shown).
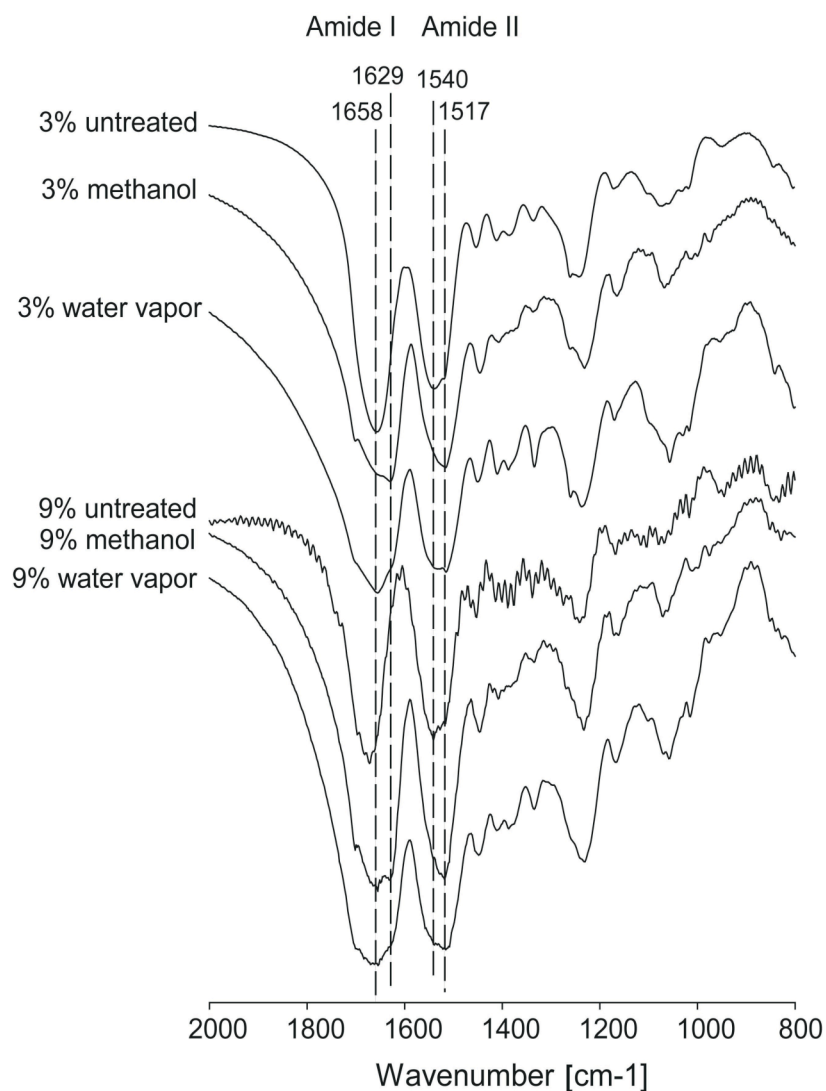
Fig. 4. *FTIR spectra of untreated, methanol treated and water vapor treated SF spheres, which were prepared from either a 3% or 9% SF solution using a nozzle with a diameter of 200 μm.*

3.2. Encapsulation efficiency

Untreated SF spheres showed similar encapsulation efficiencies (between 97.3% and 102.3%) for both salicylic acid and propranolol hydrochloride irrespective of the concentration of the SF solution used (Table 1). As expected, methanol treatment led to a significant loss of salicylic acid through leaching, causing the encapsulation efficiencies to drop to only $11.2 \pm 2.9\%$ with 3% SF solution and $25.1 \pm 0.4\%$ with 9% SF solution ($p < 0.001$). A substantial but

Table 1. Theoretical and actual drug content (expressed as wt drug/wt SF spheres) and encapsulation efficiency (calculated as percentage of actual versus theoretical drug content) of salicylic acid and propranolol hydrochloride loaded SF spheres either prepared from a 3% or 9% SF solution using a nozzle with a diameter of 200 μm. SF spheres were either left untreated, or treated with methanol or water vapor.

Encapsulated drug	Concentration of silk solution [% w/w]	Treatment	Theoretical drug content [% w/w]	Actual drug content [% w/w ± SD]	Encapsulation efficiency [% ± SD]
Salicylic acid	3	none/water vapor*	1.70	1.74 ± 0.04	102.3 ± 2.5
	3	methanol	1.70	0.20 ± 0.00	11.2 ± 2.9
	9	none/water vapor*	0.56	0.54 ± 0.01	97.3 ± 1.0
	9	methanol	0.56	0.14 ± 0.00	25.1 ± 0.4
Propranolol HCl	3	none/water vapor*	1.67	1.64 ± 0.05	97.9 ± 3.1
	3	methanol	1.67	0.35 ± 0.01	21.9 ± 2.1
	9	none/water vapor*	0.56	0.56 ± 0.01	100.8 ± 2.1
	9	methanol	0.56	0.33 ± 0.00	58.8 ± 0.5

* Corresponding to no treatment, water vapor treatment is assumed to cause no loss or leakage of embedded drug.

smaller drug loss was also observed with propranolol hydrochloride, which showed encapsulation efficiencies of 21.9 ± 2.1% with 3% SF solution and 58.8 ± 0.5% with 9% SF solution after methanol treatments ($p < 0.001$). In contrast, no drug loss could occur upon exposure to water vapor.

IGF-I encapsulation efficiencies of untreated SF spheres as determined by HPLC and ELISA were consistent. HPLC measurements revealed an IGF-I encapsulation efficiency of 96.5 ± 10.7%. The encapsulation efficiency determined by ELISA was 98.7 ± 15.7%. Upon methanol treatment no loss of IGF-I was detected by either HPLC or ELISA.

## 3.3. In vitro drug release studies

The cumulative release profiles of both model drugs from the SF spheres were studied in PBS of pH 7.4. The results are shown in Fig. 5 as a function of SF concentration and treatment. SF spheres prepared from a 3% SF solution and loaded with salicylic acid showed a burst release of 65.0 ± 6.2% (methanol treated) and 59.7 ± 7.3% (water vapor treated) within the first 2 hours. The burst release of encapsulated propranolol hydrochloride from SF spheres was less prominent: 39.4 ± 1.3% (methanol treated) and 19.2 ± 4.2% (water vapor treated). An increase in the concentration of the SF solution from 3% to 9% resulted in lower burst releases for both salicylic acid and propranolol hydrochloride loaded SF spheres. In this case, we observed a burst release of 48.9 ± 7.4% (methanol treated) and 44.6 ± 4.2% (water vapor treated) for salicylic acid loaded SF spheres versus 14.6 ± 1.4% (methanol treated) and 8.4 ± 0.9% (water vapor treated) for propranolol hydrochloride loaded SF spheres. After one day, more than 95% of the encapsulated salicylic acid was released from the SF spheres, irrespective of the concentration of the SF solution or treatment used. In contrast, within the same time period only 71.0 ± 3.4% (methanol treated) and 65.8 ± 5.2% (water vapor treated) of the loaded propranolol hydrochloride was eluted from the SF spheres prepared from a 3% SF solution. When prepared from a 9% SF solution only 41.2 ± 2.1% (methanol

treated) and 38.3 ± 2.6% (water vapor treated) propranolol hydrochloride was released after one day. After the initial burst the propranolol

hydrochloride formulations demonstrated a sustained release profile of approximately 7 days when prepared from a 3% SF solution, and of more than 21 days when using a 9% SF solution. An increase in the concentration of the SF solution from 3% to 9% resulted for both models in a further sustainment of the release. No relevant difference in the release properties between the methanol and the water vapor treated spheres was observed.

The cumulative release of IGF-I from SF spheres as prepared from a 3% SF solution and using a 200 μm nozzle is shown in Fig. 6A. Fairly continuous release was observed over a time period of 7 weeks for both methanol and water vapor treated SF spheres. According to the profile, further IGF-I release is expected to occur beyond this time. After 7 weeks, 5.7 μg ± 0.5 μg IGF-I was released from methanol treated SF spheres (41.1 ± 3.3% of the initial loading) and 5.9 μg ± 0.2 μg IGF-I from water vapor treated SF spheres (43.1 ± 1.3% of the initial loading). The bioactivity of released IGF-I was tested with a bioassay measuring the mitogenic activity of the supernatants in contact with MG-63 cells (Fig. 6B). All supernatants collected in the periods of 1.5 – 2.5 days and 10 – 16 days induced significantly higher cell proliferation than the control. This also applies to the supernatants from water vapor treated spheres collected between 0.5 and 1 day, and between 28 and 34 days. For these two intervals the respective supernatants from methanol treated spheres showed no significant increases in bioactivity above the control.

A

B
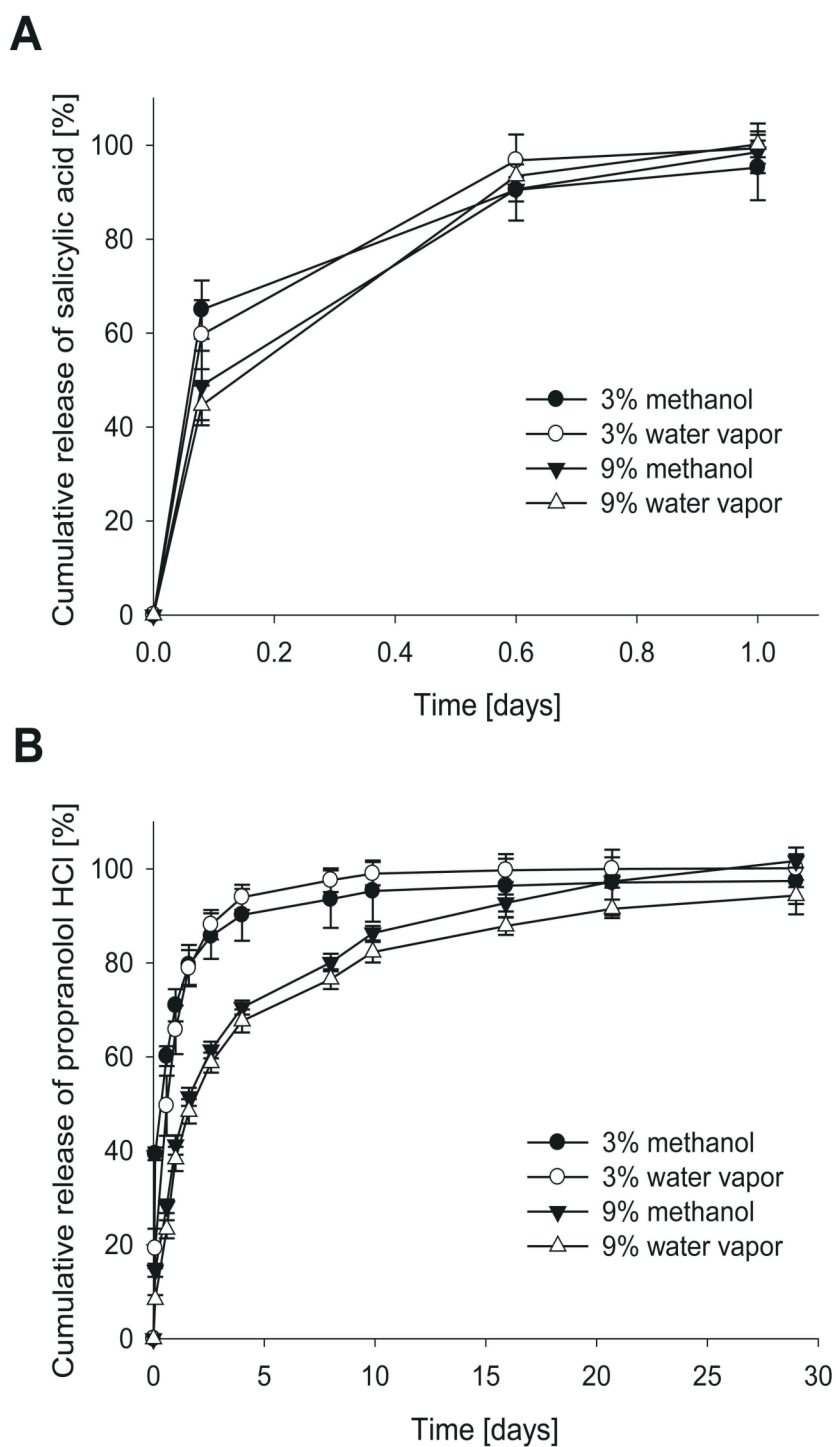
Fig. 5. *Cumulative release of salicylic acid (A) and propranolol hydrochloride (B) from either methanol or water vapor treated SF spheres prepared from either a 3% or 9% SF solution using a nozzle with a diameter of 200 μm. Data is expressed as percentage of the actual drug contents (means ± SD).*
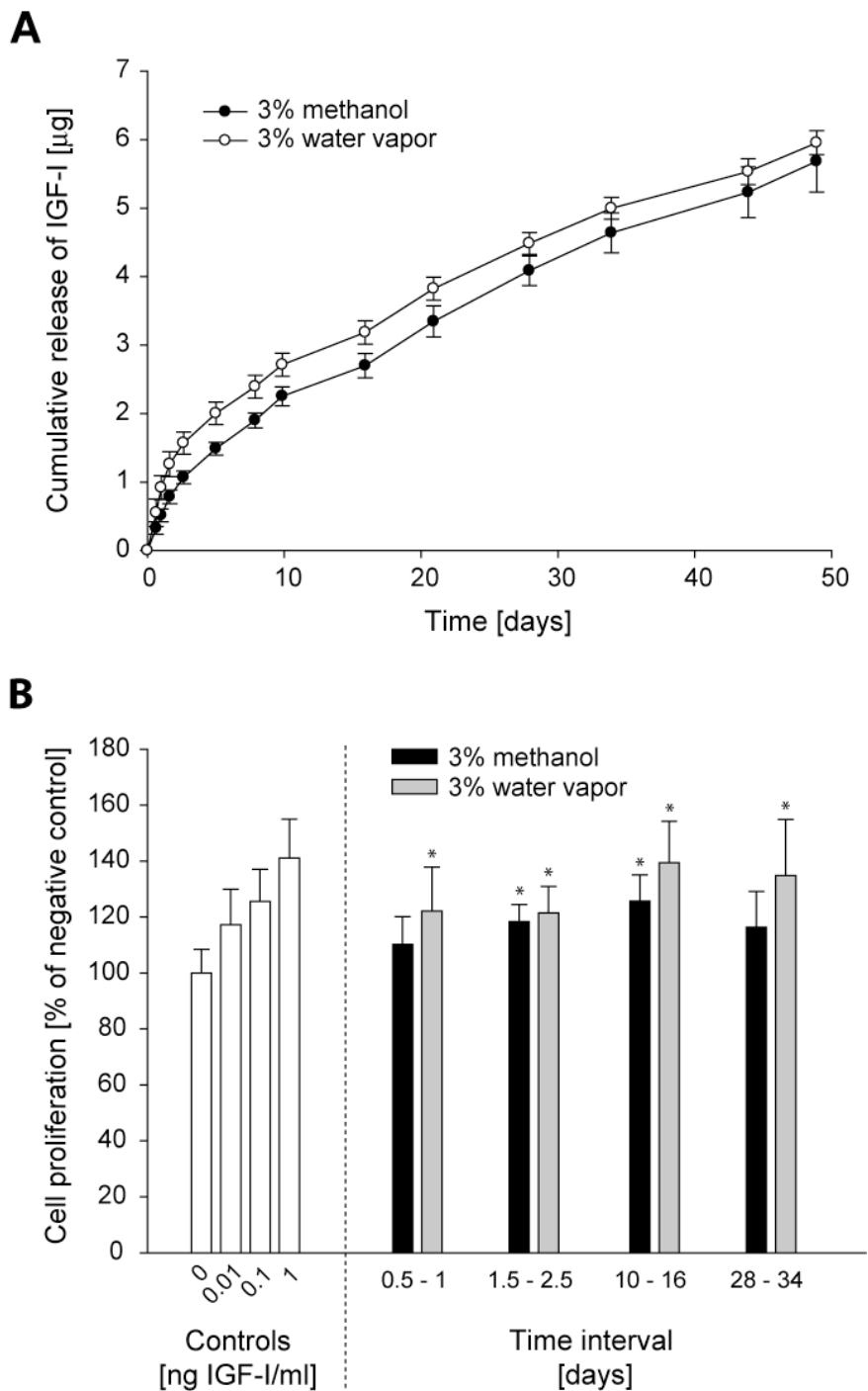
Fig. 6. *(A) Cumulative release of IGF-I of either methanol or water vapor treated SF spheres prepared from a 3% SF solution using a nozzle with a diameter of 200 μm. (B) Potency of IGF-I containing supernatants from release experiments on the proliferation of MG-63 cells. Cell proliferation was expressed as the percentage absorbance of samples relative to the negative control without IGF-I (means ± SD; *p < 0.05). Statistical differences indicated are relative to the negative control without IGF-I. Positive controls were obtained from cells incubated with 0.01, 0.1 and 1 ng IGF-I per ml medium.*

4. Discussion

For this proof-of-concept study, we fabricated SF spheres without any additional excipient, using an aqueous encapsulation process based on a laminar jet break-up induced by a nozzle vibrating at a controlled frequency and amplitude. High voltage was applied to optimize the dispersion of the beads as they approached the surface of the hardening solution (Fig. 1). This technology has been frequently used for the preparation of alginate beads for cell immobilization [23, 30, 31]. Here we introduce it for the formulation of SF spheres. This process has the advantage of being simple and scaleable. In addition, it can be carried out under very mild conditions, using only aqueous SF solutions and working at room temperature or below, which is an appealing feature for the encapsulation of sensitive biologicals. By varying the diameter of the nozzle, the concentration of the SF solution and the final treatment applied to induce water insolubility, spherical particles of varying size and morphology could be generated (Fig. 2, Fig. 3).

Obviously, depending on the site of injection, different sphere sizes are required. For the present proof-of-concept study, we applied two nozzle diameters. The use of the 80 μm instead of the 200 μm nozzle led to significantly smaller SF spheres (p < 0.05; Fig. 2). An increase in the concentration of the SF solution from 3% to 9% rendered spheres that were significantly larger in size. This can result from the fact that an increase in viscosity makes the break-up of the solution into small droplets at the same vibration frequency less likely [32]. For customized solutions, further studies may help to better define and optimize the concentrations of the SF solution, the diameters of the nozzle, and the frequencies necessary to obtain SF spheres of appropriate sizes.

Cross-sections of the SF spheres showed that untreated spheres were composed of an inner, more compact core and an outer, more porous part as determined by SEM (Fig. 3). SF spheres frozen in liquid nitrogen, freeze dried and left untreated, had a sheet-like structure. This morphology was also typical for SF fibroin solutions that were frozen at -80°C and freeze dried, resulting in parallel sheets, which were connected by thin bridges; in contrast, samples

frozen at -45°C exhibited a leaf like structure and those frozen at -18°C led to coarse porosity [33].

It has been previously reported that the prevailing molecular conformation of SF fibroin solutions frozen at temperatures below -20°C is random coil [24, 33], with characteristic FTIR absorption frequencies at 1660 cm^{-1} (amide I) and 1541 cm^{-1} (amide II) [25, 34]. FTIR spectra of the untreated SF spheres confirmed the presence of this conformation, as indicated by absorption frequencies around 1658 cm^{-1} (amide I) and at 1540 cm^{-1} (amide II) (Fig. 4).

Treatment with methanol or exposure to water vapor led to a more compact SF structure and smaller sphere size compared to untreated spheres, as determined by SEM (Fig. 3) (Fig. 2). This may be due to the fact that SF becomes densely packed when changes in its crystal structure occur [35]. Treatment with methanol has been the most frequently used method to induce water insolubility in SF. It was suggested that methanol dehydrates and, therefore, destabilizes the random coil and/or the unstable silk I state to result in the more stable silk II (predominant) conformation, characterized by an increase in β-sheet content [34, 36-38]. Indeed, FTIR measurements confirmed that methanol treated SF spheres showed an increase in β-sheet content as indicated by a typical conformational shift in the amide I and amide II band regions when compared to untreated SF spheres (Fig. 4). Nevertheless, the use of methanol caused a major loss (or leaching) of the encapsulated low molecular weight drug models. In addition, detrimental effects of organic solvents on the bioactivity of embedded protein drugs should be considered [39]. For instance, an unfavorable effect of methanol was reported for lysozyme when immobilized in SF films; induction of water insolubility with methanol resulted in a marked loss of bioactivity of the enzyme [13]. On the other hand, IGF-I embedded in porous silk scaffolds maintained significant biological activity towards the chondrogenic differentiation of human mesenchymal stem cells. Apparently SF was able to preserve the potency of IGF-I during methanol treatment [16]. In fact, here we were able to show that supernatants from the IGF-I release tests of methanol treated SF spheres were bioactive and induced the proliferation of MG-63 cells (Fig. 6B). In addition to the methanol treatment, we also applied a

water vapor treatment as a mild alternative to induce water insolubility, as described previously [21, 25, 34]. Similar to methanol treatment, water vapor induced a conformational change into β-sheet structure as indicated by a shift in the amide I and amide II band regions, but less pronounced than upon methanol treatment (Fig. 4). This corresponded to the previous results of a conformational analysis of SF films with 13C-MAS NMR [34], showing the percentage of silk II (30%) after water vapor treatment to be lower compared to a higher percentage (74%) after treatment with methanol. Min et al. explained the induction of β-sheets in electrospun SF nanofibers after exposure to water vapor by a molecular rearrangement of the SF chains due to the changes in hydrogen bonding [25].

High encapsulation efficiency is a desired feature of encapsulation technologies for controlled release [1]. It (i) minimizes the loss of therapeutics, (ii) reduces their consumption during fabrication, or (iii) helps to prolong the release rate. Our encapsulation process resulted in high encapsulation efficiencies in untreated SF spheres in the range of 100% for both model drugs, irrespective of the SF concentration used for encapsulation (Table 1). The encapsulation of IGF-I was similarly efficient. However, subsequent methanol treatments resulted in major losses of the encapsulated low-molecular-weight model drugs, salicylic acid and propranolol hydrochloride. The greater loss of salicylic acid by methanol treatment may be explained by its better solubility compared to propranolol hydrochloride [40, 41]. For both models, drug loss was reduced when a higher concentration of the SF solution (9% instead of 3%) was applied. Nevertheless, the exposure to water vapor represents an excellent alternative to induce aqueous insolubility of SF, as this treatment excludes drug leaching. Protein therapeutics are not likely to be eluted by methanol, however the denaturation potential of this solvent and the need to restrict its concentration in the final product to toxicologically acceptable levels should also be considered. Nevertheless, it is noteworthy that the encapsulation of IGF-I led to almost identical release profiles of the growth factor, with only small but non-significant differences in the levels of bioactivity, when using methanol versus water vapor treatments ($p > 0.05$).

Depending on the concentration of the SF solution and the encapsulated model drug, we obtained SF spheres with different drug release profiles (Fig. 5A and 5B). The initial burst release and the release rates from the SF spheres were reduced when using higher concentrations of the SF solution (9% instead of 3% SF). Higher SF concentration also resulted in an increase in the size of the SF spheres. Previous studies have shown that polymer concentration is a key factor in the drug release properties of particles as it resulted in bigger spheres and a drop in the release rates [42-44]. Effects of SF layer thickness were also reported when the model molecules rhodamine B, Evans blue and azoalbumin were incorporated into the multilayer structure of a SF coating made by a layer-by-layer dip-coating approach. A thicker SF layer suppressed the initial burst release and prolonged the duration of release [45].

Propranolol hydrochloride (Fig. 5B) showed a more sustained release than salicylic acid (Fig 5A). This may be due to the different hydrophobicities of the two model drugs. The aromatic moiety of propranolol hydrochloride - a naphthyl unit - is more hydrophobic than the phenyl group of salicylic acid. Therefore, differences in the hydrophobic interactions with the hydrophobic blocks (-Gly-Ala-Gly-Ala-Gly-Ser-)$_n$ of the heavy chain of the SF protein [38] are likely. The difference may also be explained by a pKa-dependent release of the two model drugs from the drug delivery system. With a pI of 4.2, due to the mainly negatively charged side chains of the hydrophilic spacers of the heavy chain [46, 47], SF is likely to interact with the protonated amine group of propranolol hydrochloride (pKa = 9.5) [40, 48] at the pH of the release studies (pH 7.4). Salicylic acid (pKa = 3.0) [41] carries a negative net charge at this pH. Consequently, repulsive charges between SF and salicylic acid may lead to enhanced release rates of this model drug compared to the release rates of propranolol hydrochloride. IGF-I, due to its higher molecular weight (7.4 kDa) showed a prolonged release. Likewise for IGF-I, ionic interactions between the mainly negatively charged side chains of the hydrophilic spacers of the heavy chain of SF and the positively charged amino acids of IGF-I (e.g. Arg) [49] may apply. Recently, an ionic interaction was described between SF and nerve growth factor (pI = 9.3), which lead to a prolonged and incomplete release [14]. In contrast, it has recently been shown that IGF-I, which has a lower pI (8.4 for

IGF-I versus 9.3 for nerve growth factor) and a lower molecular weight (7.4 kDa for IGF-I versus 26 kDa for nerve growth factor), was released more completely (i.e., 28% of the initial loading after 4 weeks) from SF scaffolds [16]. In the present study, the cumulative release of IGF-I from methanol and water vapor treated SF spheres - again, after 4 weeks - was nearly identical (i.e., about 30% and 32%, respectively, of the initial loading; Fig. 6A). As a further exploration, we performed preliminary experiments to study the ionic interaction between IGF-I and SF films. Although there was significantly less adsorption of IGF-I to SF films at pH 2.3 (both SF and IGF-I carry a positive net charge) than at pH 7.4 (SF carries a negative and IGF-I a positive net charge), the differences in adsorption were minor (60.0 ± 0.5% at pH 2.3 versus 62.2 ± 0.6% at pH 7.4, respectively). Moreover, the addition of 100 mM NaCl, 500 mM NaCl or 100 mM $MgCl_2$ to the medium at pH 7.4 did not significantly affect the adsorption of IGF-I to SF films. In conclusion, we assume the major part of the interaction to be non-Coulomb in nature since considerable protein adsorption also occurs at pH 2.3. Obviously, the interactive forces were strong enough to overcome charge repulsion. Because the heavy chain of the SF is rich in hydrophobic blocks $(-Gly-Ala-Gly-Ala-Gly-Ser-)_n$, an interaction between such blocks and the hydrophobic domain of IGF-I, featuring Leu, Val and Ile [49], is more likely.

Further studies are needed to fully understand the underlying release mechanism from SF spheres. In the first place, because of the rather slow biodegradation of SF in the range of 6 – 12 months, rate control by SF degradation is unlikely. Diffusion control alone is also unable to fully explain the release mechanism, although the influence of the molecular weight of various embedded dextrans on their release profiles from SF films, as previously documented [13], pointed towards this direction, correlating sustained release from SF films with higher molecular weights of the dextrans. Nevertheless, we found no relevant differences in the release properties between methanol and water vapor treated SF spheres, irrespective of the large differences in their porous structure, thus discounting a major impact of diffusion. More intriguing is the fact that the percentage release rates of IGF-I, as previously observed with SF scaffolds [16], closely corresponded with those found with the SF spheres

(see above), in spite of marked differences in size, shape and surface. This may indicate a rate controlling effect through the growth factor's physical entrapment or molecular interaction with SF, allowing only slow dissociation and release off the matrix.

5. Conclusions

Here we prepared SF spheres with excellent encapsulation efficiencies and sustained release kinetics using a mild encapsulation process based on a laminar jet break-up of aqueous SF solutions. Organic solvents, and even methanol turned out to be fully dispensable for the induction of water insolubility of SF. In fact, water vapor treatments were sufficient to render the SF spheres water insoluble. This technology not only helped to preserve the bioactivity of the embedded growth factor, it also allowed for a striking sustainment of its release profile. Based on the good biocompatibility record of SF as a scaffold material for bone regeneration [9, 11], the application of such SF spheres may range from the controlled delivery of labile drugs and protein therapeutics to their use as a platform for the delivery of growth factors for tissue repair.

Acknowledgements

References

1. Freiberg S, Zhu XX. Polymer microspheres for controlled drug release. Int J Pharm 2004;282(1-2):1-18.

2. Sinha VR, Trehan A. Biodegradable microspheres for protein delivery. J Control Release 2003;90(3):261-280.

3. Mano JF, Silva GA, Azevedo HS, Malafaya PB, Sousa RA, Silva SS, et al. Natural origin biodegradable systems in tissue engineering and regenerative medicine: present status and some moving trends. J R Soc Interface 2007;4(17):999-1030.

4. Malafaya PB, Silva GA, Reis RL. Natural-origin polymers as carriers and scaffolds for biomolecules and cell delivery in tissue engineering applications. Advanced drug delivery reviews 2007;59(4-5):207-233.

5. Malafaya PB, Silva GA, Reis RL. Natural-origin polymers as carriers and scaffolds for biomolecules and cell delivery in tissue engineering applications. Adv Drug Del Rev 2007;59(4-5):207-233.

6. Altman GH, Diaz F, Jakuba C, Calabro T, Horan RL, Chen J, et al. Silk-based biomaterials. Biomaterials 2003;24(3):401-416.

7. Horan RL, Antle K, Collette AL, Wang Y, Huang J, Moreau JE, et al. In vitro degradation of silk fibroin. Biomaterials 2005;26(17):3385-3393.

8. Meinel L, Hofmann S, Karageorgiou V, Kirker-Head C, McCool J, Gronowicz G, et al. The inflammatory responses to silk films in vitro and in vivo. Biomaterials 2005;26(2):147-155.

9. Meinel L, Betz O, Fajardo R, Hofmann S, Nazarian A, Cory E, et al. Silk based biomaterials to heal critical sized femur defects. Bone 2006;39(4):922-931.

10. Hofmann S, Knecht S, Langer R, Kaplan DL, Vunjak-Novakovic G, Merkle HP, et al. Cartilage-like tissue engineering using silk scaffolds and mesenchymal stem cells. Tissue Eng 2006;12(10):2729-2738.

11. Kirker-Head C, Karageorgiou V, Hofmann S, Fajardo R, Betz O, Merkle HP, et al. BMP-silk composite matrices heal critically sized femoral defects. Bone 2007;41(2):247-255.

12. Altman GH, Horan RL, Lu HH, Moreau J, Martin I, Richmond JC, et al. Silk matrix for tissue engineered anterior cruciate ligaments. Biomaterials 2002;23(20):4131-4141.

13. Hofmann S, Foo CT, Rossetti F, Textor M, Vunjak-Novakovic G, Kaplan DL, et al. Silk fibroin as an organic polymer for controlled drug delivery. J Control Release 2006;111(1-2):219-227.

14. Uebersax L, Mattotti M, Papaloizos M, Merkle HP, Gander B, Meinel L. Silk fibroin matrices for the controlled release of nerve growth factor (NGF). Biomaterials 2007;28(30):4449-4460.

15. Li C, Vepari C, Jin HJ, Kim HJ, Kaplan DL. Electrospun silk-BMP-2 scaffolds for bone tissue engineering. Biomaterials 2006;27(16):3115-3124.

16. Uebersax L, Merkle HP, Meinel L. Insulin-like growth factor I releasing silk fibroin scaffolds induce chondrogenic differentiation of human mesenchymal stem cells. J Control Release 2007;127(1):12-21.

17. Demura M, Takekawa T, Asakura T, Nishikawa A. Characterization of low-temperature-plasma treated silk fibroin fabrics by ESCA and the use of the fabrics as an enzyme-immobilization support. Biomaterials 1992;13(5):276-280.

18. Kikuchi J, Mitsui Y, Asakura T, Hasuda K, Araki H, Owaku K. Spectroscopic investigation of tertiary fold of staphylococcal protein A to explore its engineering application. Biomaterials 1999;20(7):647-654.

19. Wang L-Y, Gu Y-H, Su Z-G, Ma G-H. Preparation and improvement of release behavior of chitosan microspheres containing insulin. Int J Pharm 2006;311:187-195.

20. Bilati U, Allemann E, Doelker E. Strategic approaches for overcoming peptide and protein instability within biodegradable nano- and microparticles. Eur J Pharm Biopharm 2005;59(3):375-388.

21. Hino T, Tanimoto M, Shimabayashi S. Change in secondary structure of silk fibroin during preparation of its microspheres by spray-drying and exposure to humid atmosphere. J Colloid Interface Sci 2003;266(1):68-73.

22. Wang X, Wenk E, Matsumoto A, Meinel L, Li C, Kaplan DL. Silk microspheres for encapsulation and controlled release. J Control Release 2007;117(3):360-370.

23. Brandenberger H, Nüssli D, Piech V, Widmer F. Monodisperse particle production: a new method to prevent drop coalescence using electrostatic forces. J Electrostat 1999;45:227-238.

24. Nazarov R, Jin HJ, Kaplan DL. Porous 3-D scaffolds from regenerated silk fibroin. Biomacromolecules 2004;5(3):718-726.

25. Min BM, Jeong L, Lee KY, Park WH. Regenerated silk fibroin nanofibers: water vapor-induced structural changes and their effects on the behavior of normal human cells. Macromol Biosci 2006;6(4):285-292.

26. Sofia S, McCarthy MB, Gronowicz G, Kaplan DL. Functionalized silk-based biomaterials for bone formation. J Biomed Mater Res 2001;54(1):139-148.

27. Luginbuehl V, Wenk E, Koch A, Gander B, Merkle HP, Meinel L. Insulin-like growth factor I-releasing alginate-tricalciumphosphate composites for bone regeneration. Pharm Res 2005;22(6):940-950.

28. Pollak MN, Polychronakos C, Richard M. Insulinlike growth factor I: a potent mitogen for human osteogenic sarcoma. J Natl Cancer Inst 1990;82(4):301-305.

29. Lopaczynski W, Harris S, Nissley P. Insulin-like growth factor-I (IGF-I) dependent phosphorylation of the IGF-I receptor in MG-63 cells. Regul Pept 1993;48(1-2):207-216.

30. Seifert D, Phillips J. Production of small, monodispersed alginate beads for cell immobilization. Biotechnol Prog 1997;13:562-568.

31. Serp D, Cantana E, Heinzen C, Von Stockar U, Marison IW. Characterization of an encapsulation device for the production of monodisperse alginate beads for cell immobilization. Biotechnol Bioeng 2000;70(1):41-53.

32. Meesters G. Mechanisms of Droplet Formation. Delft University Press, Delft 1992.

33. Tsukada M, Freddi G, Minoura N, Allara G. Preparation and application of porous silk fibroin materials. J Appl Polym Sci 1994;54:507-514.

34. Asakura T, Kuzuhara A, Tabeta R, Saito H. Conformation characterization of Bombyx mori silk fibroin in the solid state by high-frequency 13C cross polarization-magic angle spinning NMR, X-ray diffraction, and infrared spectroscopy. Macromolecules 1985;18:1841-1845.

35. Rössle M, Panine P, Urban VS, Riekel C. Structural evolution of regenerated silk fibroin under shear: combined wide- and small-angle x-ray scattering experiments using synchrotron radiation. Biopolymers 2004;74(4):316-327.

36. Monti P, Freddi G, Bertoluzza A, Kasai N, Tsukada M. Raman spectroscopic studies of silk fibroin from Bombyx mori. J Raman Spectrosc 1998;29:297-304.

37. Ishida M, Asakura T, Yokoi M, Saito H. Solvent- and mechanical-treatment-induced conformational transition of silk fibroins studied by high-resolution solid-state 13C NMR spectroscopy. Macromolecules 1990;23:88-94.

38. Marsh RE, Corey RB, Pauling L. An investigation of the structure of silk fibroin. Biochim Biophys Acta 1955;16(1):1-34.

39. Pace CN, Trevino S, Prabhakaran E, Scholtz JM. Protein structure, stability and solubility in water and other solvents. Philos Trans R Soc Lond B Biol Sci 2004 Aug 29;359(1448):1225-1234; discussion 1234-1225.

40. Wade A, Reynolds J, editors. Martindale: The extra pharmacopoeia. 27th ed. London: The Pharmaceutical Press, 1977.

41. Reynolds J, Prasad A, editors. Martindale: The extra pharmacopoeia. 28th ed. London: The Pharmaceutical Press, 1982.

42. Narayani R, Rao KP. Controlled release of anticancer drug methotrexate from biodegradable gelatin microspheres. J Microencapsul 1994;11(1):69-77.

43. Bezemer JM, Radersma R, Grijpma DW, Dijkstra PJ, van Blitterswijk CA, Feijen J. Microspheres for protein delivery prepared from amphiphilic multiblock copolymers. 2. Modulation of release rate. J Control Release 2000;67(2-3):249-260.

44.   Yang Y-Y, Chung T-S, Bai X-L, Chan W-K. Effect of preparation conditions on morphology and release profiles of biodegradable polymeric microspheres containing protein fabricated by double-emulsion method. Chem Eng Sci 2000;55:2223-2236.

45.   Wang X, Hu X, Daley A, Rabotyagova O, Cebe P, Kaplan DL. Nanolayer biomaterial coatings of silk fibroin for controlled release. J Control Release 2007;121(3):190-199.

46.   Zhou CZ, Confalonieri F, Medina N, Zivanovic Y, Esnault C, Yang T, et al. Fine organization of Bombyx mori fibroin heavy chain gene. Nucleic Acids Res 2000;28(12):2413-2419.

47.   Foo CW, Bini E, Hensman J, Knight DP, Lewis RV, Kaplan DL. Role of pH and charge on silk protein assembly in insects and spiders. Appl Phys A 2006;82:223-233.

48.   Paul G, Steuernagel S, Koller H. Non-covalent interactions of a drug molecule encapsulated in a hybrid silica gel. Chem Commun (Camb) 2007;48:5194-5196.

49.   Blundell TL, Bedarkar S, Rinderknecht E, Humbel RE. Insulin-like growth factor: a model for tertiary structure accounting for immunoreactivity and receptor binding. Proc Natl Acad Sci U S A 1978;75(1):180-184.

CHAPTER III

MICROPOROUS SILK FIBROIN SCAFFOLDS EMBEDDING PLGA MICROPARTICLES FOR CONTROLLED GROWTH FACTOR DELIVERY IN TISSUE ENGINEERING

Esther Wenk, Anne J. Meinel, Sarah Wildy, Hans P. Merkle, Lorenz Meinel

Institute of Pharmaceutical Sciences, ETH Zurich, Wolfgang-Pauli-Strasse 10, CH-8093 Zurich, Switzerland

Abstract

The development of prototype scaffolds for either direct implantation or tissue engineering purposes and featuring spatiotemporal control of growth factor release is highly desirable. Silk fibroin (SF) scaffolds with interconnective pores, carrying embedded microparticles that were loaded with insulin-like growth factor I (IGF-I), were prepared by a porogen leaching protocol. Treatments with methanol or water vapor induced water insolubility of SF based on an increase in β-sheet content as analyzed by FTIR. Pore interconnectivity was demonstrated by SEM. Porosities were in the range of 70% to 90%, depending on the treatment applied, and were better preserved when methanol or water vapor treatments were prior to porogen leaching. IGF-I was encapsulated into two different types of poly(lactide-co-glycolide) microparticles (PLGA MP) using uncapped PLGA (50:50) with molecular weights of either 14 or 35 kDa to control IGF-I release kinetics from the SF scaffold. Embedded PLGA MP were located in the walls or intersections of the SF scaffold. Embedment of the PLGA MP into the scaffolds led to more sustained release rates as compared to the free PLGA MP, whereas the hydrolytic degradation of the two PLGA MP types was not affected. The PLGA types used had distinct effects on IGF-I release kinetics. Particularly the supernatants of the lower molecular weight PLGA formulations turned out to release bioactive IGF-I. Our studies justify future investigations of the developed constructs for tissue engineering applications.

1. Introduction

The spatiotemporal control of growth factors delivery to mimic physiological patterns is considered a promising approach for the regeneration of problematic bone defects resulting either from disease, fracture or surgery [1, 2]. A well known option to modulate localized growth factor release is the use of biodegradable poly(lactide-co-glycolide) microparticles (PLGA MP) [3-5]. It is well established that the release kinetics of PLGA MP may be adjusted by (i) the molecular weight of the polymer, (ii) the polymer's ratio of lactic to glycolic acid, (iii) the capped or non-capped nature of its terminal ends, (iv) the preparation technology involved, (v) the size of the fabricated MP, and (vi) by their loadings [4, 5].

IGF-I has been demonstrated to stimulate the proliferation of osteoblasts and the synthesis of new bone matrix [6]. Moreover, this 7.6 kDa polypeptide has shown stimulating effects on fracture repair *in vivo* [7-9]. The biomedical potential of IGF-I loaded biodegradable PLGA MP as a drug delivery system in bone repair has been previously demonstrated in a sheep model [3].

A delivery system designed for bone repair should ideally combine an osteoinductive growth factor for cellular differentiation and growth with an osteoconductive 3D scaffold to enhance cell recruitment and attachment, and as structural support for cells and new tissue formed in the scaffold during the initial stages post implantation [10]. The challenge of such scaffolds in mimicking endogenous release kinetics lies in (i) the preservation of growth factor integrity and functionality during preparation of the scaffold, (ii) control of appropriate growth factor release kinetics upon tissue culture or after implantation. Additional benefits may arise from (iii) an optional control of independent release rates of more than one growth factor, and (iv) the potentially targeted delivery to specific cell populations [2].

Silk fibroin (SF), a fibrous protein biopolymer derived from the silkworm *Bombyx mori*, has the advantage of being soluble in water and, therefore, allows mild fabrication conditions that are favorable for embedding sensitive agents such as growth factors. Its unique properties such as advantageous processability and superior mechanical strength as well as its biocompatibility and long-term

biodegradability [11-13] led to the exploration of SF as a biomaterial for several biomedical applications [14-17]. Recently, IGF-I has been directly embedded in a SF scaffold under mild fabrication conditions, and was shown to be released in its bioactive form with the potential to stimulate chondrogenic differentiation of human mesenchymal stem cells [18].

Little has been reported on how the release kinetics of growth factors may affect tissue repair. Its principal significance has been reported for ectopic bone formation in rats showing an interesting correlation between growth factor pharmacokinetics and osteoinduction [19]. Due to similar amino acid sequences and comparable specific activities *in vitro*, an equivalent specific potency for ectopic bone formation was expected from embedded BMP-2 versus BMP-4. However, markedly better osteoinduction was found with BMP-2 as compared to BMP-4, which was explained by better retention and, therefore, higher local concentrations of BMP-2 owing to its stronger electrostatic interactions with the applied biomaterials. Nevertheless, simple adsorption or incorporation of the growth factor onto/into a scaffold only allows limited control over the release kinetics. Using growth factor loaded MP for embedment into scaffolds is expected to better control the release kinetics not only through the scaffold itself but also through the degradation and release kinetics of the MP. Sufficient local levels of growth factors may be achieved by embedment of either suitable quantities of MP or sufficiently loaded MP. So far several studies described the positive effects of MP loaded with proteinaceous agents and embedded in scaffolds [20-24]. The advantage of embedded MP loaded with a growth factor versus adsorbed growth factor has been previously shown with glycidyl methacrylated dextran/gelatin scaffolds containing BMP loaded MP, which gained significantly more periodontal tissue regeneration as compared to BMP adsorbed on scaffolds [25].

In this study, we introduce and evaluate protocols to fabricate prototype SF scaffolds with embedded PLGA microparticles that were loaded with IGF-I. For scaffold fabrication we used aqueous SF solutions and followed a paraffin leaching protocol as previously described [18, 26]. Further integrated into scaffold fabrication was the embedment of different types of IGF-I releasing PLGA MP. Following various protocols the scaffolds were also treated with

either methanol or with water vapor as a milder alternative. Scaffolds were characterized using FTIR and SEM and analyzed in terms of shrinkage and porosity relative to prior treatments. They were further tested for their capacity to sustain IGF-I release and for the underlying mechanism of the *in vitro* degradation kinetics of the PLGA MP when embedded in the scaffolds. Also we tested the bioactivity of released IGF-I.

2. Materials and Methods

2.1. Materials

Cocoons of *Bombyx mori* were kindly supplied by Trudel Silk Inc. (Zurich, Switzerland). End-group uncapped poly(lactide-co-glycolide) (PLGA) 50:50 with a molecular weight of 14 kDa (Resomer RG502H) and a molecular weight of 35 kDa (Resomer RG503H), respectively, were from Boehringer-Ingelheim (Ingelheim, Germany). Physiogel (40 mg/ml of succinylated gelatin hydrolysate) was from Braun Medical (Sempach, Switzerland), acetonitrile from Merck (Darmstadt, Germany), dichloromethane (DCM), methanol, 2-propanol and hexane from Scharlau (Tägerig, Switzerland). Poly(vinylalcohol) (PVA, Mowiol 8-88) was from Kuraray (Frankfurt, Germany) and polysorbate 20 (Tween 20) from Hänseler (Herisau, Switzerland). For the preparation of paraffin spheres we used paraffin wax from Fluka (Buchs, Switzerland) and gelatine from Hänseler (Herisau, Switzerland). Recombinant human IGF-I was kindly provided by Chiron Corporation (Emeryville, CA). For a bioassay on its bioactivity, we used bovine serum albumin (BSA) and 3-[4,5-dimethylthiazol-2-yl]-2,5-diphenyltetrazolium bromide (MTT) from Sigma (Buchs, Switzerland), and human osteosarcoma MG-63 cells from ATCC (Manassas, VA). Eagle's MEM, fetal bovine serum (FBS), penicillin G and streptomycin, and non-essential amino acids were from Invitrogen (Paisley, UK). All other substances used were of analytical or pharmaceutical grade and obtained from Fluka (Buchs, Switzerland).

2.2. Preparation of microparticles

IGF-I loaded PLGA MP were prepared by a previously described double-emulsion solvent extraction method [27]. Briefly, 0.35 ml of internal aqueous solution containing 275 µg IGF-I and 4 mg succinylated gelatin (Physiogel) as a protein stabilizer were emulsified by ultrasonication in 3 ml DCM solution containing either 100 mg PLGA 502H or PLGA 503H. This W_1/O-dispersion was introduced into 50 ml of a 5% PVA solution, stirred at a frequency of 500 min^{-1} for 2 min to form a W_1/O/W_2-dispersion and poured into 600 ml water for DCM extraction for one hour. The resulting MP were collected by filtration and dried under reduced pressure at room temperature overnight. Controls (control PLGA 502H MP and control PLGA 503H MP) were prepared by replacing the IGF-I solution by ultrapure water.

2.3. Particle size analysis

The particle size of PLGA MP was determined by laser light diffractometry (Mastersizer X, Malvern, Worcestershire, UK) using a Fraunhofer diffraction model to analyze the raw data. Particle size was characterized by the mean diameter calculated from the volume-moment average of the size distribution, i.e. D[4,3].

2.4. IGF-I content of microparticles and encapsulation efficiency

The actual IGF-I content of the MP was analyzed as previously described [27]. Briefly, 10 mg of MP were dissolved in 0.3 ml DCM (n = 3). Then, 0.7 ml of acetone was added, and the vial was vortexed and centrifuged at a frequency of 14,000 min^{-1} for 5 min (Eppendorf centrifuge 5417R, Vaudaux-Eppendorf AG, Basel, Switzerland). The supernatant was removed, and 0.9 ml of a 3:1 acetone:DCM mixture was added. This washing procedure was repeated three times. The residue was dissolved in 0.1 M acetic acid. IGF-I was assayed by HPLC using a Merck system (Dübendorf, Switzerland) consisting of a sample cooler, an autoinjector (L-7200), a computer interface (D-7000), a pump (L-7100) and a UV detector (L-7455). Separation was performed on a Zorbax

300SB CN column (150 mm x 4.6 mm) at a flow rate of 1 ml/min. Two eluents were used: (A) consisting of 5% acetonitrile and 0.2% trifluoroacetic acid (TFA) in water, and (B) 80% acetonitrile and 0.2% TFA in water. The solvent was initially composed of 74% (v/v) eluent A. The solvent was changed over 30 min to 100% eluent B. Then, initial conditions were set to wash the column. IGF-I was detected at 214 nm and quantified by measuring peak area. Theoretical drug content was calculated assuming that the entire amount of drug was encapsulated and no drug loss occurred at any stage of MP preparation. IGF-I contents were expressed as percentage of IGF-I per PLGA (wt/wt). Encapsulation efficiencies were calculated as percentage of actual versus theoretical drug content.

2.5. Preparation of paraffin spheres

Paraffin spheres were used as a porogen for the preparation of SF scaffolds and prepared as previously described [26]. Briefly, gelatin was dissolved in ultrapure water of 80°C to obtain a concentration of 30 g/l and mixed with paraffin at a final concentration of 200 g/l. The emulsion was stirred for 15 min and then poured into ice water. The resulting paraffin spheres were collected by filtration, thoroughly washed with ultrapure water and dried under reduced pressure at room temperature. The desired paraffin spheres with a diameter of 200 to 300 μm were obtained by sieving using standard sieves (Retsch, Haan, Germany).

2.6. Preparation of SF scaffolds

Aqueous SF solution was prepared from cocoons of the silkworm *Bombyx mori* as previously described [28]. Briefly, cocoons were boiled two times for 1 h in an aqueous solution of 0.02 M Na_2CO_3 and thoroughly rinsed with water to remove sericin. Extracted SF was dissolved in a 9 M aqueous LiBr solution to obtain a 10% (w/v) solution. This solution was dialyzed against water for 2.5 days using Slide-a-Lyzer dialysis cassettes (Pierce, Woburn, MA; MWCO 3500 g/mol), followed by dialysis against a 13% (w/v) PEG (MW 6000 g/mol) solution at room temperature in order to obtain a 20% (w/v) SF solution.

SF scaffolds were prepared as previously described [26] with slight modifications. Briefly, 150 mg paraffin spheres of 200 to 300 μm diameter were filled into cylindrical molds of 8 mm inner diameter prepared from 2.5 ml syringes, and sintered by annealing at 37°C for 45 min in order to achieve sufficient pore interconnectivity within the scaffold. SF scaffolds embedding PLGA MP were prepared by mixing 5 mg previously fabricated PLGA MP with the paraffin spheres prior to sintering the spheres by annealing at 37°C for 45 min. After cooling to room temperature, 125 μl of a 20% SF solution was added to the mold and carefully aspirated to ensure a complete fill-up of the interspace between the spheres with SF solution. The constructs were then shock-frozen in liquid nitrogen and freeze-dried for 1.5 days, with the main drying period at -30°C for 16 h (Lyovac GT2, FINN-AQUA, Hurth, Germany). The influence of different treatments on the freeze-dried specimens was tested to validate a suitable method to prepare SF scaffolds for tissue engineering applications. They were therefore either (A) treated two times with hexane for 12 h to extract the paraffin spheres (code: "untreated"), (B) treated with a 90% methanol solution at room temperature for 30 min and then treated two times with hexane for 12 h to extract the paraffin spheres (code: "1st methanol") [26], (C) exposed to water vapor of 96% relative humidity by equilibration in the presence of a saturated aqueous Na_2SO_4 solution at room temperature for 24 h as previously described [29] and then treated two times with hexane for 12 h to extract the paraffin spheres (code: "1st water vapor"), (D) treated two times with hexane for 12 h to extract the paraffin spheres and then treated with a 90% methanol solution at room temperature for 30 min (code: "2nd methanol"), or (E) treated two times with hexane for 12 h to extract the paraffin spheres and then exposed to water vapor of 96% relative humidity by equilibration in the presence of a saturated aqueous Na_2SO_4 solution at room temperature for 24 h (code: "2nd water vapor") (Fig. 1). Hexane replacement was performed as described before [18, 26]. The resulting scaffolds were then dried under reduced pressure for 12 h to minimize residual hexane as previously reported [18, 26].
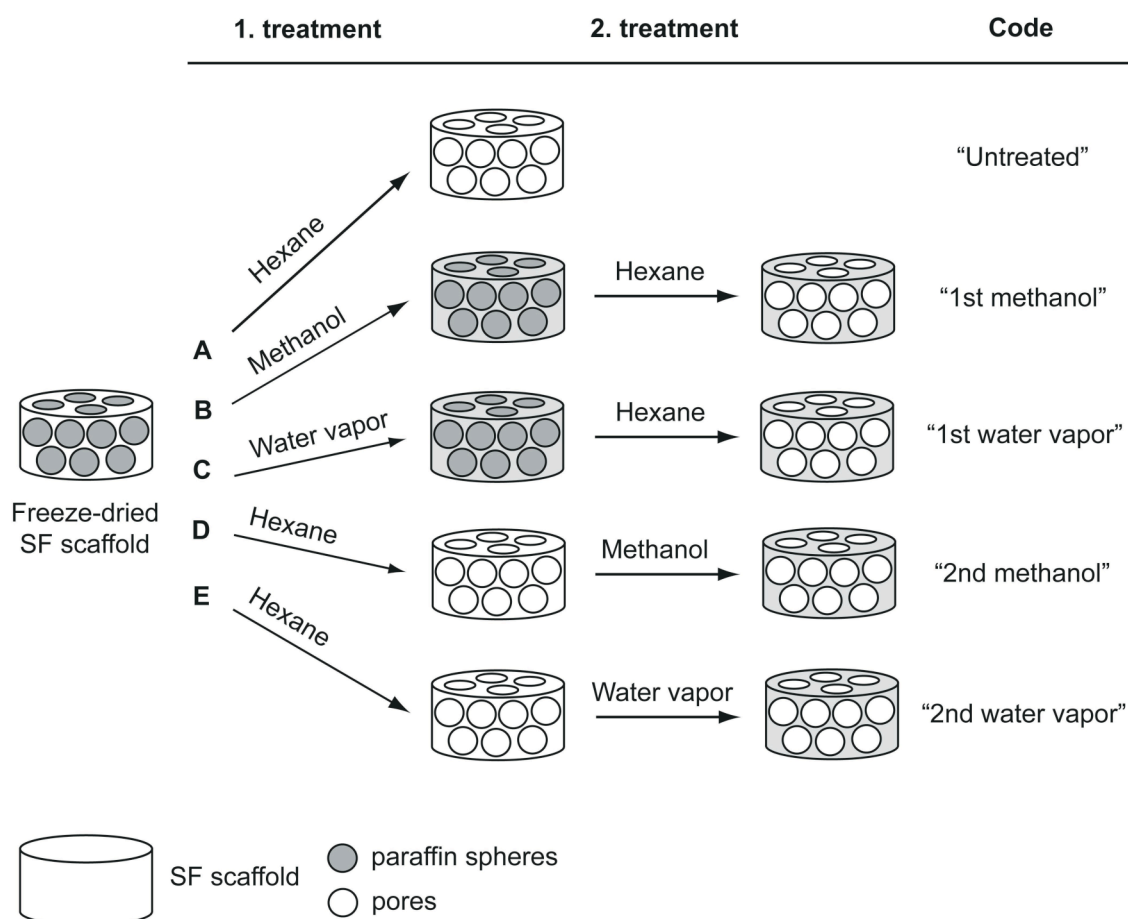
Fig. 1. *Illustration showing the different treatments applied during preparation of SF scaffolds.*

2.7. Scanning electron microscopy (SEM)

PLGA MP alone and cross-sections of SF scaffolds with and without embedded PLGA MP were platinum-coated and examined morphologically by scanning electron microscopy (SEM, Leo Gemini 1530, Zeiss, Oberkochen, Germany). Cross-sections were prepared by cutting dried SF scaffolds with a razor blade.

2.8. Shrinkage and porosity of SF scaffolds

To monitor the potential shrinkage of the SF scaffolds upon paraffin elution as well as after treatment with methanol or water vapor, the original and

final diameters of the scaffolds were measured with a slide gauge (n = 4) and were expressed as the percentage of the diameters of the original freeze-dried SF scaffolds still including the porogen.

The porosity of the SF scaffolds was analyzed by comparison of the overall scaffold volumes versus the true volumes of the SF material of the specific scaffolds, which were analyzed by means of a helium pycnometer (Accu Pic 1330, Micromeritics, Mönchengladbach, Germany; n = 3).

2.9. Fourier-transform infrared spectroscopy (FTIR)

For the analysis of their β-sheet content, SF scaffolds were ground, the samples mixed with KBr and compressed to KBr disks. FTIR spectroscopy was performed with a 2000 FT-IR Spectrometer V3,01 (Perkin Elmer, Boston, MA).

2.10. In vitro IGF-I release

IGF-I release from free PLGA MP and from PLGA MP embedded into SF scaffolds was studied in 1.0 ml release medium (50 mM sodium acetate, 100 mM sodium chloride, 0.02% polysorbate 20, 0.02% sodium azide, pH 5.4; this release medium was chosen to preserve IGF-I structure and activity [30]) at 37°C for 49 days (n = 5). Only scaffolds were tested which were previously treated two times with hexane for 12 h to extract the paraffin spheres and were then exposed to water vapor ("2nd water vapor"). The following formulations were examined: (i) 5 mg free PLGA 502H MP containing 8.1 μg IGF-I, (ii) 5 mg PLGA 502H MP containing 8.1 μg IGF-I and embedded in SF scaffold, (iii) 5 mg free PLGA 503H MP containing 6.3 μg IGF-I, (iv) 5 mg PLGA 503H MP containing 6.3 μg IGF-I and embedded in SF scaffold. Negative controls of each of the above mentioned formulations were prepared by replacing IGF-I loaded PLGA MP with control PLGA MP without IGF-I. The release medium was fully exchanged with fresh medium after 13, 37, 72, and 93 h and 7, 10, 16, 22, 26, 34, 42, and 49 days. Medium samples were immediately frozen at –20 °C, and were then analyzed using an enzyme-linked immunosorbent assay (ELISA,

DuoSet Human) according to the manufacturer's protocol (R&D Systems, Minneapolis, MN).

2.11. Bioassay for bioactivity of IGF-I

A bioassay was applied to analyze the bioactivity of the supernatants as obtained from the IGF-I release tests. IGF-I is a well-known stimulator of the *in vitro* proliferation of MG-63 cells [31, 32]. MG-63 cells were grown in growth medium (MEM containing 8.9% FBS, 1.79 mM L-glutamine, 89 U/ml penicillin G and 89 μg/ml streptomycin). Medium was exchanged every 2 – 3 days. Cells were trypsinized and diluted to 2×10^5 cells/ml in assay medium (MEM containing 0.456% BSA, 1.84 mM L-glutamine, 92 U/ml penicillin G and 92 μg/ml streptomycin). Using a 96-well plate, 100 μl of this cell suspension was added to each well, incubated at 37 °C and 5% CO_2 for 24 h, and the medium discarded. Supernatants of the *in vitro* IGF-I release study, which were collected in the time periods of 0 – 0.5 days, 4 - 7 days, 16 - 22 days and 34 - 42 days (each n = 4) were diluted 1:100 in assay medium, 100 μl of the dilution added to the assay plate and incubated at 37 °C and 5% CO_2 for 48 hours. Cells were stained with a 2% MTT solution in PBS for 4 hours. The formed formazan was solubilized with 3% sodium dodecyl sulfate (SDS) and 0.04 M HCl in 2-propanol. Absorbance was read at 570 nm. The absorbance of the supernatants of the negative controls (corresponding formulations without IGF-I) of the release study was defined as 100%. Additional samples were taken from solutions containing control cells that were incubated with 0.1, 1 and 6.25 ng IGF-I/ml assay medium (positive controls). The dilution factor of 1:100 was found to assure the range of an approximately semi-logarithmic relationship between absorbance and IGF-I concentration.

2.12. Degradation of SF scaffolds and PLGA MP

Degradation of water vapor treated SF scaffolds without PLGA MP as control was analyzed by weight before and after incubation in 1 ml release medium at 37°C for 49 days (n = 5).

To monitor the degradation of free PLGA MP and PLGA MP embedded in SF scaffolds, supernatants collected at day 3, 7, 16, 22, 26, 34 and 49 of the IGF-I release study were analyzed. Briefly, aliquots of 200 µl of the supernatants of the IGF-I release study were put into fresh tubes and the release medium was evaporated (n = 5). The residue was incubated with 50 µl of a 13.5 M NaOH solution at room temperature for 1 h and autoclaved at 121°C for 20 min to completely hydrolyze the released fragments in order to obtain the monomers glycolic acid and lactic acid [33]. 20 µl of the solution was neutralized with 33.2 µl glacial acetic acid and diluted with 53.2 µl ultrapure water. Lactic acid was determined by adding 250 µl of a lactate reagent (Trinity Biotech, St. Louis, MO) to 10 µl of the hydrolyzed and neutralized samples. The samples were incubated at room temperature for 10 min and the absorbance was read at 540 nm. As standards, 5 mg PLGA 502H MP and 5 mg PLGA 503H MP were used and treated as the samples. Degradation rate was expressed as mg PLGA per day.

2.13. Statistics

The results are expressed as means ± standard deviations. Statistical analysis was performed using the Student t-test as well as one-way analysis of variance (ANOVA) followed by the Tukey HSD test for post hoc comparison. Differences were considered significant when $p < 0.05$ and as highly significant when $p < 0.01$.

3. Results

3.1. Characterization of PLGA MP

All PLGA MP formulations were in the size range between 41.4 μm and 60.2 μm (Table 1). IGF-I encapsulation efficiencies were higher for PLGA 502H MP (59.04 ± 0.02%) as compared to PLGA 503H MP (45.55 ± 4.05%). This corresponds to a total IGF-I loading of 1.62 ± 0.04 μg/mg with PLGA 502H MP and 1.25 ± 0.11 μg/mg with PLGA 503H MP (Table 1).

Table 1. *Particle size, theoretical and actual IGF-I content (expressed as wt IGF-I/wt PLGA), encapsulation efficiency (calculated as percentage of actual versus theoretical IGF-I content) and total loading of PLGA MP prepared from PLGA 502H and 503H.*

Formulation	Particle size [μm]	Theoretical IGF-I content % (wt/wt)	Actual IGF-I content % (wt/wt) mean ± SD	Encapsulation efficiency % (wt/wt) mean ± SD	Total loading μg mg^{-1} PLGA MP, mean ± SD
502H control	41.4 ± 2.4				
503H control	60.2 ± 8.5				
502H IGF-I	44.6 ± 4.6	0.275	0.162 ± 0.004	59.044 ± 0.016	1.624 ± 0.044
503H IGF-I	50.1 ± 7.6	0.275	0.125 ± 0.011	45.547 ± 4.046	1.253 ± 0.111

3.2. Characterization of SF scaffolds

3.2.1. Scanning electron microscopy (SEM)

Cross-section analysis of the SF scaffolds by SEM revealed that all scaffolds were highly porous with marked interconnectivity (Fig. 2). After porogen leaching the SF matrix between the large pores of untreated SF scaffolds (Fig. 2A) was less porous than that of scaffolds first treated with methanol (Fig. 2B). SF scaffolds that were first treated with water vapor prior to porogen leaching showed an inhomogeneous scaffold structure. Their core section exhibited a porous fine structure between the large pores (Fig. 2C) whereas only thin walls without visible porosity were found in the peripheral section (Fig. 2D). SF scaffolds that were treated with methanol (Fig. 2E) or

water vapor (Fig. 2F) following porogen leaching showed less regular pores as compared to SF scaffolds that were first treated with either methanol or water vapor. Also a denser structure was observed in this case.
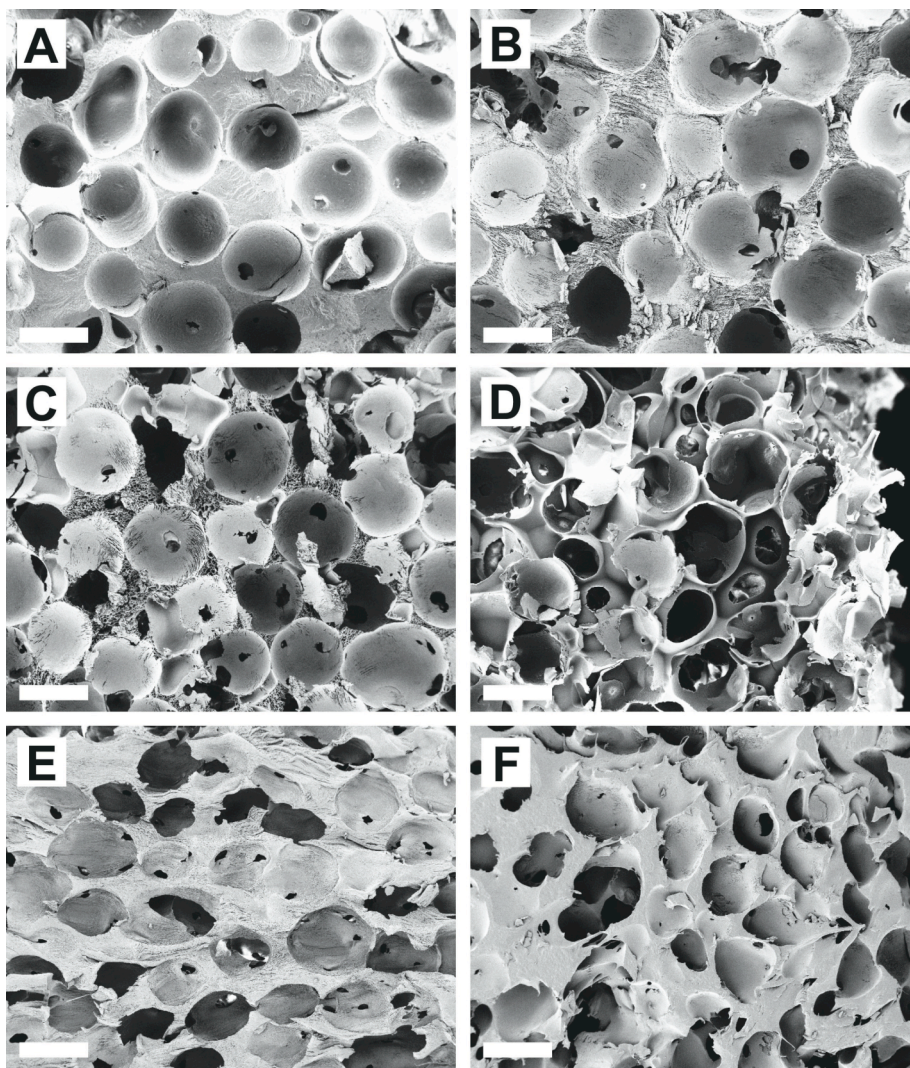
Fig. 2. *SEM images of (A) an untreated SF scaffold, (B) a SF scaffold that was first treated with methanol prior to porogen leaching, (C) the inner section of a SF scaffold that was first treated with water vapor prior to porogen leaching, (D) the outer section of a SF scaffold that was first treated with water vapor prior to porogen leaching, (E) a SF scaffold that was treated with methanol following porogen leaching, and (F) a SF scaffold that was treated with water vapor following porogen leaching. Scale bar = 200 μm.*

3.2.2. Shrinkage and porosity of SF scaffolds

Due to scaffold shrinkage, the diameters of untreated SF scaffold cylinders after porogen leaching dropped to 96.3 ± 2.3%, those that were first treated with methanol to 98.2 ± 1.2%, and those first treated with water vapor to 96.4 ± 0.7% of the original values after freeze-drying (Fig. 3A). The remaining diameters after shrinkage were thus significantly larger than those of the scaffolds that were treated with either methanol or water vapor following porogen leaching ($p < 0.01$), which shrank to 71.8 ± 3.4% and 59.1 ± 4.0%, respectively, of their original diameters after freeze-drying. No significant difference in shrinkage between the treated scaffolds was observed when they were first treated with methanol (98.2 ± 1.2%) or water vapor (96.4 ± 0.7%), whereas the diameters of the scaffolds that were treated with water vapor following porogen leaching shrank to significantly lower values (59.1 ± 4.0%) than those treated with methanol following porogen leaching (71.8 ± 3.4%) ($p < 0.05$).

Porosity measurements showed similar tendencies. The porosity of the untreated SF scaffolds after porogen leaching (97.3 ± 0.4%) as well as of those that were first treated with methanol (96.9 ± 0.8%) and water vapor (96.9 ± 0.9%) was significantly higher than that of the scaffolds that were treated with methanol (70.3 ± 11.7%) and water vapor (71.9 ± 7.1%) following porogen leaching ($p < 0.01$) (Fig. 3B).

3.2.3. FTIR

FTIR spectra of untreated SF scaffolds after porogen leaching, of SF scaffolds that were first treated with methanol or water vapor and of SF scaffolds that were treated with methanol or water vapor following porogen leaching are shown in Fig. 4. The characteristic absorption bands of untreated SF scaffolds at around 1656 cm^{-1} (amide I) and at 1543 cm^{-1} (amide II) shifted to 1628 cm^{-1} (amide I) and 1516 cm^{-1} (amide II) upon treatment with methanol and water vapor, indicating higher β-sheet based crystallinity of SF [34-37].
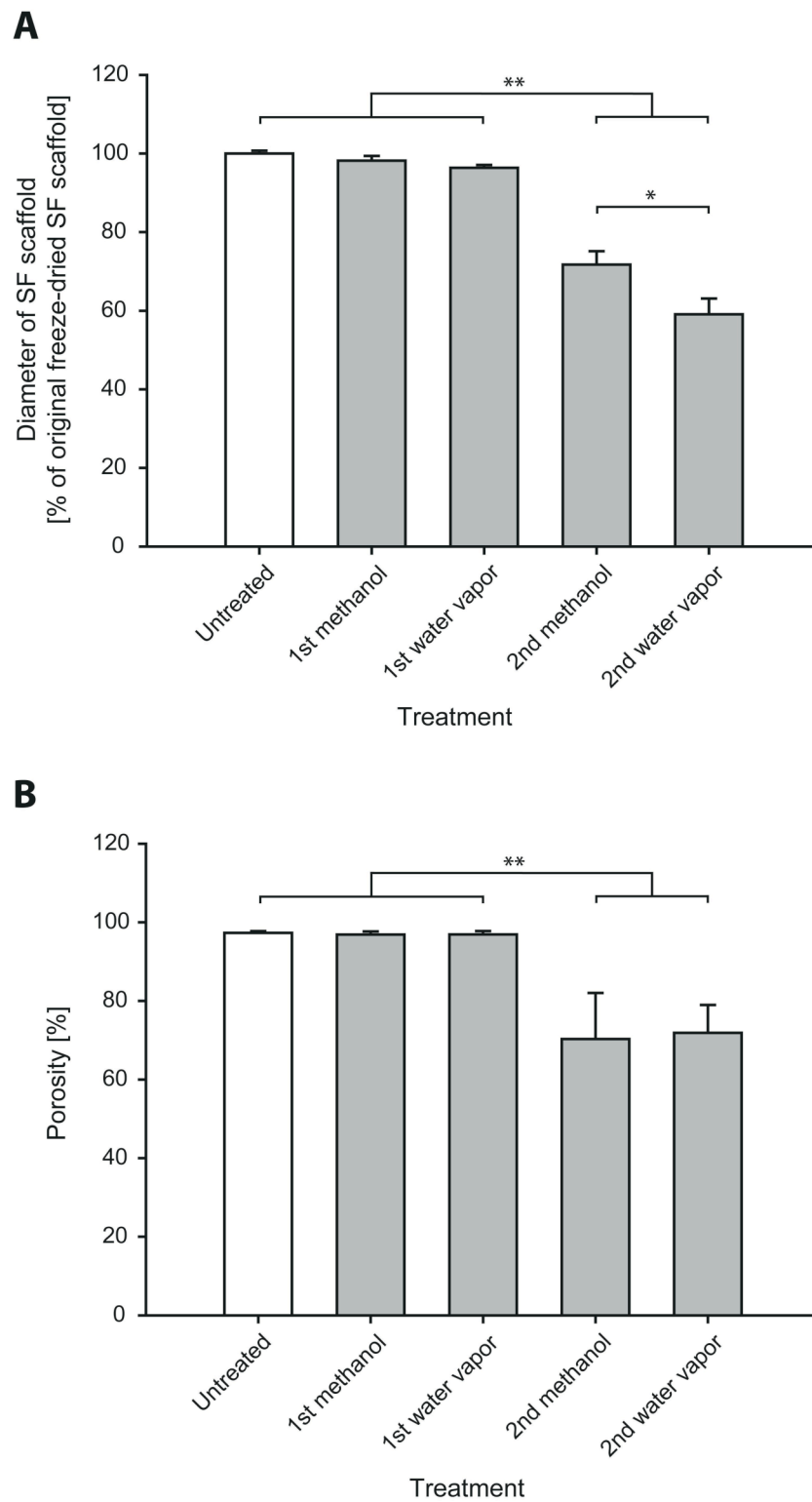
Fig. 3. *(A) Diameter of untreated and treated SF scaffolds expressed as the percentage of the diameter of the original freeze-dried SF scaffolds still including the porogen. (B) Porosity of untreated and treated SF scaffolds determined by a helium pycnometer.*
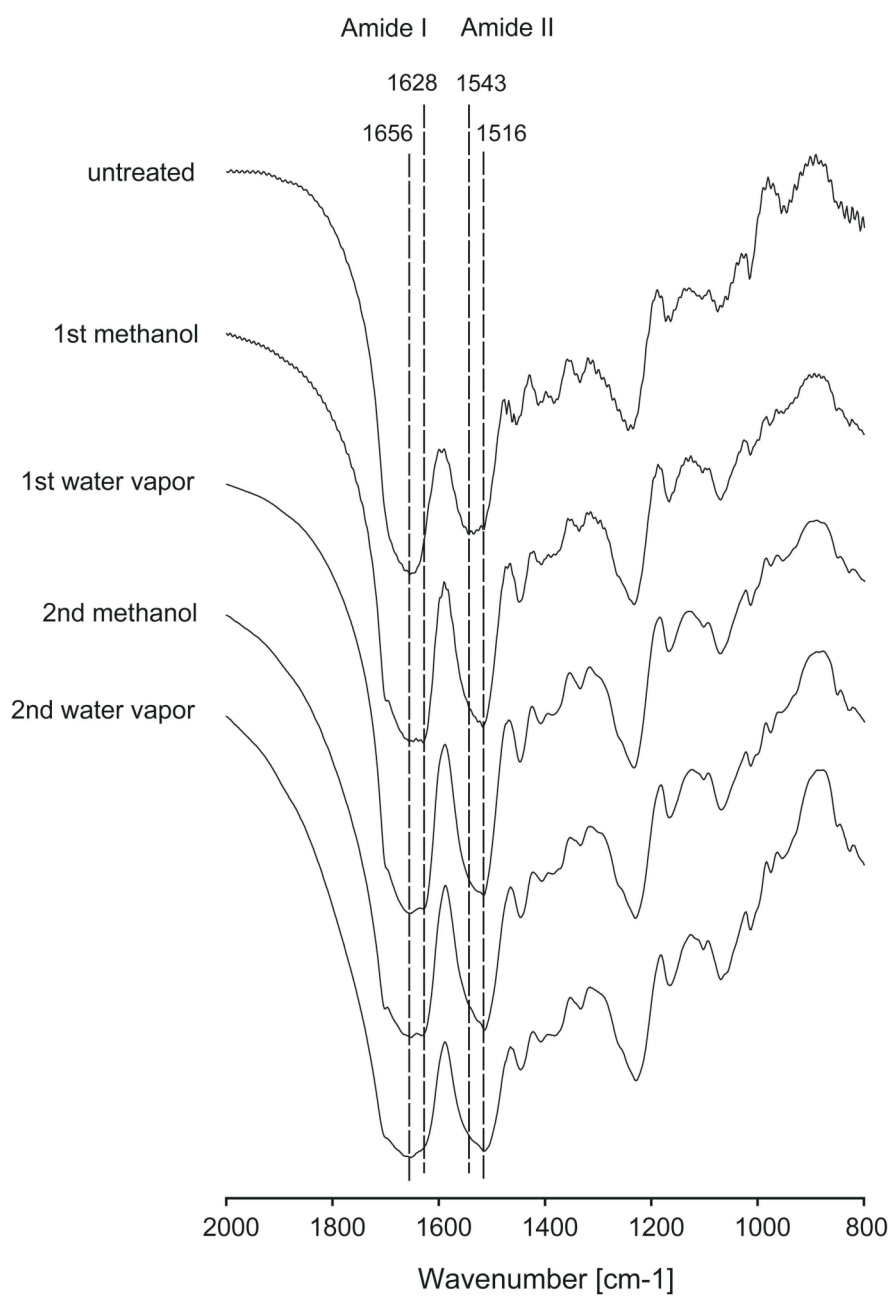
Fig. 4. *FTIR spectra of untreated and treated SF scaffolds.*

3.3. Embedment of PLGA MP in SF scaffolds

SEM studies showed that both free PLGA 502H MP and free PLGA 503H MP had a porous surface structure (Fig. 5). Cross-sections of water vapor treated SF scaffolds showed the embedded PLGA MP to be well integrated into the SF structure, strictly locating in the walls or intersections of the scaffolds. Throughout, all embedded PLGA MP appeared to be covered with a thin layer of SF. The interconnectivity of the pores was well maintained and not compromised by the embedded MP.
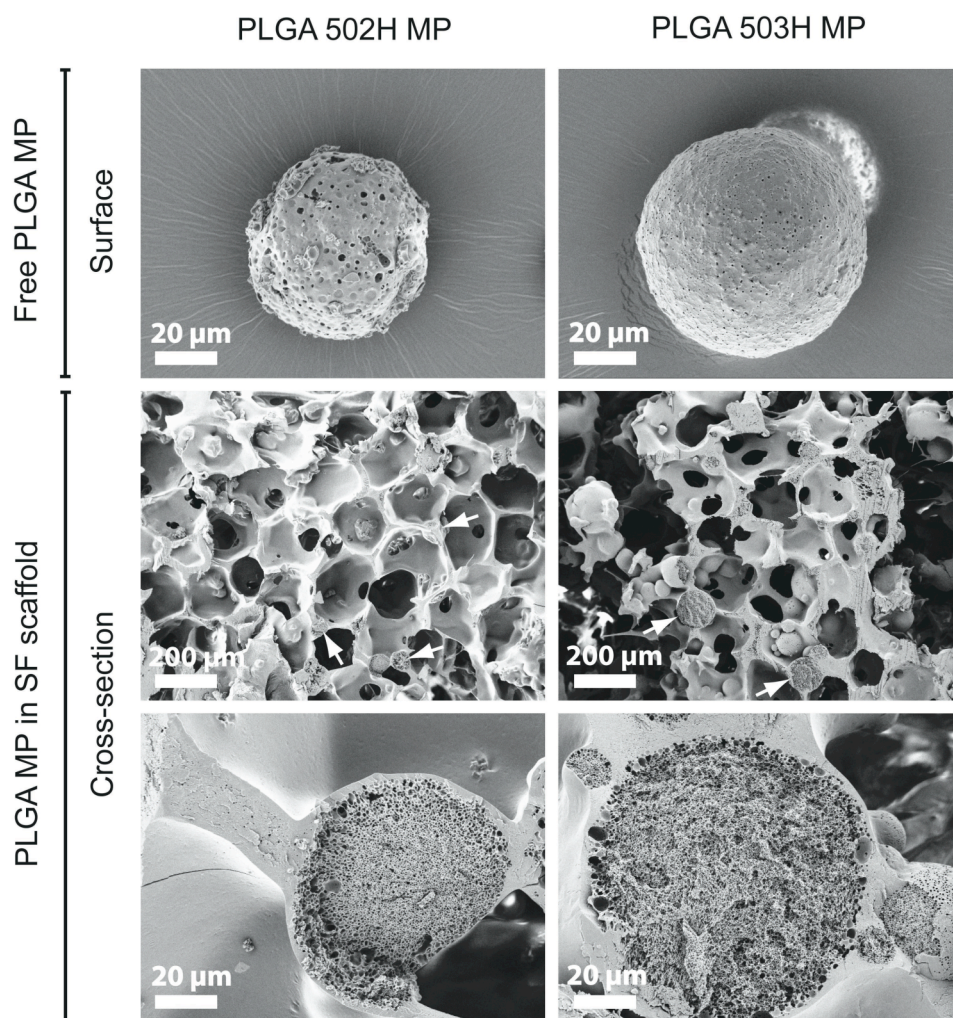

Fig. 5. *SEM images of the surface of free PLGA 502H MP and free PLGA 503H MP (first row) and cross-sections of PLGA 502H MP and PLGA 503H MP embedded in water vapor treated SF scaffolds (second and third row). Arrows = PLGA MP.*

3.4. In vitro drug release studies

The cumulative IGF-I release profiles of free PLGA MP and of PLGA MP embedded in water vapor treated SF scaffolds are shown in Fig. 6A. IGF-I release from free PLGA 502H MP and from free PLGA 503H MP was triphasic consisting of (i) a typical burst release within the first 12 h, followed by (ii) a period of low release rates until day 7 (free PLGA 502H MP) and day 16 (free PLGA 503H MP), and finally (iii) a marked increase in release from these days on. Free PLGA 502H MP and PLGA 502H MP embedded in SF scaffolds showed a burst release of 26.2 ± 5.5% and 22.4 ± 4.2%, respectively, after 0.5 d. The burst release from free PLGA 503H MP and PLGA 503H MP embedded in SF scaffolds (10.3 ± 1.1% and 3.5 ± 0.5%, respectively) was less prominent. After the burst, the release of IGF-I from embedded PLGA 502H MP was slow but continuous. Almost no IGF-I was released from embedded PLGA 503H MP until day 26, turning into a slow and continuous release from then on. After 49 days, 87.6 ± 5.8% of the initially loaded IGF-I was released from free PLGA 502H MP and 106.2 ± 3.6% from free PLGA 503H MS, respectively. On the other hand, much less, i.e. only 47.8 ± 4.5% of the initially loaded IGF-I was released from PLGA 502H MP and 23.2 ± 1.2% from PLGA 503H MP, respectively, throughout the observation period, when both were embedded in SF scaffolds. According to the obtained profiles of embedded PLGA 502H MP and embedded 503H MP, further IGF-I release is expected to occur beyond 49 days.

The bioactivity of released IGF-I was tested with a bioassay measuring the mitogenic activity of the supernatants in contact with MG-63 cells (Fig. 6B). Particularly the supernatants of the PLGA 502H formulations turned out to release bioactive IGF-I. In more detail, all supernatants collected from free PLGA 502H MP and from embedded PLGA 502H significantly enhanced cell proliferation as compared to the corresponding negative controls, irrespective of the time interval (p < 0.01). On the other hand, of the supernatants taken from free PLGA 503H MP and embedded PLGA 503H MP, only the supernatants of embedded PLGA 503H MP as collected from days 34 – 42 led to significant increases in bioactivity above the corresponding negative control (p < 0.01). No
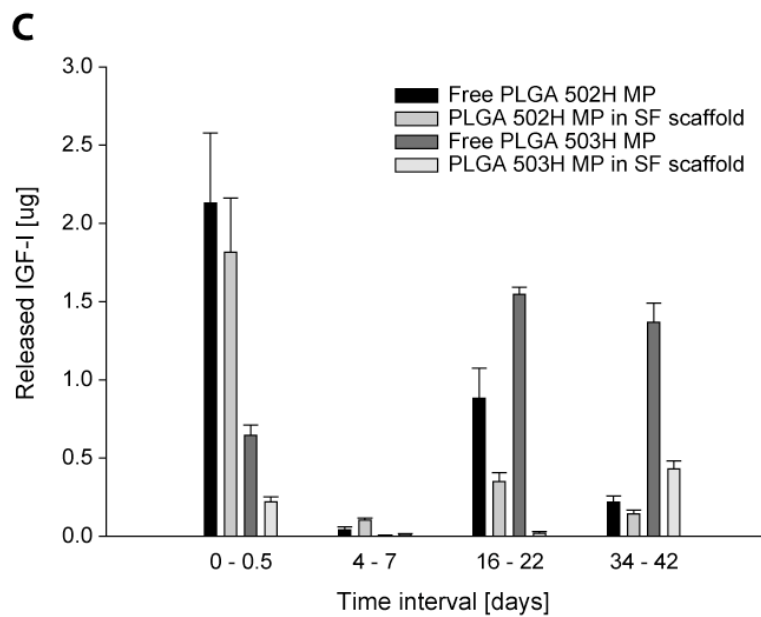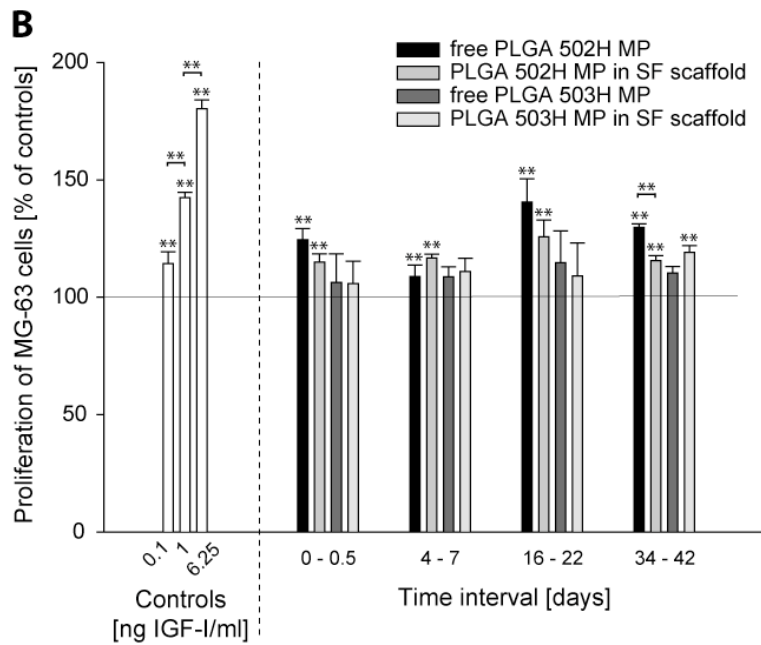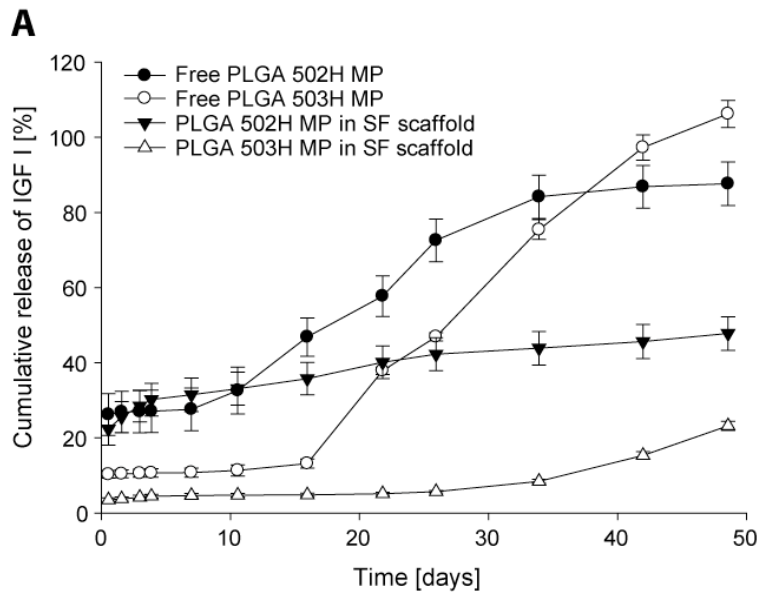
Fig. 6. *(A) Cumulative release of IGF-I either from free PLGA 502H MP, free PLGA 503H MP, PLGA 502H MP embedded in water vapor treated SF scaffolds or PLGA 503H MP embedded in water vapor treated SF scaffolds. (B) Potency of IGF-I containing supernatants from release experiments on the proliferation of MG-63 cells. Cell proliferation was expressed as the percentage absorbance of samples relative to the corresponding negative controls without IGF-I (means ± SD; **p < 0.01). Statistical differences indicated are relative to the corresponding negative controls without IGF-I. Positive controls were obtained from cells incubated with 0.1, 1 and 6.25 ng IGF-I per ml medium. (C) Released IGF-I during time intervals used for potency studies.*

significant differences were observed between supernatants collected from free PLGA MP versus embedded PLGA MP, except for the supernatants from free PLGA 502H MP and embedded PLGA 502H MP as collected from days 34 – 42. When compared with released IGF-I within the same time intervals (Fig. 6C), bioactivities followed similar trends, except for free PLGA 503H MP showing high release rates from days 16 – 22 and days 34 – 42, but low bioactivity.

3.5. Degradation studies

Degradation of water vapor treated SF scaffolds without PLGA MP as control was determined by weight before and after incubation in release medium for 49 days. Only $4.0 \pm 1.1\%$ of the scaffold was lost during this time period, roughly indicating minor hydrolytic degradation of SF under the experimental conditions.

Degradation studies of PLGA MP determined by a lactate assay showed that the degradation of the free PLGA 502H MP and the embedded PLGA 502H MP started from the beginning of the experiment and increased until day 13 (Fig. 7). On the other hand, degradation of the free PLGA 503H MP and embedded PLGA 503H MP began after a short lag around day 5 and increased until day 19. From then on the degradation rates dropped and became zero at day 45 for all formulations. Throughout the time span studied we observed no significant difference between free PLGA MP and embedded PLGA MP, except for a somewhat lower PLGA degradation of embedded PLGA 502H MP as

compared to free PLGA 502H MP at day 19 (p < 0.01). Overall, embedment into SF scaffolds did not markedly change the hydrolytic degradation profile of the two PLGA types studied.
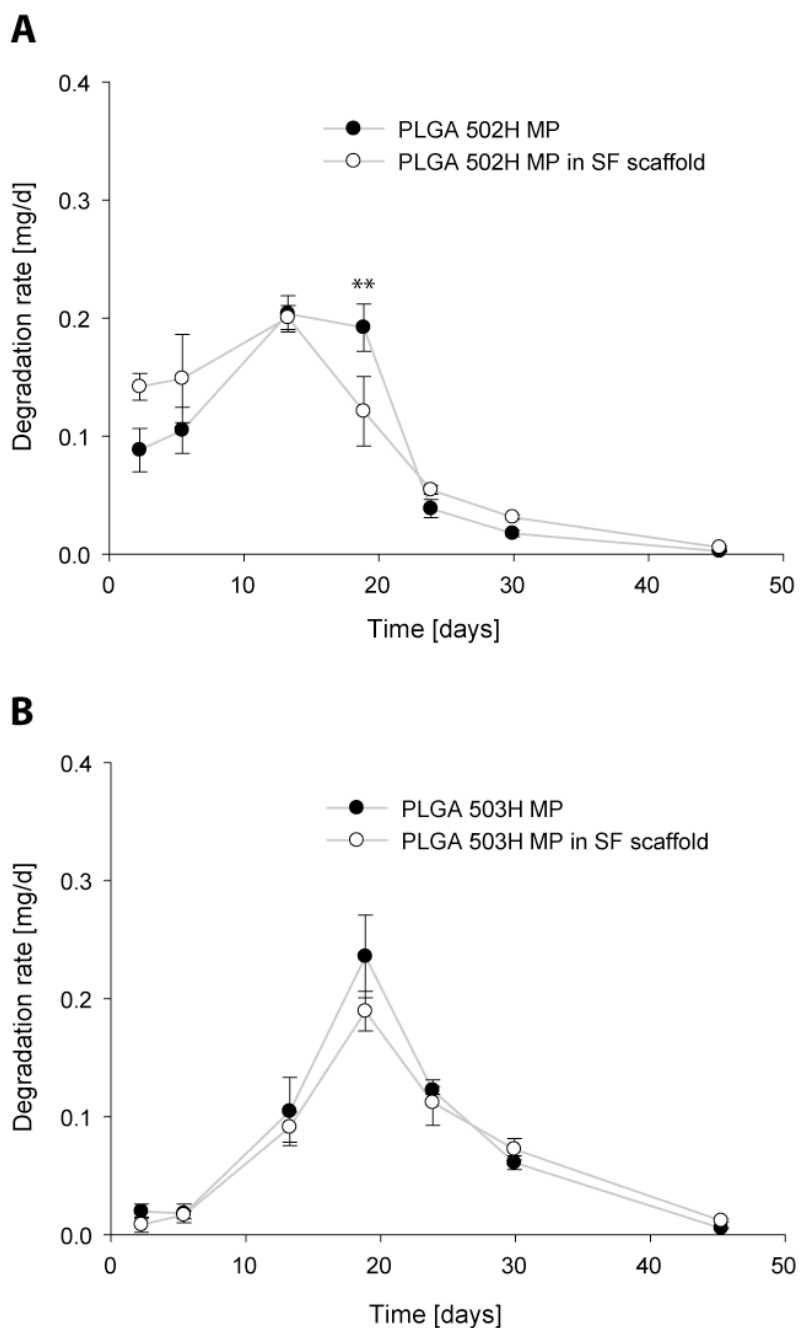
Fig. 7. *Degradation rates of (A) free PLGA 502H MP and PLGA 502H MP embedded in water vapor treated SF scaffolds, and (B) free PLGA 503H MP and PLGA 503H MP embedded in water vapor treated SF scaffolds. Data expressed as degraded PLGA in mg per day.*

4. Discussion

In physiological tissue repair biological signaling is a crucial factor controlling cellular recruitment, differentiation and proliferation. However, under critical conditions the local availability of endogenous signaling factors may be insufficient to sustain repair. Therefore, localized delivery of exogenous growth factors may be mandatory, e.g., for the repair of large (critical) bone defects [38, 39]. Incorporation of growth factors into polymeric delivery systems has been shown to provide options for stabilization and controlled delivery. Additionally, suitably designed scaffolds may be needed to support cellular attachment, differentiation and growth [10]. By combination, controlled delivery technologies and biomaterial scaffolds are expected to offer synergistic opportunities. Common methods to immobilize growth factors on scaffolds include the adsorption of growth factors onto prefabricated scaffolds prior to implantation [40] or the embedment of a growth factor during scaffold fabrication [18, 41]. Incorporation of microencapsulated growth factor into scaffolds may further improve the retention of the growth factor at the repair site, the maintenance of its bioactivity, and the sustainment of release. The stabilization of IGF-I in PLGA MP and its controlled release has been previously reported [27] and shown to have the potential to enhance new bone formation [3].

Several groups studied the incorporation of MP into scaffolds post-fabrication [20, 22, 42-45]. In contrast, incorporation of MP during fabrication of scaffolds has been less studied and mostly includes gel-like scaffolds [23, 30, 46, 47]. A common technical problem in this context is to avoid the dissolution of the MP or the premature elution of its contents into the solvent used to fabricate the scaffold. Coatings have been suggested to evade this problem. For instance, to protect PLGA MP from dissolution during fabrication of a PLGA scaffold, MP were coated with a PVA layer prior to incorporation into the scaffold [48]. In the present study, the distinctly different aqueous solubilities of the two biomaterials, PLGA and SF in its water soluble conformation, helped to avoid such problems and allowed to embed IGF-I loaded PLGA MP into SF. Here we introduce both the involved fabrication approach and a characterization of the resulting scaffold constructs, particularly in terms of their morphologies,

physical properties, *in vitro* degradation in combination with IGF-I release kinetics and mechanisms, and the bioactivities of *in vitro* released IGF-I.

Microporous SF scaffolds were prepared using aqueous SF solution and temperatures below 37°C, both favorable conditions for the incorporation of growth factors. We previously demonstrated that the bioactivity of IGF-I was maintained when using similar fabrication conditions [18]. SEM images confirmed that the treatments with hexane to elute the paraffin spheres used as porogen and the treatments with either methanol or water vapor to transform SF into its water insoluble conformation led to high pore interconnectivity (Fig. 2). For scaffolds, pore interconnectivity is crucial for cell ingrowth as well as nutrient supply and waste removal into and out of the scaffold [26]. In SF scaffolds that were treated with methanol or water vapor following porogen leaching, we observed less regular pores and a more compact structure, as determined by SEM (Fig. 2E and F), enhanced shrinkage (Fig. 3A) and a drop in porosity by about 30% (Fig. 3B) when compared to scaffolds that were first treated with methanol or water vapor prior to porogen leaching. Obviously the paraffin spheres more efficiently supported the structure of the pores and that of the scaffolds during methanol or water vapor treatment, whereas such treatments after porogen leaching caused the SF scaffolds to partly collapse and shrink in volume.

We recently described the densely packed structure of SF after treating SF spheres with methanol or exposing them to water vapor [49]. This relates to the fact that SF transforms into a β-sheet based crystalline structure during those treatments [50]. Methanol treatment has been a common method to induce water insolubility of SF by dehydration and destabilization of its random coil and unstable silk I state, leading to the silk II conformational state, which is more stable and characterized by an enrichment in β-sheet content [34-37]. Similarly, exposure to water vapor is also associated with an increase in β-sheet structure [49, 51] and has the advantage of being a mild alternative to organic solvents, especially when aiming at the incorporation of sensitive proteins such as growth factors. Indeed, increased β-sheet contents in all treated SF scaffolds were demonstrated by FTIR as indicated by a typical conformational shift in the

amide I and amide II band regions when compared to untreated SF scaffolds (Fig. 4C).

Although the pores of the SF scaffolds that were treated with methanol or water vapor following paraffin leaching were less regular and the scaffolds were subject to marked shrinkage, their pore interconnectivity was found to persist. Moreover, their porosities of about 70% as well as the porosities of scaffolds that were first treated with methanol or water vapor of about 97% were in the range of other scaffolds that were previously tested in association with bone repair both *in vitro* and *in vivo* [52].

The structure of the SF scaffolds treated with water vapor following paraffin leaching (Fig. 2F) was regular throughout the scaffolds, whereas the scaffolds that were first treated with water vapor showed differences between the core and the peripheral parts (Fig. 2C and D), which might be due to an insufficient infiltration of the water vapor during treatment when paraffin spheres were present. Therefore, water vapor treatments following paraffin leaching were preferred when IGF-I loaded PLGA MP were embedded into SF scaffolds. This mild approach was able to evade the denaturing potential of organic solvents on sensitive proteins such as many growth factors.

The decision to encapsulate IGF-I in PLGA 502H MP followed previous studies of our group [3, 27, 30]. We found similar encapsulation efficiencies and particle sizes as reported in those studies (Table 1). Additionally we prepared MP using PLGA 503H, which differed in its higher molecular weight of 35 kDa with that of PLGA 502H having a molecular weight of 14 kDa. This difference has been previously shown to largely affect the release profiles of HRP from PLGA MP [53], with the higher molecular weight showing reduced release rates. Such differences in release kinetics of a growth factor from PLGA MP may have distinct effects on bone regeneration. Here we demonstrate that both types of PLGA MP were embedded into the walls of the SF scaffolds (Fig. 5). This may be an advantage as compared to MP that are incorporated post-fabrication. This would direct the MP only into the open pores of the scaffold from where they may be easily washed out.
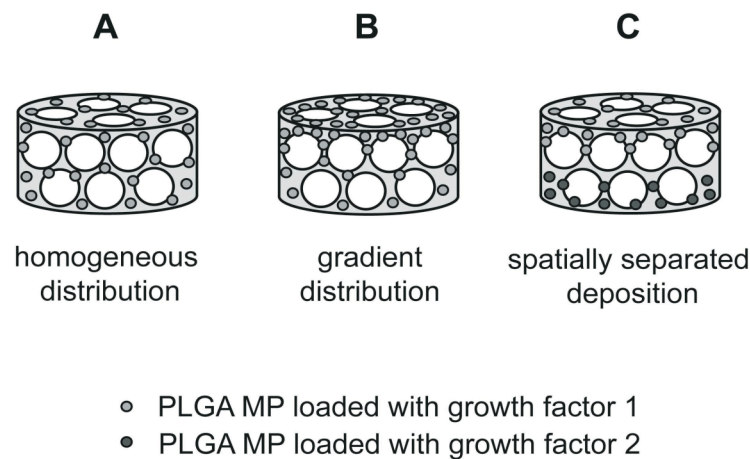
Depending on the type of PLGA used, we obtained MP with different drug release profiles (Fig. 6A). Expectedly, the initial burst from PLGA 502H MP was stronger than that from PLGA 503H MP. The main IGF-I release from free PLGA 502H MP started around one week before that of free PLGA 503H MP, resulting from the differences in molecular weight as described above. In parallel, we studied the degradation of PLGA MP using a lactate assay which confirmed the faster degradation of PLGA 502H MP, starting around one week earlier than PLGA 503H MP (Fig. 7A and B). As calculated from the free lactate levels, the degradation of both types of PLGA MP started around one week prior to the main stage of IGF-I release from free PLGA MP. IGF-I release rates from PLGA MP dropped when embedded into SF scaffolds (Fig. 6A). In contrast, there were no differences in polymer degradation rates between free PLGA MP and embedded PLGA MP. This leads to the conclusion that lactic acid and other low molecular soluble fragments of the polymers were small enough to be freely released from the SF scaffolds with essentially no additional diffusional resistance imposed. Enhanced autocatalysis of PLGA hydrolysis when embedded in the scaffold may be another explanation. In contrast, obviously owing to its much higher molecular weight of 7.6 kDa, the release of IGF-I was controlled by both PLGA degradation and diffusional resistance through the scaffold matrix. Previously we described the influence of the molecular weight of substances on their release profiles when packed into SF matrices. For instance, the higher the molecular weights of embedded dextran, the slower was its release from SF films [54]. In this context we could also show that salicylic acid, a low molecular weight molecule, was completely released from SF spheres within 1 day, whereas only around 30% of encapsulated IGF-I was released within 4 weeks [49]. Moreover, prolonged release of HRP from PLGA MP was described when the MP were coated with SF. This outcome was explained to result from the additional diffusional barrier and, possibly, by non-specific interaction between HRP and SF [55]. Another explanation for the drop in release rates of embedded PLGA MP as compared to those of free PLGA MP could be an ionic interaction between positively charged amino acids (e.g. Arg) of IGF-I (pI 8.4) [56] and the mainly negatively charged side chains of the hydrophilic spacers of the heavy chain of SF [57, 58]. An ionic interaction

between SF and positively charged growth factors, such as nerve growth factor or IGF-I, was also discussed previously [18, 41, 49]. However, the main impact of an interaction between SF and IGF-I was assumed to be of non-Coulomb character [49], as the heavy chain of SF consists of hydrophobic blocks (-Gly-Ala-Gly-Ala-Gly-Ser-)$_n$ which may interact with the hydrophobic domain of IGF-I featuring Leu, Val and Ile [56].

It is noteworthy that the bioactivity of released IGF-I from both free PLGA 502H MP and PLGA 502H MP embedded in SF scaffolds was maintained throughout all time intervals, even after 42 days (Fig. 6B). Surprisingly, supernatants taken from free PLGA 503H MP and from embedded PLGA 503H MP did not significantly induce the proliferation of MG-63 cells as compared to the corresponding negative controls, except for the supernatants from embedded PLGA 503H MP taken after 42 days. From release experiments, we would have expected high proliferation rates from supernatants taken from free PLGA 503H MP within the time interval of days 16 – 22 and days 34 – 42 when considering the high release of IGF-I in these intervals (Fig. 6C). A possible explanation may be that IGF-I in PLGA 503H MP was not as well protected as in PLGA 502H MP during fabrication or release. Nevertheless, even though less IGF-I was released from embedded PLGA 503H MP than from free PLGA 503H MP during the time interval of days 34 - 42, the supernatants from embedded PLGA 503H MP induced significantly higher cell proliferation than the respective negative control. Therefore, we assume that embedment in SF may act as additional protection factor. The protective function of SF during methanol treatment has been previously described for HRP when embedded into SF films and corresponded to its release in a bioactive form [54].

Future studies are needed to test the effect of the SF scaffolds with embedded PLGA MP loaded with IGF-I on cellular differentiation and growth and how this may be affected by the distinct release kinetics obtained from the different types of PLGA MP. A possible effect of the IGF-I that is still entrapped in the SF scaffold also has to be considered. The SF scaffold may possibly act similar to the extracellular matrix, provide a depot for growth factors that are either later released or presented surface-bound to stimulate cells in the local microenvironment [59]. Future studies should also include the

delivery of dual growth factor release from SF scaffolds as this delivery system may offer an opportunity to individually tune the release kinetics through embedment of PLGA MP of different degradation kinetics in one scaffold, even allowing spatially separated deposition and release of growth factors, a prerequisite for the repair of osteochondral defects (Fig. 8).

A	B	C
homogeneous distribution	gradient distribution	spatially separated deposition

- ◎ PLGA MP loaded with growth factor 1
- ● PLGA MP loaded with growth factor 2

Fig. 8. Illustration showing possibilities for the embedment of growth factor loaded PLGA MP in SF scaffolds: homogeneous distribution of one type of growth factor loaded PLGA MP throughout the scaffold (A), gradient distribution of one type of growth factor loaded PLGA MP (B), and spatially separated deposition of two different types of growth factor loaded PLGA MP (C).

5. Conclusions

We developed a microporous SF scaffold prototype embedding PLGA MP which we prior loaded with a growth factor. Changes in PLGA type resulted in distinct growth factor release kinetics. Embedment of PLGA MP in SF scaffolds led to more sustained release rates as compared to free PLGA MP. Based on opportunities arising from temporal control of growth factor delivery and from spatial control of growth factor deposition within the scaffolds, we expect such constructs to be advantageous for tissue engineering applications, with potential

to mimic physiological patterns more precisely. Overall, the developed scaffold prototype offers promise for promoting tissue regeneration.

Acknowledgements

References

1. Gerstenfeld LC, Cullinane DM, Barnes GL, Graves DT, Einhorn TA. Fracture healing as a post-natal developmental process: molecular, spatial, and temporal aspects of its regulation. J Cell Biochem 2003;88(5):873-884.

2. Whitaker MJ, Quirk RA, Howdle SM, Shakesheff KM. Growth factor release from tissue engineering scaffolds. J Pharm Pharmacol 2001;53(11):1427-1437.

3. Meinel L, Zoidis E, Zapf J, Hassa P, Hottiger MO, Auer JA, et al. Localized insulin-like growth factor I delivery to enhance new bone formation. Bone 2003;33(4):660-672.

4. Schrier JA, DeLuca PP. Porous bone morphogenetic protein-2 microspheres: polymer binding and in vitro release. AAPS PharmSciTech 2001;2(3):E17.

5. Woo BH, Fink BF, Page R, Schrier JA, Jo YW, Jiang G, et al. Enhancement of bone growth by sustained delivery of recombinant human bone morphogenetic protein-2 in a polymeric matrix. Pharm Res 2001;18(12):1747-1753.

6. Hock JM, Centrella M, Canalis E. Insulin-like growth factor I has independent effects on bone matrix formation and cell replication. Endocrinology 1988;122(1):254-260.

7. Schmidmaier G, Wildemann B, Gabelein T, Heeger J, Kandziora F, Haas NP, et al. Synergistic effect of IGF-I and TGF-beta1 on fracture healing in rats: single versus combined application of IGF-I and TGF-beta1. Acta Orthop Scand 2003;74(5):604-610.

8. Blumenfeld I, Srouji S, Lanir Y, Laufer D, Livne E. Enhancement of bone defect healing in old rats by TGF-beta and IGF-1. Exp Gerontol 2002;37(4):553-565.

9. Boudignon BM, Bikle DD, Kurimoto P, Elalieh H, Nishida S, Wang Y, et al. Insulin-like growth factor I stimulates recovery of bone lost after a period of skeletal unloading. J Appl Physiol 2007;103(1):125-131.

10. Rose FR, Hou Q, Oreffo RO. Delivery systems for bone growth factors - the new players in skeletal regeneration. J Pharm Pharmacol 2004;56(4):415-427.

11. Altman GH, Diaz F, Jakuba C, Calabro T, Horan RL, Chen J, et al. Silk-based biomaterials. Biomaterials 2003;24(3):401-416.

12. Horan RL, Antle K, Collette AL, Wang Y, Huang J, Moreau JE, et al. In vitro degradation of silk fibroin. Biomaterials 2005;26(17):3385-3393.

13. Meinel L, Hofmann S, Karageorgiou V, Kirker-Head C, McCool J, Gronowicz G, et al. The inflammatory responses to silk films in vitro and in vivo. Biomaterials 2005;26(2):147-155.

14. Meinel L, Betz O, Fajardo R, Hofmann S, Nazarian A, Cory E, et al. Silk based biomaterials to heal critical sized femur defects. Bone 2006;39(4):922-931.

15. Hofmann S, Knecht S, Langer R, Kaplan DL, Vunjak-Novakovic G, Merkle HP, et al. Cartilage-like tissue engineering using silk scaffolds and mesenchymal stem cells. Tissue Eng 2006;12(10):2729-2738.

16. Kirker-Head C, Karageorgiou V, Hofmann S, Fajardo R, Betz O, Merkle HP, et al. BMP-silk composite matrices heal critically sized femoral defects. Bone 2007;41(2):247-255.

17. Altman GH, Horan RL, Lu HH, Moreau J, Martin I, Richmond JC, et al. Silk matrix for tissue engineered anterior cruciate ligaments. Biomaterials 2002;23(20):4131-4141.

18. Uebersax L, Merkle HP, Meinel L. Insulin-like growth factor I releasing silk fibroin scaffolds induce chondrogenic differentiation of human mesenchymal stem cells. J Control Release 2008;127(1):12-21.

19. Uludag H, D'Augusta D, Golden J, Li J, Timony G, Riedel R, et al. Implantation of recombinant human bone morphogenetic proteins with biomaterial carriers: A correlation between protein pharmacokinetics and osteoinduction in the rat ectopic model. J Biomed Mater Res 2000;50(2):227-238.

20. Wei G, Jin Q, Giannobile WV, Ma PX. Nano-fibrous scaffold for controlled delivery of recombinant human PDGF-BB. J Control Release 2006;112(1):103-110.

21. Hedberg EL, Tang A, Crowther RS, Carney DH, Mikos AG. Controlled release of an osteogenic peptide from injectable biodegradable polymeric composites. J Control Release 2002;84(3):137-150.

22. Lee M, Chen TT, Iruela-Arispe ML, Wu BM, Dunn JC. Modulation of protein delivery from modular polymer scaffolds. Biomaterials 2007;28(10):1862-1870.

23. Ungaro F, Biondi M, d'Angelo I, Indolfi L, Quaglia F, Netti PA, et al. Microsphere-integrated collagen scaffolds for tissue engineering: effect of microsphere formulation and scaffold properties on protein release kinetics. J Control Release 2006;113(2):128-136.

24. Perets A, Baruch Y, Weisbuch F, Shoshany G, Neufeld G, Cohen S. Enhancing the vascularization of three-dimensional porous alginate scaffolds by incorporating controlled release basic fibroblast growth factor microspheres. J Biomed Mater Res 2003;65(4):489-497.

25. Chen FM, Zhao YM, Zhang R, Jin T, Sun HH, Wu ZF, et al. Periodontal regeneration using novel glycidyl methacrylated dextran (Dex-GMA)/gelatin scaffolds containing microspheres loaded with bone morphogenetic proteins. J Control Release 2007;121(1-2):81-90.

26. Uebersax L, Hagenmuller H, Hofmann S, Gruenblatt E, Muller R, Vunjaknovakovic G, et al. Effect of scaffold design on bone morphology in vitro. Tissue eng 2006;12(12):3417-3429.

27. Meinel L, Illi OE, Zapf J, Malfanti M, Peter Merkle H, Gander B. Stabilizing insulin-like growth factor-I in poly(D,L-lactide-co-glycolide) microspheres. J Control Release 2001;70(1-2):193-202.

28. Sofia S, McCarthy MB, Gronowicz G, Kaplan DL. Functionalized silk-based biomaterials for bone formation. J Biomed Mater Res 2001;54(1):139-148.

29. Hino T, Tanimoto M, Shimabayashi S. Change in secondary structure of silk fibroin during preparation of its microspheres by spray-drying and exposure to humid atmosphere. J Colloid Interface Sci 2003;266(1):68-73.

30. Luginbuehl V, Wenk E, Koch A, Gander B, Merkle HP, Meinel L. Insulin-like growth factor I-releasing alginate-tricalciumphosphate composites for bone regeneration. Pharm Res 2005;22(6):940-950.

31. Pollak MN, Polychronakos C, Richard M. Insulinlike growth factor I: a potent mitogen for human osteogenic sarcoma. J Natl Cancer Inst 1990;82(4):301-305.

32. Lopaczynski W, Harris S, Nissley P. Insulin-like growth factor-I (IGF-I) dependent phosphorylation of the IGF-I receptor in MG-63 cells. Regul Pept 1993;48(1-2):207-216.

33. Gupta RK, Chang AC, Griffin P, Rivera R, Guo YY, Siber GR. Determination of protein loading in biodegradable polymer microspheres containing tetanus toxoid. Vaccine 1997;15(6-7):672-678.

34. Asakura T, Kuzuhara A, Tabeta R, Saito H. Conformation characterization of Bombyx mori silk fibroin in the solid state by high-frequency 13C cross polarization-magic angle spinning NMR, X-ray diffraction, and infrared spectroscopy. Macromolecules 1985;18:1841-1845.

35. Monti P, Freddi G, Bertoluzza A, Kasai N, Tsukada M. Raman spectroscopic studies of silk fibroin from Bombyx mori. J Raman Spectrosc 1998;29:297-304.

36. Ishida M, Asakura T, Yokoi M, Saito H. Solvent- and mechanical-treatment-induced conformational transition of silk fibroins studied by high-resolution solid-state 13C NMR spectroscopy. Macromolecules 1990;23:88-94.

37. Marsh RE, Corey RB, Pauling L. An investigation of the structure of silk fibroin. Biochim Biophys Acta 1955;16(1):1-34.

38. Ma PX. Biomimetic materials for tissue engineering. Adv Drug Deliv Rev 2008;60(2):184-198.

39. Malafaya PB, Silva GA, Baran ET, Reis RL. Drug delivery therapies I. General trends and its importance on bone tissue engineering applications. Curr Opin Solid State Mater Sci 2002;6:283-295.

40. Karageorgiou V, Tomkins M, Fajardo R, Meinel L, Snyder B, Wade K, et al. Porous silk fibroin 3-D scaffolds for delivery of bone morphogenetic protein-2 in vitro and in vivo. J Biomed Mater Res 2006;78(2):324-334.

41. Uebersax L, Mattotti M, Papaloizos M, Merkle HP, Gander B, Meinel L. Silk fibroin matrices for the controlled release of nerve growth factor (NGF). Biomaterials 2007;28(30):4449-4460.

42. Jin Q, Wei G, Lin Z, Sugai JV, Lynch SE, Ma PX, et al. Nanofibrous Scaffolds Incorporating PDGF-BB Microspheres Induce Chemokine Expression and Tissue Neogenesis In Vivo. PLoS ONE 2008;3(3):e1729.

43. Lee JE, Kim SE, Kwon IC, Ahn HJ, Cho H, Lee SH, et al. Effects of a chitosan scaffold containing TGF-beta1 encapsulated chitosan microspheres on in vitro chondrocyte culture. Artif Organs 2004;28(9):829-839.

44. Deng T, Huang S, Zhou S, He L, Jin Y. Cartilage regeneration using a novel gelatin-chondroitin-hyaluronan hybrid scaffold containing bFGF-impregnated microspheres. J Microencapsul 2007;24(2):163-174.

45. Kim SE, Park JH, Cho YW, Chung H, Jeong SY, Lee EB, et al. Porous chitosan scaffold containing microspheres loaded with transforming growth factor-beta1: implications for cartilage tissue engineering. J Control Release 2003;91(3):365-374.

46. Defail AJ, Edington HD, Matthews S, Lee WC, Marra KG. Controlled release of bioactive doxorubicin from microspheres embedded within gelatin scaffolds. J Biomed Mater Res 2006;79(4):954-962.

47. DeFail AJ, Chu CR, Izzo N, Marra KG. Controlled release of bioactive TGF-beta 1 from microspheres embedded within biodegradable hydrogels. Biomaterials 2006;27(8):1579-1585.

48. Hu Y, Hollinger JO, Marra KG. Controlled release from coated polymer microparticles embedded in tissue-engineered scaffolds. J Drug Target 2001;9(6):431-438.

49. Wenk E, Wandrey AJ, Merkle HP, Meinel L. Silk fibroin spheres as a platform for controlled drug delivery. J Control Release 2008;132:26-34.

50. Rössle M, Panine P, Urban VS, Riekel C. Structural evolution of regenerated silk fibroin under shear: combined wide- and small-angle x-

ray scattering experiments using synchrotron radiation. Biopolymers 2004;74(4):316-327.

51.	Min BM, Jeong L, Lee KY, Park WH. Regenerated silk fibroin nanofibers: water vapor-induced structural changes and their effects on the behavior of normal human cells. Macromol Biosci 2006;6(4):285-292.

52.	Karageorgiou V, Kaplan D. Porosity of 3D biomaterial scaffolds and osteogenesis. Biomaterials 2005;26(27):5474-5491.

53.	Zilberman M, Grinberg O. HRP-loaded bioresorbable microspheres: effect of copolymer composition and molecular weight on microstructure and release profile. J Biomater Appl 2008;22(5):391-407.

54.	Hofmann S, Foo CT, Rossetti F, Textor M, Vunjak-Novakovic G, Kaplan DL, et al. Silk fibroin as an organic polymer for controlled drug delivery. J Control Release 2006;111(1-2):219-227.

55.	Wang X, Wenk E, Hu X, Castro GR, Meinel L, Wang X, et al. Silk coatings on PLGA and alginate microspheres for protein delivery. Biomaterials 2007;28(28):4161-4169.

56.	Blundell TL, Bedarkar S, Rinderknecht E, Humbel RE. Insulin-like growth factor: a model for tertiary structure accounting for immunoreactivity and receptor binding. Proc Natl Acad Sci U S A 1978;75(1):180-184.

57.	Zhou CZ, Confalonieri F, Medina N, Zivanovic Y, Esnault C, Yang T, et al. Fine organization of Bombyx mori fibroin heavy chain gene. Nucleic Acids Res 2000;28(12):2413-2419.

58.	Foo CW, Bini E, Hensman J, Knight DP, Lewis RV, Kaplan DL. Role of pH and charge on silk protein assembly in insects and spiders. Appl Phys A 2006;82:223-233.

59.	Macri L, Silverstein D, Clark RA. Growth factor binding to the pericellular matrix and its importance in tissue engineering. Adv Drug Deliv Rev 2007;59(13):1366-1381.

CHAPTER IV

THE USE OF SULFONATED SILK FIBROIN DERIVATIVES TO CONTROL BINDING, DELIVERY AND POTENCY OF FGF-2 IN TISSUE REGENERATION

Esther Wenk[1], Amanda R. Murphy[2], David L. Kaplan[2], Lorenz Meinel[1], Hans P. Merkle[1], Lorenz Uebersax[1]

[1]Institute of Pharmaceutical Sciences, ETH Zurich, Wolfgang-Pauli-Strasse 10, CH-8093 Zurich, Switzerland

[2]Department of Biomedical Engineering, 4 Colby Street, Tufts University, Medford, MA 02155, United States

Abstract

The development of biomaterials that mimic the physiological binding of growth factors to the extracellular matrix (ECM) is an appealing strategy for advanced growth factor delivery systems. *In vivo*, fibroblast growth factor 2 (FGF-2) binds to the sulfated glycosaminoglycan heparan sulfate, which is a major component of the ECM. Therefore, we tested whether silk fibroin (SF) decorated with a sulfonated moiety could mimic the natural ECM environment and lead to advanced delivery of this heparin-binding growth factor. Using a diazonium coupling reaction, modified SF derivatives containing approximately 20, 40, 55 and 70 sulfonic acid groups per SF molecule were obtained. Films of the SF derivative decorated with 70 sulfonic acid groups per SF molecule resulted in a 2-fold increase in FGF-2 binding as compared to native SF. More than 99% of bound FGF-2 could be retained on all SF derivatives. However, protection of FGF-2 potency was only achieved with at least 40 sulfonic acid groups per SF molecule, as observed by reduced metabolic activity and enhanced levels of phosphorylated extracellular signal-regulated kinases (pERK1/2) in cultured human mesenchymal stem cells (hMSCs). This study introduces a first step towards the development of an ECM-mimicking biomaterial for sustained, non-covalent binding, controlled delivery and preserved potency of biomolecules.

1. Introduction

The extracellular matrix (ECM) regulates mammalian cell behavior such as migration, survival, proliferation and differentiation. Therefore, mimicking the ECM by scaffold design, e.g. by introducing mechanical and/or biochemical cues, has been suggested to optimize cell interactions and differentiation in tissue regeneration [1]. The ECM represents a hydrated protein- and proteoglycan-based gel network consisting of collagens, non-collageneous glycoproteins such as elastin, laminin or fibronectin, and hydrophilic proteoglycans with large glycosaminoglycan side chains [2]. Entire decellularized ECM has been used as biological scaffold for a variety of therapeutic applications [3], but bears the potential for immunogenicity, disease transfer and variability. By contrast, individual components of the ECM such as collagen, laminin, fibrin and hyaluronic acid can be isolated and purified to create well-defined biomaterials with biological function [4]. In this context, synthetic constructs and biomaterials derivatized with ECM-derived peptides or protein fragments have been suggested to improve biological recognition and cellular interaction [5-7].

Beyond its function to provide a physiological matrix for cellular accommodation, the ECM also acts as a local storage for growth factors, delivers them on demand, protects their potency, and, in some cases, enhances binding to cell surface receptors [2]. For instance, fibroblast growth factor 2 (FGF-2), a heparin-binding growth factor, specifically interacts with a major component of the ECM, the sulfated glycosaminoglycan heparan sulfate [8-10]. FGFs are a family of growth factors involved in angiogenesis, wound healing, and embryonic development and represent key-players for the proliferation and differentiation of a wide variety of cells and tissues. Accordingly, FGF-2 shows mitogenic effects on fibroblasts, endothelial cells, smooth muscle cells and osteoblasts [8] making it a strong candidate for biomedical applications in tissue regeneration. Interaction with ECM- and cell-surface associated heparan sulfate proteoglycans (HSPGs) is essential for FGF signal transduction. It has been shown that cell-surface associated HSPGs, which have been detected on the cell surface of most mammalian cells and also on hMSCs [11, 12], play an active

role in the presentation of ECM-bound FGF-2 to its cell surface receptors. Therefore, HSPGs function as regulators of growth factor activity [13-16]. This explains the marked interest in studying the molecular interaction of heparan sulfate, heparin and modifications or mimics thereof with FGF-2 [17, 18]. For instance, silyl-heparin, a chemically modified analogue of heparin, has been synthesized and found to be a useful vehicle for the local delivery of FGF-2 [19]. Moreover, binding to sulfated colominic acid increased the mitogenic activity of FGF-2 [17]. Similar attributes have also been observed with sulfonated polymers. In fact, sulfonated poly(γ-glutamic acid) has been demonstrated to strongly interact with FGF-2, and better preserve the bioactivity of FGF-2 than the non-sulfonated polymer [20].

Here we tested the hypothesis that a decoration of silk fibroin (SF) with sulfonic acid moieties leads to a sustained, non-covalent binding of this heparin-binding growth factor, controls its delivery, and preserves its potency. SF is a fibrous protein extracted from the cocoons of the domestic silkworm *Bombyx mori* [21], and has been widely investigated for tissue engineering applications [22-25], owing to its unique properties, such as aqueous processability under mild conditions, exceptional mechanical strength, as well as biocompatibility and biodegradability. However, SF lacks cell adhesion or growth factor binding sites *per se*. Nevertheless, as a polypeptide, SF features various amino acid residues allowing ready bioconjugation of functional groups to make it a potential ECM mimic. For instance, coupling of an RGD sequence has been suggested to enhance osteoblast-like cell adhesion on SF [7]. Several reports have been made on the chemical decoration of the tyrosine residues in SF [26-28]. Recently, SF derivatives were introduced that were modified through diazonium coupling chemistry using several aniline derivatives featuring carboxylic acid, amine, ketone, sulfonic acid or alkyl groups. It has been shown that human mesenchymal stem cells (hMSCs) were able to attach, proliferate and differentiate into the osteogenic lineage on all of these SF derivatives [26].

Using diazonium coupling chemistry, we reacted SF with the diazonium salt of 4-sulfanilic acid to produce SF derivatives with varying numbers of sulfonic acid moieties. Binding of FGF-2 to films of native SF and sulfonated SF derivatives was studied to determine their binding capacities for the growth

factor. We further examined FGF-2 release profiles of the derivatives and their potential for growth factor retention. The biological potency of FGF-2 was studied by seeding hMSCs onto films of native SF and sulfonated SF derivatives, and analyzing the effect of free as well as bound FGF-2 on the metabolic turnover in cell culture as well as on the phosphorylation of the extracellular signal-regulated kinase (ERK), indicating the activation of the Ras pathway [29, 30]. This study introduces a first step towards the development of an ECM-mimicking SF derivative for sustained, non-covalent binding, controlled delivery, and preserved potency of a growth factor for tissue regeneration.

2. Materials and Methods

2.1. Materials

Cocoons of *Bombyx mori* were obtained from Tajima Shoji Co. (Yokohoma, Japan). FGF-2 was from R&D Systems (Minneapolis, MN). For cell culture studies, we used fetal bovine serum (FBS), RPMI 1640 medium, Dulbecco's Modified Eagle Medium (DMEM), penicillin G and streptomycin, fungizone, trypsin and non-essential amino acids (NEAA) from Invitrogen (Paisley, UK). All other substances used were of analytical or pharmaceutical grade and obtained from Sigma or Fluka (St. Louis, MO; Buchs, Switzerland) unless otherwise indicated.

2.2. Preparation of SF solution

SF solutions were prepared from cocoons of the silkworm *B. mori* as previously described [26]. Cocoons were boiled for 1 h in an aqueous solution of 0.02 M Na_2CO_3 and thoroughly rinsed with water to remove the sericin. The extracted SF was dissolved in a 9 M aqueous LiBr solution at 60 °C for 45 min to obtain a 20% (w/v) solution. This solution was filtered through a 5 μm syringe filter and dialyzed against distilled water for 2 days using Slide-a-Lyzer dialysis cassettes (MWCO 3500 g/mol; Pierce, Woburn, MA), followed by dialysis against borate buffer (100 mM borate, 150 mM NaCl, pH 9) (BupH

borate buffer pak; Pierce, Woburn, MA) for an additional day changing the buffer 2 times. The SF solution had a final concentration of ~ 9% (w/v).

2.3. Diazonium coupling reaction

The diazonium coupling reaction was performed as previously described [26]. Briefly, 68 mg (0.40 mmol) of 4-sulfanilic acid was dissolved in 2 mL water, and then combined with 1 mL of a 1.6 M aqueous solution of p-toluenesulfonic acid. This mixture was cooled on ice, and then combined with 1 mL of a cooled 0.8 M aqueous solution of $NaNO_2$. The mixture was vortexed briefly, and then placed in an ice bath for 15 min. The resulting diazonium salt stock solution was then reacted with the silk solution in borate buffer. To control the level of modification, differing amounts of the diazonium salt were added. In a typical experiment, the total reaction volume was 5 mL, where 4 mL of the silk solution was combined with 0, 250, 500, 750, or 1000 µL of the stock diazonium salt solution, which approximately corresponds to the addition of 0.10, 0.15, 0.25, and 0.35 equivalents of the diazonium salt relative to the number of tyrosine residues in SF. In cases where less than 1000 µL of the diazonium salt stock was used, the stock solution was first diluted with water to give a total volume of 1000 µL. The diazonium salt was allowed to react with the SF solutions for 20 min. The reaction mixtures were then purified by passing them through disposable Sephadex size exclusion columns (NAP-25, GE Healthcare), pre-equilibrated with distilled water. The resulting solutions of sulfonated SF derivatives had a concentration of about 4% (w/v) in water, and were diluted with water to about 2% (w/v) before further use. The level of azo incorporation for each of the derivatives was analyzed in water with UV-Vis spectroscopy using a GBC 916 spectrophotometer. UV-Vis: λmax (pH 7) = 215 nm (carbonyl) and 325 nm (azo).

The native SF control was obtained by passing the silk solution in borate buffer through a Sephadex size exclusion column pre-equilibrated with distilled water to remove the buffer salts. UV-Vis: λmax (pH 7) = 215 nm (carbonyl) and 275 nm (tyrosine).

2.4. Fourier-transform infrared (FTIR) spectroscopy

Films of native SF and sulfonated SF derivatives were measured directly by FTIR spectroscopy with a 2000 FT-IR Spectrometer V3,01 (Perkin Elmer, Boston, MA) in a similar way as previously reported in detail for KBr disks [31, 32].

2.5. Contact angle measurements

Aqueous solutions (2%) of native SF and sulfonated SF derivatives were spread on glass slides and the films dried overnight. Films were then exposed to water vapor of 96% relative humidity by equilibration in the presence of a saturated aqueous Na_2SO_4 solution at room temperature for 12 h as previously described [31, 33] and dried. This treatment will further be denoted as water vapor treatment. Advancing water-contact angles were analyzed using a drop shape analyzer DSA100 (Krüss, Hamburg, Germany) with a drop size of 11 µL.

2.6. Preparation of films used for binding and release of FGF-2 and for cell culture

For binding and release studies solutions with 2% (w/v) native SF or sulfonated SF derivatives were obtained by dilution with water and subsequent sterile filtration through a 0.22 µm filter. Films were prepared by coating the wells of a 96-well plate with 100 µL solution each. The films were dried overnight in a laminar flow hood and treated with water vapor as previously described [31, 33].

2.7. FGF-2 binding and release

To study the binding of FGF-2, films of native SF and sulfonated SF derivatives were incubated with 100 µL PBS of pH 7.4 containing 0.1% BSA (for stabilization) and 100 ng FGF-2 (corresponding to 1000 ng/mL FGF-2) at room temperature (n = 4). Control films (films of native SF and sulfonated SF derivatives without bound FGF-2) were treated with 100 µL PBS of pH 7.4

containing 0.1% BSA. Samples of 5 µL were taken after 1, 2 and 4 h. Bound FGF-2 was analyzed indirectly by measuring FGF-2 remaining in the supernatant using an enzyme-linked immunosorbent assay (ELISA, DuoSet Human) according to the manufacturer's protocol (R&D Systems, Minneapolis, MN). Data was expressed as percentage of the initial amount of FGF-2.

For the release studies, the supernatants of the binding study after 4 h were removed and films were washed with fresh PBS. FGF-2 release from the films was studied at 37 °C in 100 µL PBS of pH 7.4, again containing 0.1% BSA (for stabilization; n = 4). The release medium was fully exchanged with fresh medium after 1, 2, 3, 4 and 6 days. Medium samples were analyzed using an ELISA as described above. Data was expressed as percentage of the initially bound FGF-2.

2.8. Cell isolation, expansion and characterization

Human mesenchymal stem cells (hMSCs) were isolated and characterized as previously described [34-37]. Briefly, bone marrow of a healthy male donor obtained from Cambrex Bio Science Walkersville, Inc. (Walkersville, Maryland, MD) was diluted in isolation medium, consisting of RPMI supplemented with 5% FBS. The cells were pelleted, resuspended in expansion medium (DMEM, 10% FBS, penicillin-streptomycin, fungizone, 1% NEAA, 1 ng/mL bFGF) and seeded in 175 cm^2 flasks at a density of 5 x 10^4 cells/cm^2. After reaching approximately 80% confluence (12–17 days for the first passage), cells were trypsinized and replated every 6–8 days at approximately 80% confluence. The second passage (P2) cells were detached and frozen in liquid nitrogen until used for cell culture. The hMSCs were characterized prior to use by their surface antigen pattern and the ability to selectively differentiate along the chondrogenic and osteogenic lineages in response to environmental stimuli, as previously described [37].

2.9. Cell culture

Cell culture studies were performed in order to evaluate the biological response of hMSCs to FGF-2 - either free or bound to films of native SF or sulfonated SF derivatives - in terms of metabolic activity as well as phosphorylated extracellular signal-regulated kinases (pERK1/2). For this purpose P2 hMSCs were thawed, suspended in expansion medium (DMEM, 10% FBS, penicillin-streptomycin, fungizone, 1% NEAA, 1 ng/mL bFGF) and seeded in 175 cm^2 flasks at a density of 5 x 10^4 cells per cm^2 until they reached approximately 80% confluence. For seeding hMSCs were detached and dispersed in 100 µL control medium (DMEM, 10% FBS, 100 U/mL penicillin, 100 µg/mL streptomycin, 0.5 µg/mL fungizone). Cell culture experiments were performed in 96-well plates of tissue culture plastic (TCP). Wells were either coated with films of native SF or sulfonated SF derivatives as described above. Details for the loading of films with FGF-2 is given below. Controls were as follows: (i) wells coated with films of native SF or sulfonated SF derivatives without FGF-2 (FGF-2-free film control), (ii) wells containing free FGF-2 in control medium, without SF films (free FGF-2 control), and (iii) wells containing control medium, without SF films and without FGF-2 (all-negative control). Background fluorescence from the alamarBlue solution in medium was subtracted when measuring metabolic activity. A summary of the samples and controls used for the cell culture studies is given in Table 1.

Table 1. Samples and controls used for cell culture studies.

	Wells	Code
Samples	Films of native SF with bound FGF-2 Films of sulfonated SF derivatives[a] with bound FGF-2	
Controls	Films of native SF without FGF-2 Films of sulfonated SF derivatives[a] without FGF-2	FGF-2-free film control FGF-2-free film control
	Free FGF-2 in control medium (without SF films) Control medium (without SF films, without FGF-2)	Free FGF-2 control All-negative control

[a] Films of SF derivatives with 20, 40, 55 or 70 sulfonic acid groups per silk molecule

For analysis of metabolic activity the wells were seeded with about 500 hMSCs in 100 µL control medium per well, whereas about 10^4 cells in 100 µL control medium per well were used for the determination of pERK1/2. After cell seeding 96-well plates were incubated at 37 °C in humidified 5% CO_2 atmosphere for 2, 4, 7 and 9 days when used for the analysis of metabolic activity (n = 4), or for 24 h when used for the determination of pERK1/2 (n = 3). Throughout cell culture medium was exchanged with fresh control medium every 2 to 3 days. Medium exchange in wells containing free FGF-2 was with fresh control medium supplemented with FGF-2 at the same concentration.

Loading of films of native SF and films of sulfonated SF derivatives with FGF-2 for cell culture experiments was as follows: Previously prepared films of native SF or sulfonated SF derivatives in 96-wells were incubated with 100 µL PBS containing 100 or 1000 ng/mL FGF-2 (corresponding to 10 or 100 ng per film) and 0.1% BSA (for stabilization) for 4 h. Supernatants were removed, films washed with PBS and then seeded with hMSCs in control medium as described above.

The experimental conditions for the controls were as following: FGF-2-free film controls were prepared from native SF and sulfonated SF derivatives and pretreated with FGF-2-free PBS containing 0.1% BSA at room temperature for 4 h, washed with PBS and then seeded with hMSCs as described above. For free FGF-2 controls, hMSCs were directly seeded into the wells of the tissue culture plastic (TCP) and were cultured with 100 µL control medium containing either 100 or 1000 ng/mL of FGF-2 per well. The amounts of free FGF-2 were chosen according to the range of FGF-2 that was found to bind to films of native SF and sulfonated SF derivatives in order to provide the same amount of growth factor in an unbound state. Finally, all-negative controls were performed with control medium alone.

2.10. Metabolic activity

Metabolic activity of hMSCs was determined using the alamarBlue assay (Invitrogen, Paisley, UK) according to the manufacturer's protocol. The active ingredient of alamarBlue (resazurin) is a non-fluorescent indicator dye which is

converted to bright red-fluorescent resorufin via reduction by metabolically active cells [38]. Briefly, 10% alamarBlue solution was added to the medium of each well and incubated for 3 h. 100 μL from each well was analyzed for fluorescence with an excitation wavelength of 560 nm and an emission wavelength of 590 nm.

2.11. Phosphorylated ERK1/2 (pERK1/2)

To determine pERK1/2, cells were lysed with 150 μL cell lysis buffer (Cell Signaling Technology, Danvers, MA) given to each well and incubated for 5 min. The cells were harvested, briefly sonicated on ice, centrifuged at 14,000 x g at 4 °C for 10 min and the supernatants transferred to new tubes. pERK1/2 was analyzed using the PathScan® Phospho-p44/42 MAPK (Thr202/Tyr204) Sandwich ELISA Kit (Cell Signaling Technology, Danvers, MA) according to the manufacturer's protocol.
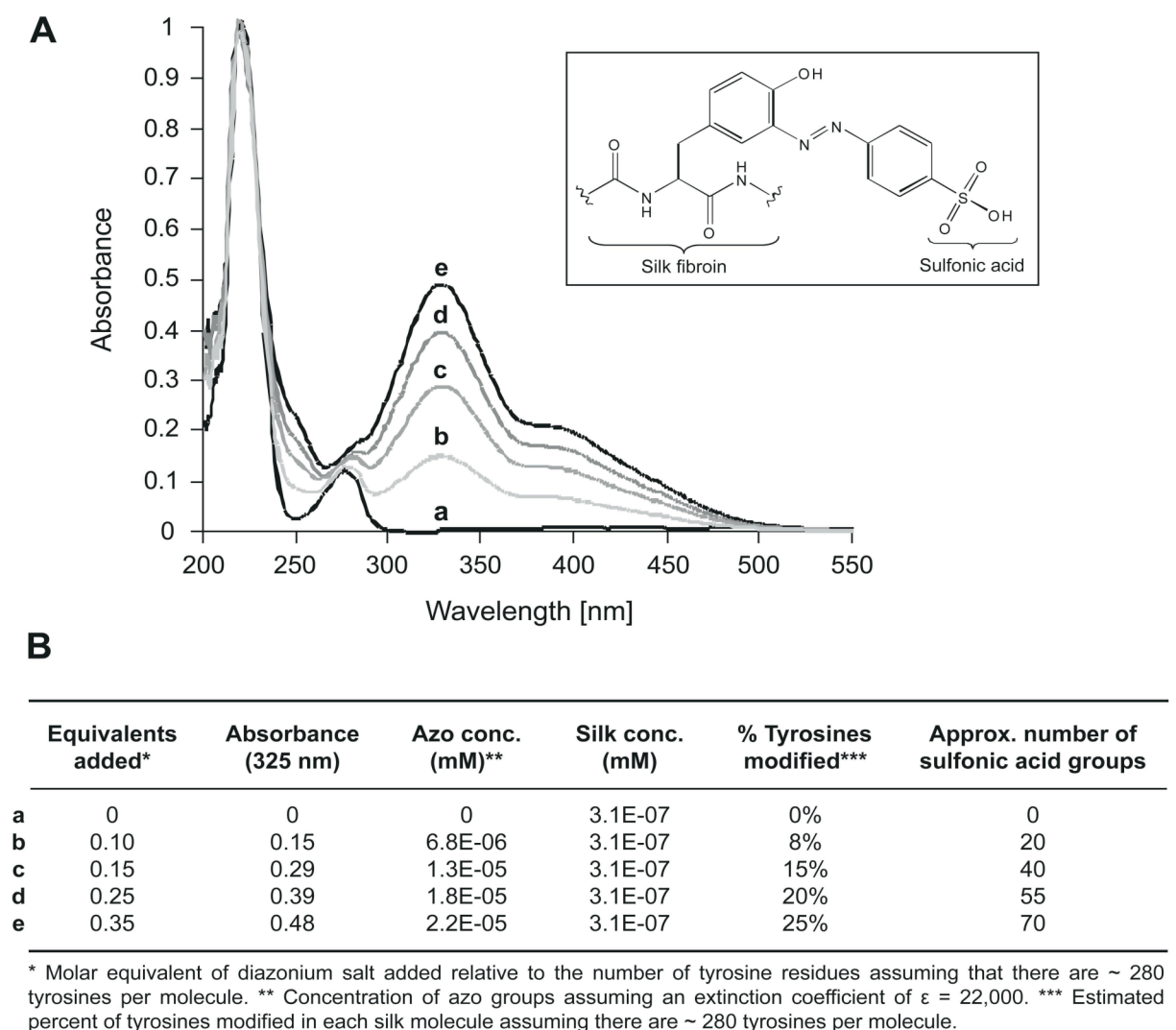
2.12. Statistics

Results are expressed as means ± standard deviations. Statistical analysis was performed using the Student t-test as well as one-way analysis of variance (ANOVA) followed by the Tukey HSD test for post-hoc comparison. Differences were considered highly significant when $p < 0.01$ and significant when $p < 0.05$.

3. Results

3.1. Synthesis and analysis of sulfonated SF derivatives

The tyrosine residues in native SF were chemically modified using diazonium coupling chemistry to introduce a sulfonic acid moiety [26], as shown in the insert in Fig. 1. The degree of sulfonation of the final SF derivative was controlled by treating the native protein with either 0.10, 0.15, 0.25, or 0.35 molar equivalents of the diazonium salt of 4-sulfanilic acid relative to the number of tyrosine residues. The number of sulfonic acid-decorated tyrosines in

A

B

	Equivalents added*	Absorbance (325 nm)	Azo conc. (mM)**	Silk conc. (mM)	% Tyrosines modified***	Approx. number of sulfonic acid groups
a	0	0	0	3.1E-07	0%	0
b	0.10	0.15	6.8E-06	3.1E-07	8%	20
c	0.15	0.29	1.3E-05	3.1E-07	15%	40
d	0.25	0.39	1.8E-05	3.1E-07	20%	55
e	0.35	0.48	2.2E-05	3.1E-07	25%	70

* Molar equivalent of diazonium salt added relative to the number of tyrosine residues assuming that there are ~ 280 tyrosines per molecule. ** Concentration of azo groups assuming an extinction coefficient of ε = 22,000. *** Estimated percent of tyrosines modified in each silk molecule assuming there are ~ 280 tyrosines per molecule.

Fig. 1. *(A) UV-Vis spectra of native (a) and sulfonated silk fibroin (SF) derivatives (b − e) in water at pH 7 (normalized to the carbonyl peak at 210 nm). Insert: Sulfonated SF derivative obtained by functionalizing the tyrosine residues in SF with the diazonium salt of 4-sulfanilic acid. (B) Estimated number of tyrosine residues modified with increasing amounts of the diazonium salt of 4-sulfanilic acid based on UV absorbance and approximate number of sulfonic acid groups per silk molecule.*

each SF derivative was estimated using UV-Vis spectroscopy (Fig. 1A) by calculating the concentration of azobenzene groups from the absorbance at 325 nm (Fig. 1B) [26]. SF contains about 280 tyrosine amino acids per molecule [39]; therefore, the percentage of decorated tyrosines in a SF derivative solution of known concentration could be calculated. Accordingly, SF derivatives

containing approximately 20, 40, 55 and 70 sulfonic acid moieties per silk molecule (Fig. 1B) were obtained and further investigated in subsequent experiments.

3.2. FTIR spectroscopy

FTIR spectra of untreated and water vapor treated films of native SF and sulfonated SF derivatives were recorded. Characteristic absorption bands of the films were observed at around 1658 cm^{-1} (amide I) and at 1540 cm^{-1} (amide II). The bands shifted to 1629 cm^{-1} (amide I) and 1517 cm^{-1} (amide II), respectively, upon treatment with water vapor. The spectra (data not shown) corresponded well with previous data [40-42], indicating higher β-sheet based crystallinity of SF upon water vapor treatment. Accordingly, as previously described by Murphy et al. [26], sulfonated SF derivatives were still able to form a β-sheet structure when dehydrated with organic solvents such as methanol.

3.3. Contact angles

The change in hydrophilicity with increasing degrees of sulfonation was determined by measuring the advancing contact angles of films made of native SF and sulfonated SF derivatives prior treated with water vapor (Fig. 2). Films of native SF showed contact angles of about 71°, whereas films of the sulfonated derivatives had significantly lower contact angles of less than 50° ($p < 0.01$). Water contact angles were observed to drop with increasing degrees of sulfonation, and remained constant at around 40° corresponding to 55 sulfonic acid groups per silk molecule or more. The contact angles on films of the SF derivative decorated with 55 sulfonic acid groups per silk molecule were significantly lower than those on SF derivatives featuring 20 ($p < 0.01$) or 40 ($p < 0.05$) sulfonic acid groups per silk molecule.
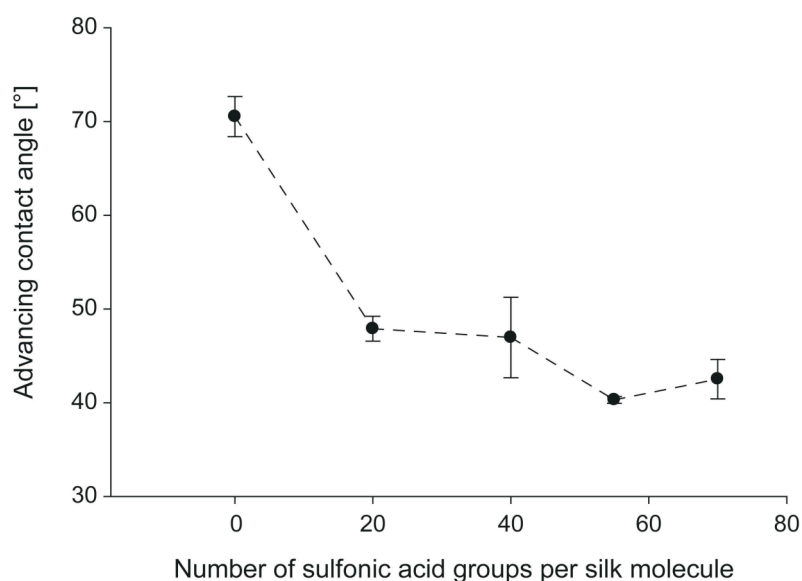
Fig. 2. *Advancing contact angles of films of native SF and SF derivatives with 20, 40, 55 and 70 sulfonic acid groups per silk molecule.*

3.4. FGF-2 binding and release

We further examined the capacity of native SF and sulfonated SF derivatives to bind and release FGF-2. Preliminary adsorption experiments have shown a nearly exhaustive FGF-2 binding to films of the SF derivative with the highest degree of sulfonation (70 sulfonic acid groups per silk molecule) after 4 h incubation with concentrations of 1, 10 and 100 ng/mL FGF-2 (corresponding to 0.1, 1 and 10 ng FGF per film). In contrast, when using 1000 ng/mL FGF-2 (corresponding to 100 ng FGF per film), FGF-2 was found to be in excess and binding approximately at 95% of the total amount of FGF-2. This concentration was chosen to test the capacity of SF films with different degrees of sulfonation to bind and release FGF-2. When incubated at a concentration of 1000 ng/mL FGF-2 for 1, 2 and 4 h there was increasing binding of FGF-2 to the films depending on the degree of sulfonation (except for a single outlier for the derivative with 40 sulfonic acid groups per silk molecule after 2 hours). The cumulative binding of FGF-2 to native SF and sulfonated SF derivatives is given in Fig. 3A. After 4 h, native SF bound only 48.5 ± 15.1% of the total amount of FGF-2. The total amount of FGF-2 bound to the modified SF derivatives

correlated linearly with the number of sulfonic acid groups present (Fig. 3B). SF films with the highest degree of sulfonation were able to bind up to 95.2 ± 2.2%, twice as much as native SF.
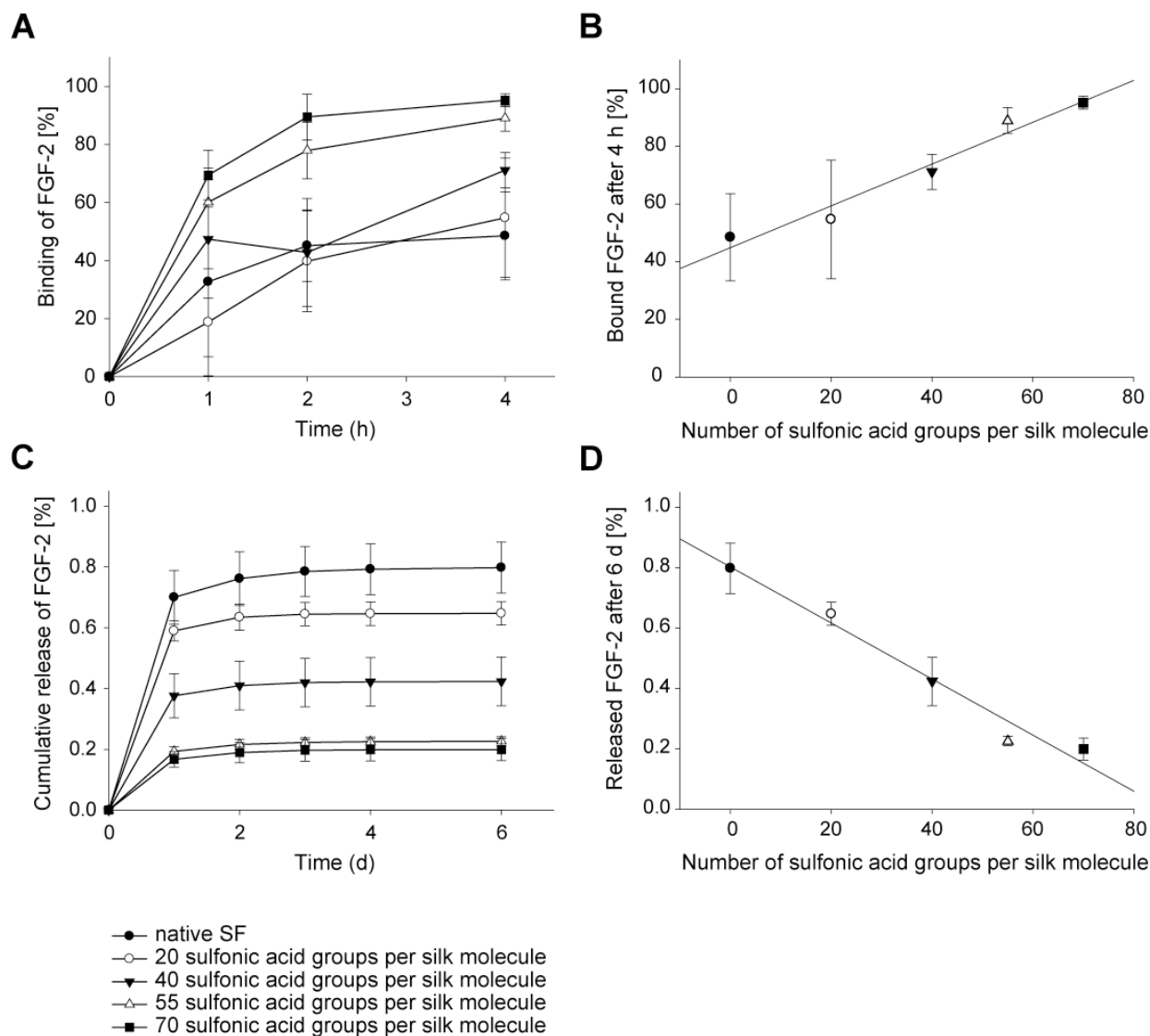
Fig. 3. *(A) Cumulative adsorption of FGF-2 to films of native SF and sulfonated SF derivatives. (B) FGF-2 bound to films of native SF and sulfonated SF derivatives after 4 h. (C) Cumulative release of FGF-2 from films of native SF and sulfonated SF derivatives. (D) Released FGF-2 from films of native SF and sulfonated SF derivatives after 6d. Binding is expressed as percentage of the initial amount of FGF-2, release as percentage of the bound FGF-2 (n = 4; means ± SD).*

The cumulative release of bound FGF-2 from films of native SF or SF derivatives was studied in PBS of pH 7.4 containing 0.1% BSA (Fig. 3C). The amounts of bound FGF-2 that were released from the films were low and depended inversely on the degree of sulfonation. The highest amount was released from native SF ($0.79 \pm 0.08\%$ after 6 d) and the lowest amount from SF derivatives with the highest degree of sulfonation ($0.20 \pm 0.04\%$ after 6 d). After 3 days, practically no further release was observed. After 6 d an apparently linear relationship between the level of sulfonation and released FGF-2 was observed (Fig. 3D).

3.5. Effect of free versus bound FGF-2 on the metabolic activity of hMSCs

As a control experiment we first analyzed how the metabolic activity of hMSCs was affected when exposed to free FGF-2 in the absence of native SF or sulfonated SF derivatives. For this purpose hMSCs were directly cultured in TCP wells. Their metabolic activity was examined after 2, 4, 7 and 9 days in culture using the alamarBlue assay. After 2, 4 and 7 days, no significant differences between the metabolic activities of hMSCs treated with or without free FGF-2 were observed (data not shown). On day 9, hMSCs that were treated with 100 and 1000 ng/mL FGF-2 showed significantly lower metabolic activities as compared to hMSCs treated with control medium without FGF-2 ($p < 0.05$ and $p < 0.01$, respectively) (Fig. 4A). The drop in metabolic activity was $23.5 \pm 8.4\%$ and $29.2 \pm 2.4\%$, respectively (Fig. 4B), and was not significantly different between the two FGF-2 concentrations.

In a similar way we investigated the effect of FGF-2 when bound to films of the SF derivative with the highest degree of sulfonation (70 sulfo groups per silk molecule) that were treated with either 100 or 1000 ng/mL FGF-2 prior to cell seeding. The total amounts of FGF-2 in these experiments were in the same range as involved in the experiments with free FGF-2 as described above.

Again, the metabolic activity of hMSCs was significantly reduced as compared to the corresponding FGF-2-free film control ($p < 0.01$) (Fig. 4A). The decrease in metabolic activity was $34.9 \pm 6.1\%$ and $32.6 \pm 4.1\%$ (Fig. 4B) for the two FGF-2 concentrations applied and again not significantly different

A

B
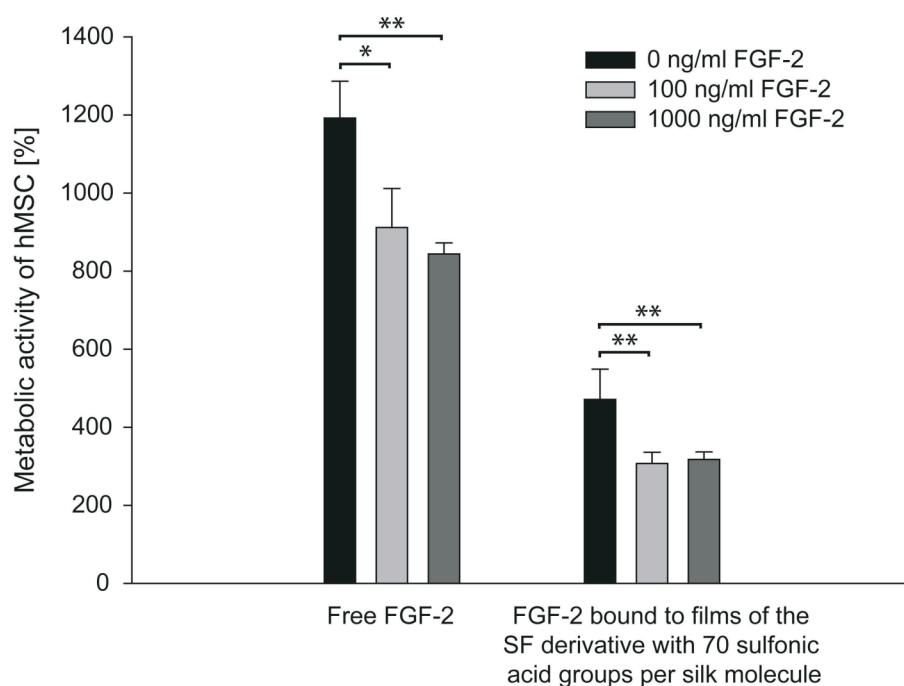
Sample	FGF-2 conc. [ng/ml]	Free FGF-2 [ng/well]	Adsorbed FGF-2 [ng/film]	Drop in metabolic activity [%]	Significance of drop in metabolic acitivity
Free FGF-2	100	10		23.5 ± 8.4	*
Free FGF-2	1000	100		29.2 ± 2.4	**
70	100		10.0 ± 0.1	34.9 ± 6.1	**
70	1000		90.3 ± 3.1	32.6 ± 4.1	**

Fig. 4. *(A) Metabolic activity of hMSCs determined after 9 days using the alamarBlue assay. hMSCs were seeded on tissue culture plastic (TCP) and incubated with 0, 100 and 1000 ng/mL FGF-2 in control medium. Data is expressed as percentage of the control without cells. Additionally, hMSCs were cultured on films of the SF derivative with 70 sulfonic acid groups per silk molecule that were treated with 0, 100 and 1000 ng/ml FGF-2 prior to cell seeding. Data is expressed as percentage of the corresponding control films without cells. (B) Summary of Fig. 4A: Drop in metabolic activity of hMSCs cultured on tissue culture plastic (TCP) and treated with 100 and 1000 ng/mL FGF-2 in control medium or cultured on films of the SF derivative with 70 sulfonic acid groups per silk molecule (70) that were treated with 100 and 1000 ng/ml FGF-2 prior to cell seeding as compared to cells treated with 0 ng/mL FGF-2 (n = 4; means ± SD; *p < 0.05, **p < 0.01).*
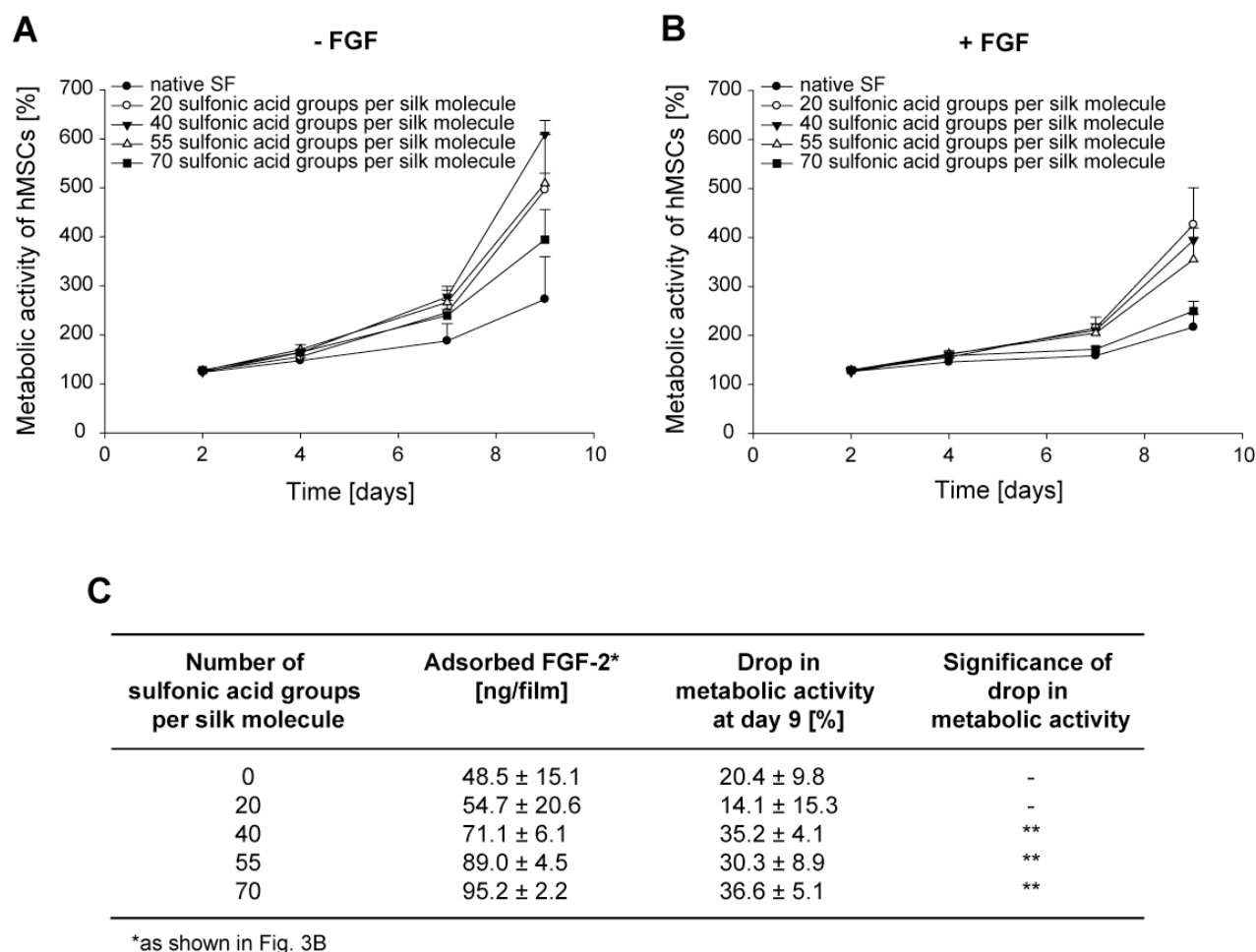
between the two FGF-2 concentrations. Overall, the drops in metabolic activity as observed with free FGF-2 versus FGF-2 bound to the sulfonated SF derivative were similar. Therefore, whether added as free FGF-2 or bound to the SF derivative, under the prevailing experimental conditions hMSCs responded by lowering their metabolic activity. This corresponds well with the biological effect of FGF-2 as previously observed in fibroblast cell culture, rat bone graft and demineralized bone matrix studies [43-45].

3.6. Metabolic activities of hMSCs as affected by FGF-2 bound to sulfonated SF derivatives with different degrees of sulfonation

Given the principal observation that FGF-2 - whether in a free or bound state - caused the metabolic activity of hMSCs to drop, we further investigated the incremental effects of FGF-2 bound to films of various sulfonated SF derivatives featuring increasing degrees of sulfonation. As controls we used films of native SF with bound FGF-2 and the corresponding FGF-2-free film controls. Again, the metabolic activities were determined at day 2, 4, 7 and 9. Under all culture conditions, the greatest increase in metabolic activity was seen between 7 and 9 days (Fig. 5A,B). After 9 days in culture the metabolic activity assessed in the cell cultures depended on the sulfonation of the SF derivative and on the FGF-2. Both in the absence and presence of bound FGF-2 we found the highest metabolic activity in hMSC cultures at intermediate levels of sulfonation. Metabolic activity was at a maximum in the absence of FGF-2 with hMSCs cultured on films containing 40 sulfonic acid groups per SF molecule, while in the presence of bound FGF-2 cells cultured on films containing 20 sulfonic acid groups had higher metabolic activity. With or without bound FGF-2 the metabolic activities on native SF films were the lowest. As compared to native SF, the SF derivatives with 20, 40 and 55 sulfonic acid groups per SF molecule showed significant increases in metabolic activities ($p < 0.01$). Overall, the principal response of the hMSCs to bound FGF-2 was a significant drop in metabolic activity by about one third (Fig. 5A,B), very much corresponding to the trend seen with the experiments using free FGF-2 (see above). Similar but minor trends were also observed after 7 days in culture, and

no significant effects were found at day 2 and 4. A summary of the effects after 9 days in culture is given in Fig. 5C.

Number of sulfonic acid groups per silk molecule	Adsorbed FGF-2* [ng/film]	Drop in metabolic activity at day 9 [%]	Significance of drop in metabolic activity
0	48.5 ± 15.1	20.4 ± 9.8	-
20	54.7 ± 20.6	14.1 ± 15.3	-
40	71.1 ± 6.1	35.2 ± 4.1	**
55	89.0 ± 4.5	30.3 ± 8.9	**
70	95.2 ± 2.2	36.6 ± 5.1	**

*as shown in Fig. 3B

Fig. 5. *Metabolic activity of hMSCs determined at day 2, 4, 7 and 9 using the alamarBlue assay. (A) hMSCs cultured on films of native SF and SF derivatives without FGF-2. (B) hMSCs cultured on films of native SF and SF derivatives following binding of FGF-2 as shown in Fig. 3B. (C) Summary of Fig. 5A and 5B at day 9: Drop in metabolic activity of hMSCs cultured on SF films with bound FGF-2 compared to the metabolic activity of cells cultured on the corresponding SF films without FGF-2 (n = 4; means ± SD; **p < 0.01).*

3.7. Effect of free versus bound FGF-2 on the phosphorylation of ERK1/2 of hMSCs

As a control experiment we analyzed how the phosphorylation of ERK1/2 of hMSCs was affected when exposed to free FGF-2 in the absence of films of native SF or sulfonated SF derivatives. For this, hMSCs were directly cultured in the TCP wells. The determination of pERK1/2 was carried out after 24 h. hMSCs that were treated with 100 ng/mL FGF-2 showed significantly higher levels of pERK1/2 as compared to hMSCs treated with control medium without FGF-2 ($p < 0.01$) (Fig. 6A). The increase in levels of pERK1/2 was $51.6 \pm 13.6\%$ (Fig. 6B).

Similarly, we investigated the effect of FGF-2 when bound to SF films with the highest level of sulfonation (70 sulfo groups per silk molecule) that were treated with either 100 or 1000 ng/mL FGF-2 prior to cell seeding. Again, the levels of pERK1/2 in hMSCs were significantly enhanced as compared to the corresponding FGF-2-free film control ($p < 0.01$) (Fig. 6A). The increase in the levels of ERK1/2 was $46.1 \pm 12.2\%$ and $44.1 \pm 5.3\%$, respectively (Fig. 6B) and was not significantly different between the two FGF-2 concentrations. Overall the increase in the levels of pERK1/2 as observed with free FGF-2 versus FGF-2 bound to films of the sulfonated SF derivative was similar. Therefore, whether added as free FGF-2 or bound to the films of the SF derivative, under the prevailing experimental conditions hMSCs responded by increasing their levels of pERK1/2.

3.8. Level of pERK1/2 of hMSCs as affected by FGF-2 bound to sulfonated SF derivatives with different degrees of sulfonation
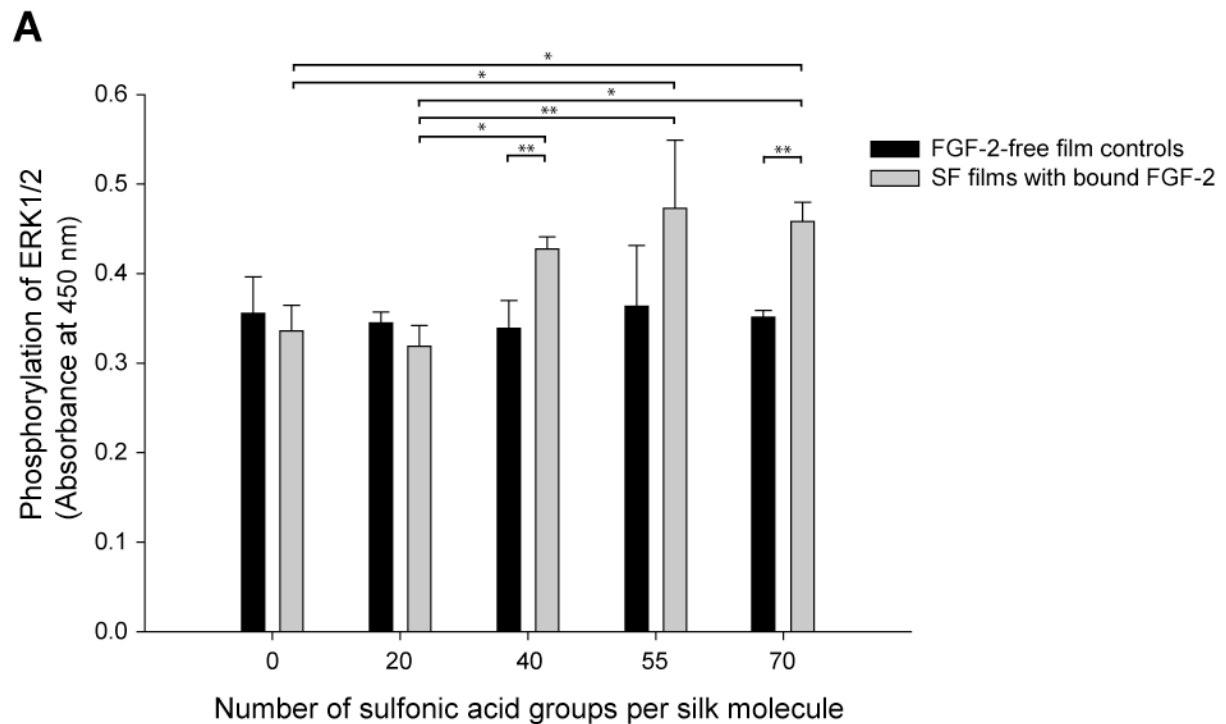
Given the principal observation that free and bound FGF-2 enhanced the levels of pERK1/2, we further investigated the effect of FGF-2 bound to films of various sulfonated SF derivatives featuring increasing degrees of sulfonation. As controls we used films of native SF with bound FGF-2 and the corresponding FGF-2-free film controls. Again, the levels of pERK1/2 were determined after

A

B
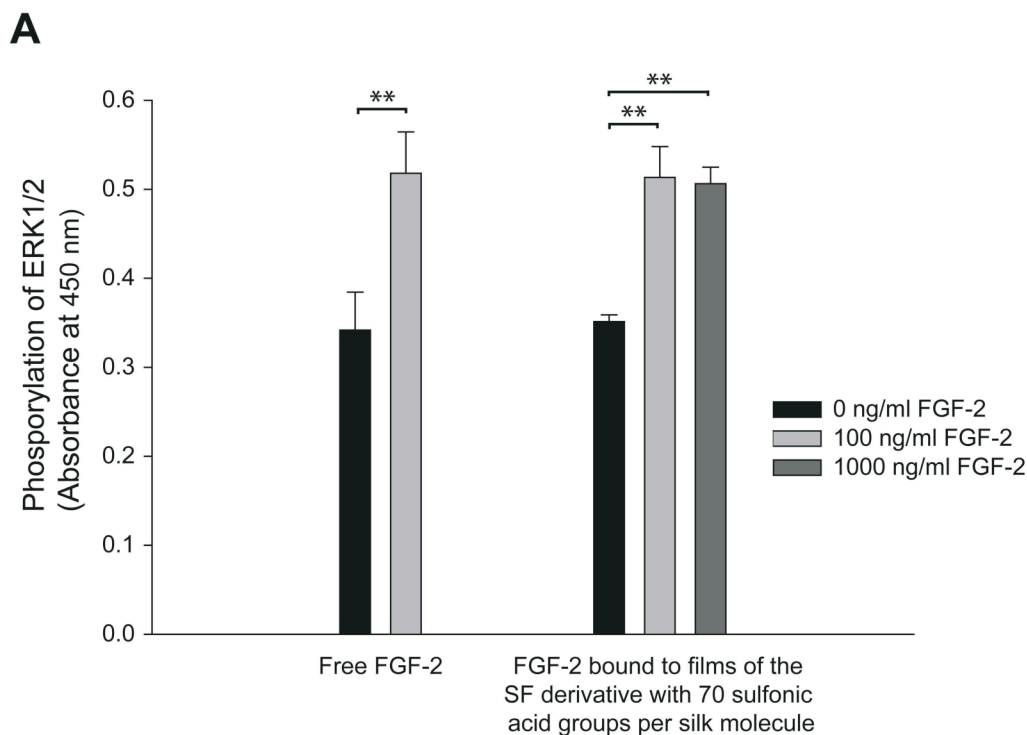
Sample	FGF-2 conc. [ng/ml]	Free FGF-2 [ng/well]	Adsorbed FGF-2 [ng/film]	Increase in pERK1/2 [%]	Significance of increase in pERK1/2
Free FGF-2	100	10		51.6 ± 13.6	**
70	100		10.1 ± 0.1	46.1 ± 12.2	**
70	1000		90.5 ± 3.1	44.1 ± 5.3	**

Fig. 6. (A) Phosphorylation of ERK1/2 of hMSCs determined after 24 h. hMSCs were seeded on tissue culture plastic (TCP) and incubated with 0 and 100 ng/mL FGF-2 in control medium. Additionally, hMSCs were cultured on films of the SF derivative with 70 sulfonic acid groups per silk molecule that were treated with 0, 100 and 1000 ng/mL FGF-2 prior to cell seeding. Data is expressed as absorbance measured at 450 nm. (B) Summary of Fig. 6A: Increase in pERK1/2 of hMSCs cultured on TCP and treated with 100 ng/mL FGF-2 in control medium or cultured on films of the SF derivative with 70 sulfonic acid groups per silk molecule (70) that were treated with 100 and 1000 ng/mL FGF-2 prior to cell seeding as compared to cells treated with 0 ng/mL FGF-2 (n = 3; means ± SD; **p < 0.01).

Fig. 7. *(A) Phosphorylation of ERK1/2 of hMSC determined after 24 h. hMSCs were cultured on films of native SF and sulfonated SF derivatives following FGF-2 binding as shown in Fig. 3B. Data is expressed as absorbance measured at 450 nm (means ± SD; *p < 0.05, **p < 0.01). (B) Summary of Fig. 7A: Increase in levels of pERK1/2 of hMSCs cultured on SF films with bound FGF-2 as compared to the levels of pERK1/2 of cells cultured on the corresponding SF films without FGF-2 (n = 3; means ± SD; **p < 0.01).*

24 h (Fig. 7A). No significant difference in the levels of pERK1/2 was observed between the FGF-2-free film controls irrespective of the number of sulfonic acid groups per silk molecule. When comparing SF films with bound FGF-2, films of

SF derivatives with 55 and 70 sulfonic acid groups per silk molecule showed significantly higher levels of pERK1/2 than films of native SF ($p < 0.05$) or films of the SF derivative with 20 sulfonic acid groups per silk molecule ($p < 0.01$ for films of SF derivative with 55 and $p < 0.05$ for films of SF derivative with 70 sulfonic acid groups per silk molecule). The presence of bound FGF-2 on films of SF derivatives with 40 and 70 sulfonic acid groups per silk molecule led to significantly higher levels of pERK1/2 as compared to the corresponding FGF-2-free film controls ($p < 0.01$). This increase was $26.2 \pm 4.0\%$ and $30.5 \pm 6.0\%$ for hMSCs cultured on films of SF derivatives with 40 and 70 sulfonic acid groups per silk molecule, respectively (Fig. 7B). Nevertheless, tendencies to higher levels of pERK1/2 were also seen for films of the SF derivative with 55 sulfonic acid groups per silk molecule with bound FGF-2 compared to the corresponding FGF-2-free film controls.

Overall, the principal response of the hMSCs to FGF-2 bound to films of SF derivatives with more than 20 sulfonic acid groups per silk molecule was an increase in the levels of pERK1/2 by about one third (Fig. 7B), whereas no change was observed with hMSCs cultured on films of native SF or SF derivative with 20 sulfonic acid groups per silk molecule.

4. Discussion

Analogous to nature where the sulfated glycosaminoglycan heparan sulfate is employed for physiological storage of FGF-2 in the ECM, we tested the hypothesis of whether SF could be decorated with moieties containing sulfonic acid groups in order to endow it with high capacity for non-covalent storage and sustained release of this heparin-binding growth factor for tissue engineering purposes. Recently, several approaches have been investigated to covalently immobilize growth factors to biomaterials [46-48]. However, covalent linkage of growth factors to biomaterials usually suffers from efficiency problems, leaving significant amounts of growth factor unconjugated or compromising its potency due to detrimental coupling conditions. Moreover, extensive washing steps may be necessary in order to remove residual coupling reagents that might

compromise the biocompatibility of the material. Therefore, the decoration of biomaterials with chemical moieties that could enhance the affinity of a growth factor to bind to this material may improve the loading efficiency as well as the immobilization and stabilization of the growth factor, thereby mimicking the biological storage of growth factors by components of the ECM. For this work, we utilized a simple protocol employing diazonium coupling chemistry to conjugate sulfonic acid functional groups to SF [26]. Films prepared from these sulfonated SF derivatives have been previously shown to support proliferation and differentiation of hMSCs [26]. For the present study, we synthesized various sulfonated SF derivatives containing approximately 20, 40, 55 and 70 sulfonic acid groups per SF molecule (Fig. 1), and analyzed their capacity to bind FGF-2. Furthermore, we examined the cellular response of hMSCs when seeded onto films of such conjugates that were prior loaded with FGF-2.

It is well known that cell adhesion and subsequent activity are generally enhanced on more hydrophilic surfaces [49]. The decoration of SF with sulfonated moieties drastically increased the hydrophilicity of SF (Fig. 2). This had a profound effect on the metabolic activity of hMSCs on films of SF derivatives (Fig. 5A), leading to higher metabolic activities as compared to cells grown on films of native SF with a maximum at a sulfonation degree of about 40 sulfonic acids per SF molecule. The observation that the highest metabolic activity in hMSC cultures was at intermediate levels of sulfonation is consistent with other studies that have reported that cell adhesion and proliferation preferentially occur on surfaces with intermediate levels of hydrophilicity [50-52]. The reduced metabolic activity on films with the highest degree of sulfonation (~70 sulfonic acids per SF molecule) may be explained by an increased negative charge density on the films which may possibly lead to an increased repulsion of negatively charged cell membranes [49].

The decoration with sulfonated moieties resulted in increased binding of FGF-2 to the films as compared to films of native SF (Fig. 3A) making these SF derivatives appealing biomaterials for FGF-2 storage. Increased binding of FGF-2 to various matrices decorated with heparin-like molecules has been previously reported [53-55]. Binding of FGF-2 obviously originates from an enhanced ionic interaction between the negatively charged sulfonic acid groups of the SF

derivative and the basic amino acid residues of FGF-2 [18]. As FGF-2 binding also occured with films of native SF, an additional contribution is also likely to occur from the interaction between the mainly negatively charged side chains of the hydrophilic spacers of the heavy chain of SF [56, 57] and the basic amino acid residues of FGF-2. Moreover, an interaction between the hydrophobic blocks (-Gly-Ala-Gly-Ala-Gly-Ser-)$_n$ of the heavy chain of SF and the hydrophobic core of FGF-2 [8] may be considered. Overall, the linear correlation between the degree of sulfonation and bound FGF-2 allows for predictable loading of FGF-2 (Fig. 3B) with high capacity. Within the experimental conditions of this study, loss of unbound FGF-2 was minor, suggesting an economic advantage over covalent linkage approaches.

More than 99% of bound FGF-2 was retained during incubation in buffer for up to 6 days (Fig. 3C), indicating a strong interaction not only between FGF-2 (pI = 9.6) and the sulfonic acid groups, but also between FGF-2 and SF itself. Similarly, strong retention of growth factors by matrices of native SF was also observed in other studies. For instance, depending on the preparation method of SF matrices, only 0.3% - 13% of nerve growth factor (pI = 9.3) was released within 22 days [58]. The somewhat lower retention of IGF-I by SF spheres and SF scaffolds, releasing approximately 30% of the initial loading within 4 weeks, may be explained by reduced ionic interaction due to its lower pI of 8.4 [31, 59] and suggests individual differences between growth factors. The inverse relationship between the degree of sulfonation and the release of FGF-2 in this study (Fig. 3D) indicates progressive retention with increasing degree of sulfonation. It also signifies a favorable premise to control FGF-2 binding and delivery under tissue engineering conditions *in vitro* or *in vivo*.

In nature, the ECM acts as a physiological reservoir for growth factors such as FGF-2 that is delivered upon cellular demand by expression of various enzymes [60]. On the other hand, growth factors interact with cell surface receptors even when bound to components of the ECM or to a substrate [61-63]. For instance, FGF-2 immobilized on a plastic substrate retained its bioactivity, stimulated ERK1/2 phosphorylation, cell proliferation and motility in endothelial cells [62]. Moreover, immobilized EGF on a polystyrene plate switched PC12 cells from growth to neural differentiation, whereas soluble EGF

was ineffective. EGF immobilized on a polystyrene plate caused a long lasting stimulation of ERK/MAPK [64]. In this context, we examined the biological response of hMSCs to FGF-2 bound to films of native SF or sulfonated SF derivatives. Only when bound to films of SF derivatives featuring at least 40 sulfonated moieties per SF molecule, FGF-2 showed preserved potency and significantly reduced the metabolic activity of adherent hMSCs (Fig. 5C). As the drop in metabolic activity was seen for free FGF-2 as well as for FGF-2 bound to SF films, we expected the inhibition to be an inherent FGF-2 characteristic. A dose dependent effect of FGF-2 featuring a drop in metabolic activity when using high FGF-2 concentrations on proliferation has been described elsewhere [43-45] and is not the focus of this study. For instance, concentrations of 100 ng/mL FGF-2 in medium supplemented with 2% FCS have been reported to inhibit serum-stimulated fibroblast proliferation by 29% over 3 days as compared to the controls without FGF-2 [43]. It also needs to be considered that the medium containing free FGF-2 was exchanged with fresh control medium supplemented with FGF-2 at the same concentration every 2 to 3 days. In contrast, FGF-2 was only bound once to films of native SF or SF derivatives and no further FGF-2 was added during the duration of the experiments. Therefore, it is even more evident that the drop in metabolic activity from free FGF-2 was not significantly different to FGF-2 bound to films of SF derivatives with at least 40 sulfonic acid groups (Fig. 4B and Fig. 5C), leading to the assumption that these SF derivatives were able to stabilize FGF-2. Speculatively a ceiling effect of FGF-2 may be also considered.

FGF-2 bound to films of native SF and sulfonated SF derivatives was further tested for its effect on the phosphorylation of ERK1/2 in hMSCs (Fig. 7). Activated ERK1/2 regulates cell function by phosphorylation of substrates such as downstream kinases, cytoskeletal elements, regulators of apoptosis, and several transcription factors, and is involved in cell proliferation, survival, differentiation, apoptosis, motility and metabolism [65, 66]. The importance of the ERK pathway for the proliferation of adult hMSC has been demonstrated [66]. Exclusively FGF-2 bound to films of SF derivatives with at least 40 sulfonic acid groups could retain the potency of FGF-2 as shown in an increase in pERK1/2. These results were thus in agreement with the results of the

metabolic activity (Fig. 5C). Therefore, SF derivatives with a sufficient degree of sulfonation may stabilize FGF-2, prevent rapid wash-out *in vivo* and act as a biomaterial substrate for local storage of potent growth factors.

FBS was used in all studies in order to mimic the interaction of serum components with the growth factor loaded SF film, which is likely to happen in an *in vivo* situation. Components of the FBS such as growth factors that affect cell behavior may preferably bind to films of native SF or films of the sulfonated SF derivatives or replace already bound growth factor changing its release kinetics. The presence of serum components might change the effect of the loaded SF film on seeded cells. However, no difference between the levels of pERK1/2 of hMSCs cultured on TCP and hMSCs cultured on films of the SF derivative with 70 sulfonic acid groups per silk molecule was detected when medium with FBS was used (Fig. 6A). This suggests a biological response irrespective of a potential binding of other components of FBS. Therefore, the difference in metabolic activity between hMSCs cultured on TCP and hMSCs cultured on SF films of sulfonated SF derivatives is likely to be the result of the difference in hydrophobicities of the substrates.

The *in vivo* performance of SF derivates decorated with sulfonic acid groups has still to be determined. Highly charged polyanionic polymers were shown to modulate various enzymatic cascades in plasma, affecting coagulation, fibrinolysis, inflammation and vasculature function [67, 68]. Highly sulfated polysaccharides were shown to be able to initiate activation of the contact system [67, 69]. Recently, oversulfated chondroitin sulfate (OSCS), a compound contaminating heparin supplies worldwide, has been associated with severe anaphylactoid reactions that have occurred after intravenous heparin administration [70]. Moreover, the importance of an accurate sulfation of the extracellular matrix is underscored by the pathogenesis of several chondrodysplasias. This disease is associated to undersulfation of proteoglycans due to mutations of the diastrophic dysplasia sulfate transporter, a transmembrane glycoprotein with a critical role for the sulfation of proteoglycans [71]. Therefore, the performance of the SF derivatives decorated with sulfonic acid moieties has to be tested for each individual application.

In this study, we showed that films of SF derivatives decorated with sulfonic acid moieties resulted in superior binding of bioactive FGF-2 as compared to films of native SF. This allowed for predictable non-covalent loading and sustained binding of FGF-2 on SF substrates. Moreover, the potency of FGF-2 was exclusively retained when bound to films of sulfonated SF derivatives, resulting in reduced metabolic activities of hMSC and increased levels of pERK1/2. Based on our results, sulfonated SF derivatives represent a promising biomaterial for efficient loading of growth factors and should be further investigated as ECM-mimic for tissue regeneration. Further studies are encouraged to elucidate this potential in the context of angiogenesis using cell types such as fibroblasts and endothelial cells. *In vivo* corroboration of the data would be another objective.

Acknowledgements

References

1.	Ma PX. Biomimetic materials for tissue engineering. Adv. Drug Deliv. Rev. 2008;60(2):184-198.

2.	Lutolf MP, Hubbell JA. Synthetic biomaterials as instructive extracellular microenvironments for morphogenesis in tissue engineering. Nat. Biotechnol. 2005;23(1):47-55.

3.	Badylak SF. The extracellular matrix as a biologic scaffold material. Biomaterials 2007;28(25):3587-3593.

4.	Chan G, Mooney DJ. New materials for tissue engineering: towards greater control over the biological response. Trends Biotechnol. 2008;26(7):382-392.

5.	Taylor PM. Biological matrices and bionanotechnology. Philos. Trans. R. Soc. Lond. 2007;362(1484):1313-1320.

6.	Shin H, Jo S, Mikos AG. Biomimetic materials for tissue engineering. Biomaterials 2003;24(24):4353-4364.

7.	Sofia S, McCarthy MB, Gronowicz G, Kaplan DL. Functionalized silk-based biomaterials for bone formation. J. Biomed. Mater. Res. 2001;54(1):139-148.

8.	Nugent MA, Iozzo RV. Fibroblast growth factor-2. Int. J. Biochem. Cell Biol. 2000;32(2):115-120.

9.	Ornitz DM. FGFs, heparan sulfate and FGFRs: complex interactions essential for development. Bioessays 2000;22(2):108-112.

10.	Harmer NJ. Insights into the role of heparan sulphate in fibroblast growth factor signalling. Biochem. Soc. Trans. 2006;34(Pt 3):442-445.

11.	Manton KJ, Leong DF, Cool SM, Nurcombe V. Disruption of heparan and chondroitin sulfate signaling enhances mesenchymal stem cell-derived osteogenic differentiation via bone morphogenetic protein signaling pathways. Stem cells (Dayton, Ohio) 2007;25(11):2845-2854.

12.	Hashi CK, Zhu Y, Yang GY, Young WL, Hsiao BS, Wang K, et al. Antithrombogenic property of bone marrow mesenchymal stem cells in nanofibrous vascular grafts. Proc. Natl. Acad. Sci. U.S.A. 2007;104(29):11915-11920.

13. Vlodavsky I, Miao HQ, Medalion B, Danagher P, Ron D. Involvement of heparan sulfate and related molecules in sequestration and growth promoting activity of fibroblast growth factor. Cancer Metastasis Rev. 1996;15(2):177-186.

14. Ruoslahti E, Yamaguchi Y. Proteoglycans as modulators of growth factor activities. Cell 1991;64(5):867-869.

15. Whitelock JM, Graham LD, Melrose J, Murdoch AD, Iozzo RV, Underwood PA. Human perlecan immunopurified from different endothelial cell sources has different adhesive properties for vascular cells. Matrix Biol. 1999;18(2):163-178.

16. Yayon A, Klagsbrun M, Esko JD, Leder P, Ornitz DM. Cell surface, heparin-like molecules are required for binding of basic fibroblast growth factor to its high affinity receptor. Cell 1991;64(4):841-848.

17. Kunou M, Koizumi M, Shimizu K, Kawase M, Hatanaka K. Synthesis of sulfated colominic acids and their interaction with fibroblast growth factors. Biomacromolecules 2000;1(3):451-458.

18. Coltrini D, Rusnati M, Zoppetti G, Oreste P, Isacchi A, Caccia P, et al. Biochemical bases of the interaction of human basic fibroblast growth factor with glycosaminoglycans. New insights from trypsin digestion studies. Eur. J. Biochem. 1993;214(1):51-58.

19. Zamora PO, Tsang R, Pena LA, Osaki S, Som P. Local delivery of basic fibroblast growth factor (bFGF) using adsorbed silyl-heparin, benzyl-bis(dimethylsilylmethyl)oxycarbamoyl-heparin. Bioconjug. Chem. 2002;13(5):920-926.

20. Matsusaki M, Serizawa T, Kishida A, Akashi M. Novel functional biodegradable polymer II: fibroblast growth factor-2 activities of poly(gamma-glutamic acid)-sulfonate. Biomacromolecules 2005;6(1): 400-407.

21. Altman GH, Diaz F, Jakuba C, Calabro T, Horan RL, Chen J, et al. Silk-based biomaterials. Biomaterials 2003;24(3):401-416.

22. Meinel L, Betz O, Fajardo R, Hofmann S, Nazarian A, Cory E, et al. Silk based biomaterials to heal critical sized femur defects. Bone 2006;39(4):922-931.

23. Hofmann S, Knecht S, Langer R, Kaplan DL, Vunjak-Novakovic G, Merkle HP, et al. Cartilage-like tissue engineering using silk scaffolds and mesenchymal stem cells. Tissue Eng. 2006;12(10):2729-2738.

24. Kirker-Head C, Karageorgiou V, Hofmann S, Fajardo R, Betz O, Merkle HP, et al. BMP-silk composite matrices heal critically sized femoral defects. Bone 2007;41(2):247-255.

25. Altman GH, Horan RL, Lu HH, Moreau J, Martin I, Richmond JC, et al. Silk matrix for tissue engineered anterior cruciate ligaments. Biomaterials 2002;23(20):4131-4141.

26. Murphy AR, St John P, Kaplan DL. Modification of silk fibroin using diazonium coupling chemistry and the effects on hMSC proliferation and differentiation. Biomaterials 2008;29(19):2829-2838.

27. Gotoh Y, Tsukada M, Minoura N, Imai Y. Synthesis of poly(ethylene glycol)-silk fibroin conjugates and surface interaction between L-929 cells and the conjugates. Biomaterials 1997;18(3):267-271.

28. Tamada Y. Sulfation of silk fibroin by chlorosulfonic acid and the anticoagulant activity. Biomaterials 2004;25(3):377-383.

29. Zheng Q, Huang G, Yang J, Xu Y, Guo C, Xi Y, et al. Could the effect of modeled microgravity on osteogenic differentiation of human mesenchymal stem cells be reversed by regulation of signaling pathways? Biol. Chem. 2007;388(7):755-763.

30. Giuliani R, Bastaki M, Coltrini D, Presta M. Role of endothelial cell extracellular signal-regulated kinase1/2in urokinase-type plasminogen activator upregulation and in vitro angiogenesis by fibroblast growth factor-2. J. Cell Sci. 1999;112:2597-2606.

31. Wenk E, Wandrey AJ, Merkle HP, Meinel L. Silk fibroin spheres as a platform for controlled drug delivery. J. Control. Release 2008;132(1):26-34.

32. Wenk E, Meinel AJ, Wildy S, Merkle HP, Meinel L. Microporous silk fibroin scaffolds embedding PLGA microparticles for controlled growth factor delivery in tissue engineering. Biomaterials 2009;30:2571-2581.

33. Hino T, Tanimoto M, Shimabayashi S. Change in secondary structure of silk fibroin during preparation of its microspheres by spray-drying and

exposure to humid atmosphere. J. Colloid. Interface Sci. 2003;266(1):68-73.

34. Meinel L, Hofmann S, Betz O, Fajardo R, Merkle HP, Langer R, et al. Osteogenesis by human mesenchymal stem cells cultured on silk biomaterials: comparison of adenovirus mediated gene transfer and protein delivery of BMP-2. Biomaterials 2006;27(28):4993-5002.

35. Meinel L, Karageorgiou V, Fajardo R, Snyder B, Shinde-Patil V, Zichner L, et al. Bone tissue engineering using human mesenchymal stem cells: effects of scaffold material and medium flow. Ann. Biom. Eng. 2004;32(1):112-122.

36. Meinel L, Karageorgiou V, Hofmann S, Fajardo R, Snyder B, Li C, et al. Engineering bone-like tissue in vitro using human bone marrow stem cells and silk scaffolds. J. Biomed. Mater Res 2004;71(1):25-34.

37. Hagenmüller H, Hofmann S, Kohler T, Merkle HP, Kaplan DL, Vunjak-Novakovic G, et al. Non-invasive time-lapsed monitoring and quantification of engineered bone-like tissue. Ann. Biom. Eng. 2007;35(10):1657-1667.

38. Nakayama GR, Caton MC, Nova MP, Parandoosh Z. Assessment of the Alamar Blue assay for cellular growth and viability in vitro. J. Immunol. Methods 1997;204(2):205-208.

39. Zhou CZ, Confalonieri F, Jacquet M, Perasso R, Li ZG, Janin J. Silk fibroin: structural implications of a remarkable amino acid sequence. Proteins 2001;44(2):119-122.

40. Asakura T, Kuzuhara A, Tabeta R, Saito H. Conformation characterization of Bombyx mori silk fibroin in the solid state by high-frequency 13C cross polarization-magic angle spinning NMR, X-ray diffraction, and infrared spectroscopy. Macromolecules 1985;18:1841-1845.

41. Monti P, Freddi G, Bertoluzza A, Kasai N, Tsukada M. Raman spectroscopic studies of silk fibroin from Bombyx mori. J. Raman Spectrosc. 1998;29:297-304.

42. Marsh RE, Corey RB, Pauling L. An investigation of the structure of silk fibroin. Biochim. Biophys. Acta 1955;16(1):1-34.

43. Garcia-Maya M, Anderson AA, Kendal CE, Kenny AV, Edwards-Ingram LC, Holladay A, et al. Ligand concentration is a driver of divergent signaling and pleiotropic cellular responses to FGF. J. Cell. Physiol. 2006;206(2):386-393.

44. Wang JS, Aspenberg P. Basic fibroblast growth factor enhances bone-graft incorporation: dose and time dependence in rats. J. Orthop. Res. 1996;14(2):316-323.

45. Wang JS, Aspenberg P. Basic fibroblast growth factor and bone induction in rats. Acta Orthop. Scand. 1993;64(5):557-561.

46. Karageorgiou V, Meinel L, Hofmann S, Malhotra A, Volloch V, Kaplan D. Bone morphogenetic protein-2 decorated silk fibroin films induce osteogenic differentiation of human bone marrow stromal cells. J. Biomed. Mater. Res. 2004;71(3):528-537.

47. Geer DJ, Swartz DD, Andreadis ST. Biomimetic delivery of keratinocyte growth factor upon cellular demand for accelerated wound healing in vitro and in vivo. Am. J. Pathol. 2005;167(6):1575-1586.

48. Chen PR, Chen MH, Lin FH, Su WY. Release characteristics and bioactivity of gelatin-tricalcium phosphate membranes covalently immobilized with nerve growth factors. Biomaterials 2005;26(33):6579-6587.

49. Wilson CJ, Clegg RE, Leavesley DI, Pearcy MJ. Mediation of biomaterial-cell interactions by adsorbed proteins: a review. Tissue Eng. 2005;11(1-2):1-18.

50. Kim MS, Shin YN, Cho MH, Kim SH, Kim SK, Cho YH, et al. Adhesion behavior of human bone marrow stromal cells on differentially wettable polymer surfaces. Tissue Eng. 2007;13(8):2095-2103.

51. Tamada Y, Ikada Y. Effect of preadsorbed proteins on cell adhesion to polymer surfaces. J. Colloid. Interface Sci. 1993;155:334-339.

52. Neff JA, Tresco PA, Caldwell KD. Surface modification for controlled studies of cell-ligand interactions. Biomaterials 1999;20(23-24):2377-2393.

53. Wissink MJ, Beernink R, Poot AA, Engbers GH, Beugeling T, van Aken WG, et al. Improved endothelialization of vascular grafts by local release

of growth factor from heparinized collagen matrices. J. Control. Release 2000;64(1-3):103-114.

54. Bos GW, Scharenborg NM, Poot AA, Engbers GH, Beugeling T, van Aken WG, et al. Proliferation of endothelial cells on surface-immobilized albumin-heparin conjugate loaded with basic fibroblast growth factor. J. Biomed. Mater. Res. 1999;44(3):330-340.

55. Freeman I, Kedem A, Cohen S. The effect of sulfation of alginate hydrogels on the specific binding and controlled release of heparin-binding proteins. Biomaterials 2008;29(22):3260-3268.

56. Zhou CZ, Confalonieri F, Medina N, Zivanovic Y, Esnault C, Yang T, et al. Fine organization of Bombyx mori fibroin heavy chain gene. Nucleic Acids Res. 2000;28(12):2413-2419.

57. Foo CW, Bini E, Hensman J, Knight DP, Lewis RV, Kaplan DL. Role of pH and charge on silk protein assembly in insects and spiders. Appl. Phys. A 2006;82:223-233.

58. Uebersax L, Mattotti M, Papaloizos M, Merkle HP, Gander B, Meinel L. Silk fibroin matrices for the controlled release of nerve growth factor (NGF). Biomaterials 2007;28(30):4449-4460.

59. Uebersax L, Merkle HP, Meinel L. Insulin-like growth factor I releasing silk fibroin scaffolds induce chondrogenic differentiation of human mesenchymal stem cells. J. Control. Release 2008;127(1):12-21.

60. Whitelock JM, Murdoch AD, Iozzo RV, Underwood PA. The degradation of human endothelial cell-derived perlecan and release of bound basic fibroblast growth factor by stromelysin, collagenase, plasmin, and heparanases. J. Biol. Chem. 1996;271(17):10079-10086.

61. Smith JC, Singh JP, Lillquist JS, Goon DS, Stiles CD. Growth factors adherent to cell substrate are mitogenically active in situ. Nature 1982;296(5853):154-156.

62. Tanghetti E, Ria R, Dell'Era P, Urbinati C, Rusnati M, Ennas MG, et al. Biological activity of substrate-bound basic fibroblast growth factor (FGF2): recruitment of FGF receptor-1 in endothelial cell adhesion contacts. Oncogene 2002;21(24):3889-3897.

63. Vincent TL, McLean CJ, Full LE, Peston D, Saklatvala J. FGF-2 is bound to perlecan in the pericellular matrix of articular cartilage, where it acts as a chondrocyte mechanotransducer. Osteoarthr. Cartil. 2007;15(7):752-763.

64. Ito Y, Chen G, Imanishi Y, Morooka T, Nishida E, Okabayashi Y, et al. Differential control of cellular gene expression by diffusible and non-diffusible EGF. J. Biochem. 2001;129(5):733-737.

65. Chua CC, Rahimi N, Forsten-Williams K, Nugent MA. Heparan sulfate proteoglycans function as receptors for fibroblast growth factor-2 activation of extracellular signal-regulated kinases 1 and 2. Circ. Res. 2004;94(3):316-323.

66. Carcamo-Orive I, Tejados N, Delgado J, Gaztelumendi A, Otaegui D, Lang V, et al. ERK2 protein regulates the proliferation of human mesenchymal stem cells without affecting their mobilization and differentiation potential. Exp. Cell Res. 2008;314(8):1777-1788.

67. Hojima Y, Cochrane CG, Wiggins RC, Austen KF, Stevens RL. In vitro activation of the contact (Hageman factor) system of plasma by heparin and chondroitin sulfate E. Blood 1984;63(6):1453-1459.

68. Henry SP, Giclas PC, Leeds J, Pangburn M, Auletta C, Levin AA, et al. Activation of the alternative pathway of complement by a phosphorothioate oligonucleotide: potential mechanism of action. J. Pharmacol. Exp. Ther. 1997;281(2):810-816.

69. Silverberg M, Diehl SV. The activation of the contact system of human plasma by polysaccharide sulfates. Ann. N. Y. Acad. Sci. 1987;516:268-279.

70. Kishimoto TK, Viswanathan K, Ganguly T, Elankumaran S, Smith S, Pelzer K, et al. Contaminated heparin associated with adverse clinical events and activation of the contact system. N. Engl. J. Med 2008;358(23):2457-2467.

71. Hastbacka J, de la Chapelle A, Mahtani MM, Clines G, Reeve-Daly MP, Daly M, et al. The diastrophic dysplasia gene encodes a novel sulfate transporter: positional cloning by fine-structure linkage disequilibrium mapping. Cell 1994;78(6):1073-1087.

FINAL DISCUSSION AND OUTLOOK

Silk fibroin (SF) has previously shown to represent an attractive biomaterial for tissue regeneration, obviously due to its favorable processability, biocompatibility, long-term biodegradability and superior mechanical strength [1-3]. To further improve and widen the performance of SF constructs for this purpose, the combination of the SF matrix with growth factors is a promising objective. In order to maintain the potency of such sensitive therapeutics in the final product, its fabrication needs to be carefully planned. A suitable fabrication process should ideally circumvent the use of elevated temperatures, organic solvents, water/solvent interfaces and/or cross-linking reagents. Mild fabrication conditions should allow a straightforward introduction of the growth factor into the process, e.g., by simply mixing a solution of the growth factor with a SF solution. Otherwise, the incorporation of the growth factor may be performed through adsorption or covalent coupling to a prefabricated system. But unless efficiently bound by specific interaction, the adsorption of growth factors may be troubled by low binding capacity, loss of unbound material and rapid release. Covalent linkage of growth factors to SF and other biomaterials has shown to be an alternative [4-6], but usually suffers from efficiency problems, leaving significant amounts of growth factor unconjugated or with compromised potency due to detrimental coupling conditions. Steric hindrance may be another pending problem and requires careful selection of conjugation sites and spacers. Moreover, extensive washing steps may be necessary in order to remove residual coupling reagents that might compromise the biocompatibility of the material. Altogether, the ability to modify the release of growth factors through adsorption or covalent coupling to a biomaterial is limited.

Against this background, the main objective of the present PhD thesis was an investigation on the potential of silk fibroin (SF) as a platform for controlled drug delivery, with a major focus on growth factors for tissue regeneration. In particular, this work covers the following aspects:

(i)   A new fabrication approach for a mild and efficient incorporation of highly sensitive biologicals such as insulin-like growth factor I (IGF-I) into SF spheres for tissue regeneration applications.

(ii)   The assembly of IGF-I loaded poly-(lactide-co-glycolide) microparticles (PLGA MP) into porous SF scaffolds as an approach to combine the capacity of PLGA MP for controlled growth factor delivery with the mechanical support exerted by SF scaffolds.

(iii)   The implementation of natural concepts for growth factor storage and delivery, using chemically modified SF for enhanced non-covalent binding and controlled delivery of fibroblast growth factor 2 (FGF-2).

SF spheres were prepared by means of a laminar jet break-up technology using a nozzle vibrating at controlled frequency and amplitude. In contrast to other methods for the preparation of spheres, their fabrication occured under mild conditions, using an aqueous SF solution and by working at room temperature or below. As a more gentle alternative to the most frequently used methanol treatment to induce water insolubility through β-sheet enrichment, the thus produced SF spheres were treated with water vapor, thus bypassing the use of organic solvents that may be detrimental to growth factor stability. Variations in the diameter of the nozzle, SF concentration, and subsequent treatment turned out to result in spheres with distinct modifications in size, morphology and release rates. In contrast to most other fabrication methods, the applied technology resulted in high encapsulation efficiencies, being in the range of 100% for both the model compounds salicylic acid and propranolol hydrochloride, as well as for the growth factor IGF-I. Particularly for costly therapeutics, high encapsulation efficiency is a crucial feature for controlled release formulations. It minimizes the mass loss of such therapeutics during fabrication and helps to better sustain their release upon application. The biological potency of IGF-I released from such SF spheres was found to be preserved.

The desired size of such spheres obviously depends on the intended site of injection and application. The laminar jet break-up technology chosen was

particularly suitable for the preparation of relatively large spheres. By choosing a nozzle with a much smaller diameter, free flow through the nozzle may become difficult, especially when using SF solutions of high viscosity. Smaller SF micro- and nanospheres could be envisaged using a modified electrospinning approach, e.g., by adjusting the applied voltage or the concentration or viscosity of the SF solution [7-9]. The produced particles may be collected in pre-cooled methanol or frozen in liquid nitrogen. High encapsulation efficiencies can be equally assumed.

As an approach to better confine growth factor loaded particles to the site of administration and add capacity for bearing mechanical load, we combined porous SF scaffolds with PLGA microparticles (PLGA MP) comprising IGF-I. In fact, PLGA MP represent a well-known option to modulate growth factor release [10-12]. Their biomedical potential as IGF-I delivery system for bone repair has been previously demonstrated in a sheep model [10]. In contrast to a direct embedment of IGF-I into SF scaffolds [13], the incorporation of IGF-I loaded PLGA MP was expected to further protect the growth factor during fabrication of the delivery system and to better control the release of the growth factor. In fact, the release kinetics of the growth factor were not only governed by the SF scaffold itself but also by the biodegradation kinetics of the PLGA MP. This adds further opportunities to better keep the release of growth factors from scaffolds under control. Further studies are necessary to investigate the impact of the obtained release kinetics on the cellular differentiation and proliferation on and in the scaffold. The present study focusing on a single growth factor load may be also expanded towards a combination of growth factors, e.g., for dual growth factor delivery, to better comply with the physiological process.

Although SF scaffolds incorporating growth factor loaded PLGA MP show advantages, their fabrication is complex and certainly not exclusive to deliver growth factors. A more straightforward option would be the sequential assembly of the components, consisting of a prior fabrication of the SF scaffold equipped with sufficient binding capacity, followed by a subsequent protocol to load the growth factor. This would not only speed up the development and manufacturing of such delivery systems, but also help to maintain the potency of

embedded growth factor due to the fact that the necessary sterilization of the SF scaffold may be performed before loading the growth factor. Additionally, the growth factor may be safely kept in a dry and stable state, and bound just prior to administration. In order to provide sufficient binding capacity for the growth factor and to enhance cell adherence, we decorated SF with sulfonic acid moieties, mimicking the binding capacity of sulfated glycosaminoglycan heparan sulfate, which represents a major component of the extracellular matrix (ECM) of mammalian tissue and is known to bind FGF-2. In fact, we could demonstrate that films of SF derivatives decorated with sulfonic acid moieties resulted in superior binding of FGF-2 as compared to films of native SF. This allowed for predictable non-covalent loading and sustained binding of FGF-2 on SF substrates. The potency of FGF-2 was readily retained when bound to films of sulfonated SF derivatives, as demonstrated by reduced metabolic turnover as well as enhanced phosphorylation of extracellular signal-regulated kinases in human mesenchymal stem cells. Based on our results, sulfonated SF derivatives represent an advanced biomaterial for efficient loading of this growth factor and should be tested as an ECM-mimic for tissue regeneration. What still needs to be resolved is whether the biological response to such constructs was induced by bound or continuously released FGF-2. A possible systemic toxicity of sulfonated SF derivatives would be another important issue to be tested. Further studies are also encouraged to elucidate the potential of decorated SF in the context of angiogenesis. *In vivo* corroboration of the data could be another objective. To which extent sulfonic acid moieties, differing in conjugation site, size and structure, would affect their interaction with the growth factor or with cellular receptors, would be interesting to be investigated in more detail as well.

The present PhD thesis has shown several options to sustain the release of growth factors from SF as a biomaterial. The knowledge of the interaction between therapeutics and SF may lead to a better control of drug release rates from SF matrices. Nevertheless, it should be carefully considered whether the common approach to let the growth factor be released from the matrix or the more recently raised substrate-mediated approach calling for a firm attachment of the growth factor to the matrix is more promising. Signaling induced by certain growth factors firmly attached to a biomaterial may induce a stronger

response than signaling by a soluble factor, while other factors may show better results when being released [14]. A more sufficient understanding of the interplay of specific biological, chemical and physical cues on the quality of *in vitro* and *in vivo* engineered tissue is required for optimal tissue regeneration. The challenge will be to accurately adjust the involved variables according to the physiological and therapeutic needs.

References

1. Altman GH, Diaz F, Jakuba C, Calabro T, Horan RL, Chen J, et al. Silk-based biomaterials. Biomaterials 2003;24(3):401-416.

2. Horan RL, Antle K, Collette AL, Wang Y, Huang J, Moreau JE, et al. In vitro degradation of silk fibroin. Biomaterials 2005;26(17):3385-3393.

3. Meinel L, Hofmann S, Karageorgiou V, Kirker-Head C, McCool J, Gronowicz G, et al. The inflammatory responses to silk films in vitro and in vivo. Biomaterials 2005;26(2):147-155.

4. Karageorgiou V, Meinel L, Hofmann S, Malhotra A, Volloch V, Kaplan D. Bone morphogenetic protein-2 decorated silk fibroin films induce osteogenic differentiation of human bone marrow stromal cells. J Biomed Mater Res A 2004;71(3):528-537.

5. Geer DJ, Swartz DD, Andreadis ST. Biomimetic delivery of keratinocyte growth factor upon cellular demand for accelerated wound healing in vitro and in vivo. Am J Pathol 2005;167(6):1575-1586.

6. Chen PR, Chen MH, Lin FH, Su WY. Release characteristics and bioactivity of gelatin-tricalcium phosphate membranes covalently immobilized with nerve growth factors. Biomaterials 2005;26(33):6579-6587.

7. Wang H, Zhang Y, Shao H, Hu X. Electrospun ultra-fine silk fibroin fibers from aqueous solutions. J Mater Sci 2005;40:5359-5363.

8. Sukigara S, Gandhi M, Ayutsede J, Micklus M, Ko F. Regeneration of Bombyx mori silk by electrospinning-part 1: processing parameters and geometric properties. Polymer 2003;44:5721-5727.

9. Meechaisue C, Wutticharoenmongkol P, Waraput R, Huangjing T, Ketbumrung N, Pavasant P, et al. Preparation of electrospun silk fibroin fiber mats as bone scaffolds: a preliminary study. Biomed Mater 2007;2(3):181-188.

10. Meinel L, Zoidis E, Zapf J, Hassa P, Hottiger MO, Auer JA, et al. Localized insulin-like growth factor I delivery to enhance new bone formation. Bone 2003;33(4):660-672.

11. Woo BH, Fink BF, Page R, Schrier JA, Jo YW, Jiang G, et al. Enhancement of bone growth by sustained delivery of recombinant human bone morphogenetic protein-2 in a polymeric matrix. Pharm Res 2001;18(12):1747-1753.

12. Schrier JA, DeLuca PP. Porous bone morphogenetic protein-2 microspheres: polymer binding and in vitro release. AAPS PharmSciTech 2001;2(3):E17.

13. Uebersax L, Merkle HP, Meinel L. Insulin-like growth factor I releasing silk fibroin scaffolds induce chondrogenic differentiation of human mesenchymal stem cells. J Control Release 2008;127(1):12-21.

14. Dinbergs ID, Brown L, Edelman ER. Cellular response to transforming growth factor-beta1 and basic fibroblast growth factor depends on release kinetics and extracellular matrix interactions. J Biol Chem 1996;271(47):29822-29829.

CURRICULUM VITAE

Esther Wenk

born in Wattwil, Switzerland

on September 29th, 1978

EDUCATION

07. 2004 – 01. 2009	**Ph.D thesis and teaching assistant**
	(ETH Zurich, Switzerland)
	Institute of Pharmaceutical Sciences Drug Formulation and Delivery Group Advisors: Prof. H.P. Merkle, Dr. Dr. L. Meinel Thesis: „Silk fibroin as a vehicle for drug delivery in tissue regeneration"
11. 2003	**Swiss Federal Diploma of Pharmacy**
10. 1998 – 11. 2003	**Undergraduate studies in Pharmacy**
	(ETH Zurich, Switzerland)
	Diploma thesis: "Biologische Zellantwort von kultivierten Osteoblasten auf mit Wachstumsfaktor beladene PLGA Mikrosphären"
08. 1994 – 08. 1998	**Matura Typus C**
	(Gymnasium Wattwil, Switzerland)

PROFESSIONAL EXPERIENCE

02. 2009 – present	**Swiss Federal Office of Public Health**
	(Bern, Switzerland)
	Scientific associate

12. 2003 – 02. 2004	**Falken Apotheke**
05. 2004 – 06. 2004	(Zurich, Switzerland)
	Part-time work as pharmacist

03. 2004 – 04. 2004	**Health Center Nkambe**
	(Nkambe, Cameroon, Africa)
	Work as pharmacist

2002 – 2004	**Apotheke Wattwil**
	(Wattwil, Switzerland)
	Part-time work as pharmacist

08. 2000 – 08. 2001	**Apotheke Wattwil**
	(Wattwil, Switzerland)
	Practical training as a cand. pharm. in the context of the undergraduate studies in pharmacy

SCIENTIFIC CONTRIBUTIONS

Publications

Wenk E, Merkle HP, Meinel L. Silk fibroin as a vehicle for drug delivery applications. To be submitted.

Wenk E, Murphy AR, Kaplan DL, Merkle HP, Meinel L, Uebersax L. The use of sulfonated silk fibroin derivatives to control binding, delivery and potency of FGF-2 for tissue regeneration. Biomaterials 2010,31(6):1403-1413.

Yildirim S, Borer ME, **Wenk E**, Meinel L, Lacroix C. Development of silk fibroin-based beads for immobilized cell fermentations. J Microencapsul 2010;27(1):1-9.

Wenk E, Meinel AJ, Wildy S, Merkle HP, Meinel L. Microporous silk fibroin scaffolds embedding PLGA microparticles for controlled growth factor delivery in tissue engineering. Biomaterials 2009; 30:2571-2581.

Wenk E, Wandrey AJ, Merkle HP, Meinel L. Silk fibroin spheres as a platform for controlled drug delivery. J Control Release 2008;132(1):26-34.

Wang X, **Wenk E**, Zhang X, Meinel L, Vunjak-Novakovic G, Kaplan DL. Growth factor gradients via microsphere delivery in biopolymer scaffolds for osteochondral tissue engineering. J Control Release 2008;34:81-90.

Wang X, **Wenk E**, Matsumoto A, Meinel L, Li C, Kaplan DL. Silk microspheres for encapsulation and controlled release. J Control Release 2007;117(3):360-370.

Wang X, **Wenk E**, Hu X, Castro GR, Meinel L, Wang X, et al. Silk coatings on PLGA and alginate microspheres for protein delivery. Biomaterials 2007;28(28):4161-4169.

Luginbuehl V, **Wenk E**, Koch A, Gander B, Merkle HP, Meinel L. Insulin-like growth factor I-releasing alginate-tricalciumphosphate composites for bone regeneration. Pharm Res 2005;22(6):940-950.

Oral presentations

E. Wenk, Preparation and application of silk spheres for controlled drug delivery, Zurich-Geneva Joint Seminar Series in Drug Formulation & Delivery, February 15 – 16, 2007, Geneva, Switzerland.

E. Wenk, Microparticulate polymeric systems for drug delivery and tissue engineering, "Doktorandentag", Faculty of Pharmacy, October 18, 2006, Zurich, Switzerland.

E. Wenk, Preparation of silk spheres for controlled drug delivery, 33rd Annual Meeting and Exposition of the Controlled Release Society, July 22 – 26, 2006, Vienna, Austria.

E. Wenk, Preparation of silk spheres for controlled drug delivery, Zurich-Geneva Joint Seminar Series in Drug Formulation & Delivery, October 7 - 8, 2004, Zurich, Switzerland.

Poster presentations

E. Wenk, FGF-2 binding to modified silk fibroin films mimicking the extracellular matrix, 14th Swiss Conference on Biomaterials, May 8, 2008, Basel, Switzerland.

E. Wenk, Silk scaffolds as a new application system for IGF-I loaded PLGA microspheres, 34th Annual Meeting and Exposition of the Controlled Release Society, July 7 – 11, 2007, Long Beach, California, USA.

E. Wenk, Silk scaffolds as a new application system for IGF-I loaded PLGA microspheres, 2nd MRC Graduate Symposium, June 27, 2007, Zurich, Switzerland.

E. Wenk, Preparation of silk spheres for controlled drug delivery, 1st MRC Graduate Symposium, June 29, 2006, Zurich, Switzerland.

E. Wenk, Preparation of silk spheres for drug delivery, Annual Meeting Swiss Society for Biomedical Engineering, September 1 – 2, 2005, Lausanne, Switzerland.

ACKNOWLEDGEMENTS

related problems. A big thank you to all other members of the former and present Drug Formulation and Delivery group contributing to a great atmosphere.

I would like to thank my family and friends for their constant support and advice in all situations of life.